



This is a repository copy of *Transition metal complexes as photosensitisers in one- and two-photon photodynamic therapy*.

White Rose Research Online URL for this paper:
<http://eprints.whiterose.ac.uk/130249/>

Version: Accepted Version

Article:

McKenzie, L.K., Bryant, H.E. and Weinstein, J.A. (2019) Transition metal complexes as photosensitisers in one- and two-photon photodynamic therapy. *Coordination Chemistry Reviews*, 379. pp. 2-29. ISSN 0010-8545

<https://doi.org/10.1016/j.ccr.2018.03.020>

Reuse

This article is distributed under the terms of the Creative Commons Attribution-NonCommercial-NoDerivs (CC BY-NC-ND) licence. This licence only allows you to download this work and share it with others as long as you credit the authors, but you can't change the article in any way or use it commercially. More information and the full terms of the licence here: <https://creativecommons.org/licenses/>

Takedown

If you consider content in White Rose Research Online to be in breach of UK law, please notify us by emailing eprints@whiterose.ac.uk including the URL of the record and the reason for the withdrawal request.



eprints@whiterose.ac.uk
<https://eprints.whiterose.ac.uk/>

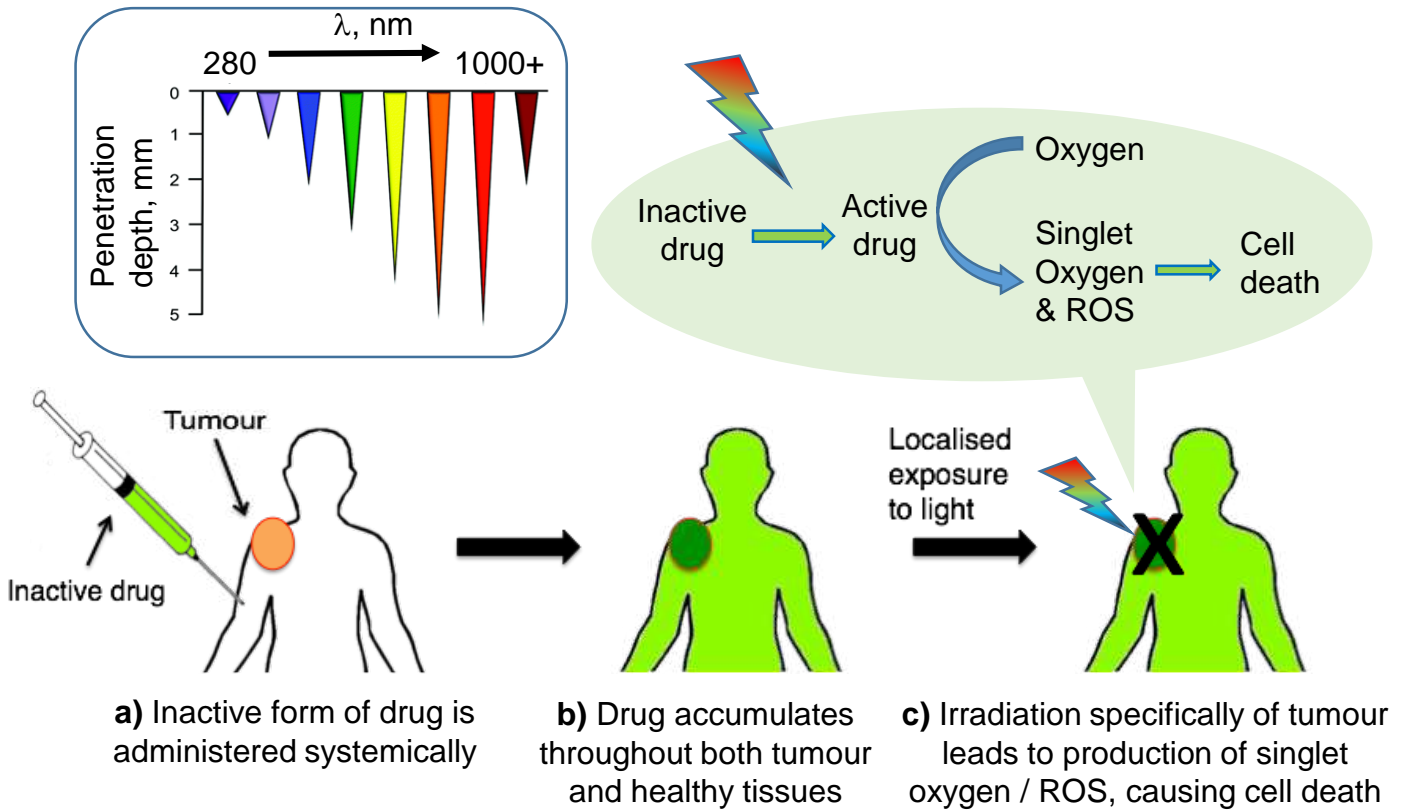


Figure 1. A schematic of PDT treatment of cancer: a) non-active form of drug is administered; b) drug is left to accumulate in tumour and healthy tissue; c) specific radiation of tumour tissue leads to production of singlet oxygen/ reactive oxygen species leading to targeted cell death. Top left: Depth of tissue penetration as a function of wavelength of light, adapted from [2].

Figure 2

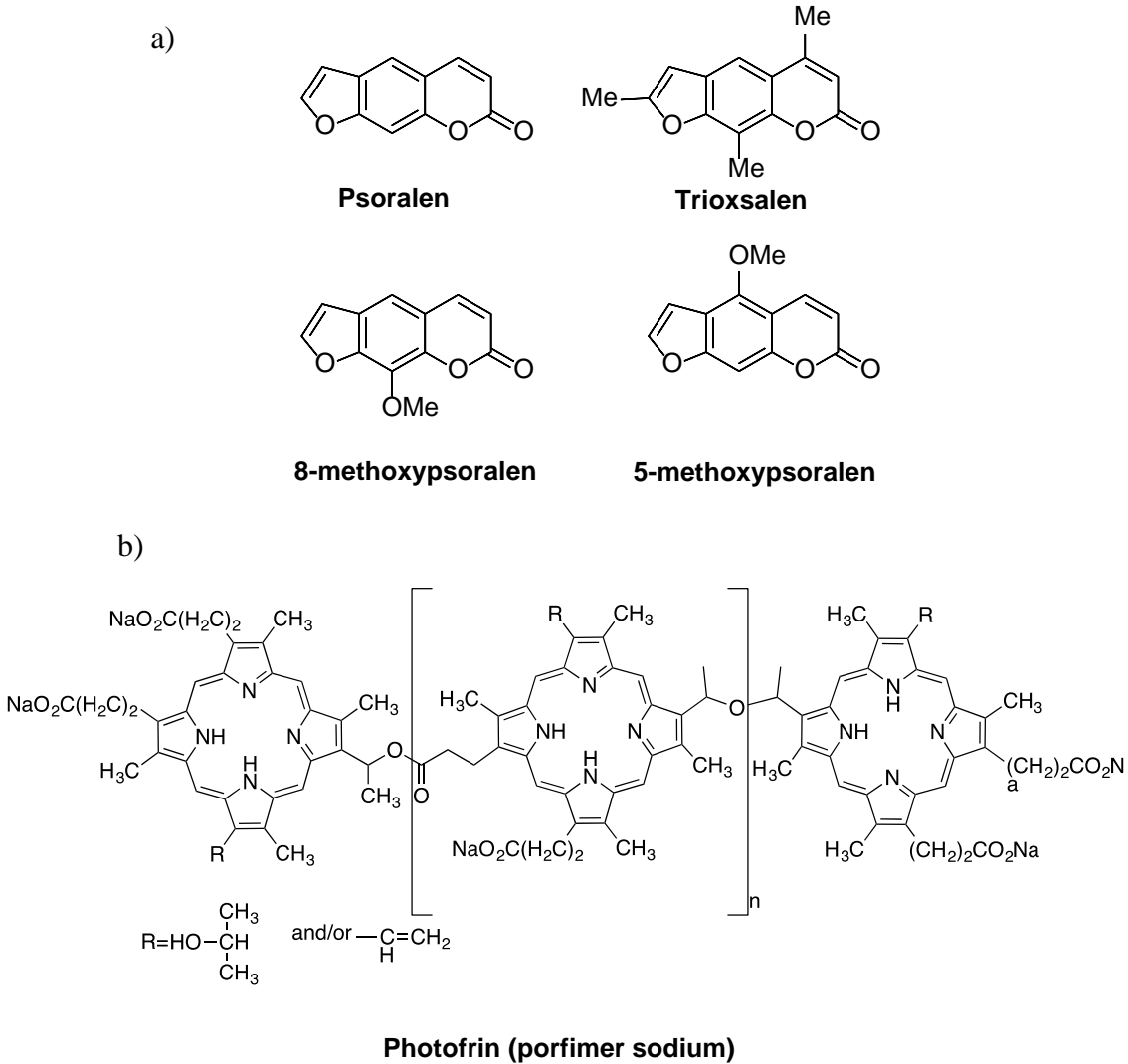


Figure 2. a) Structure of Psoralen and related molecules; b) Structure of Photofrin.

Figure 3

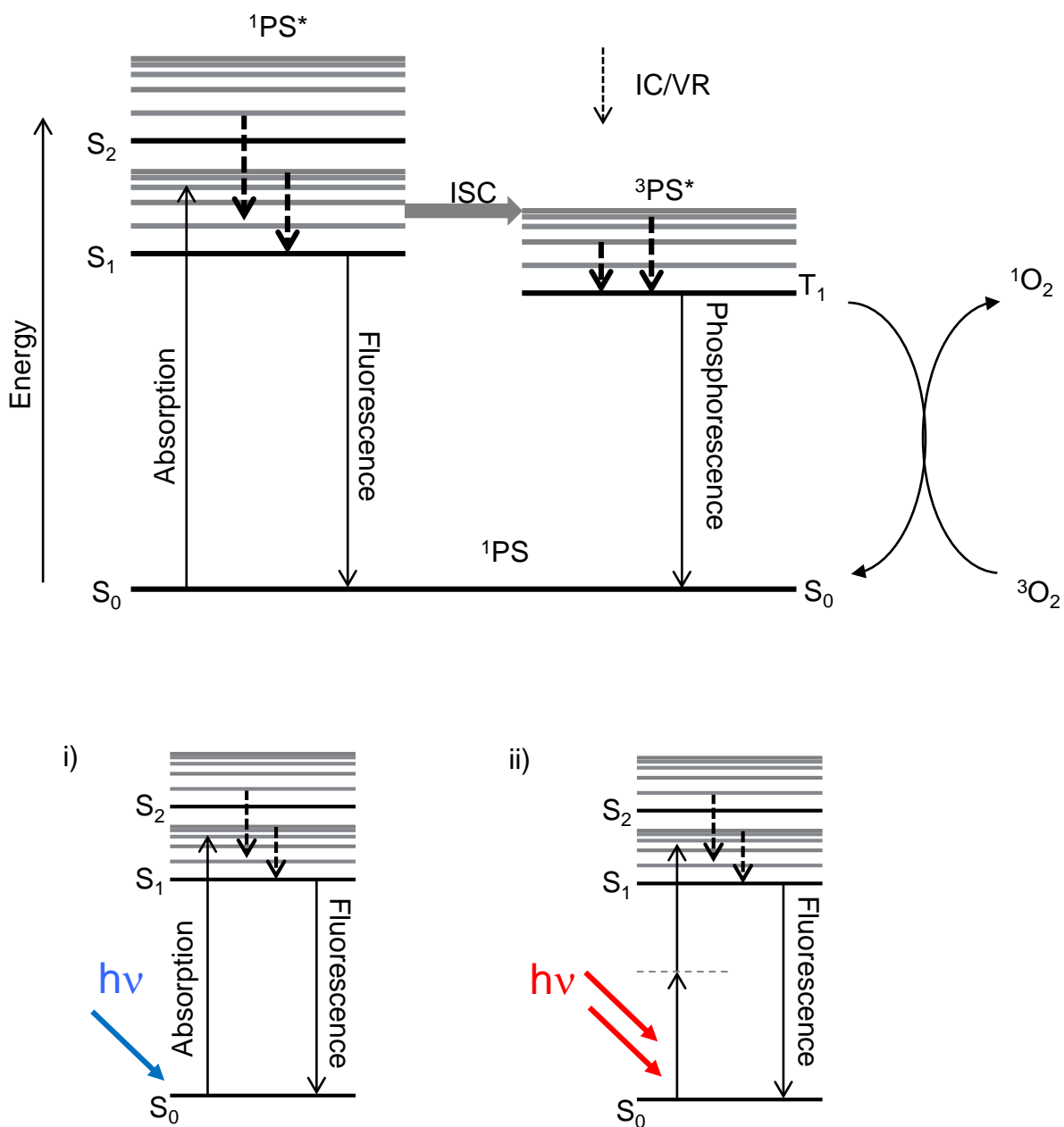


Figure 3. A simplified Jablonski diagram showing typical energy levels and transitions relevant to the formation of the triplet state of photosensitiser, and photosensitization of molecular oxygen. IC = internal conversion, VR = vibrational relaxation, ISC = intersystem crossing.

Figure 4

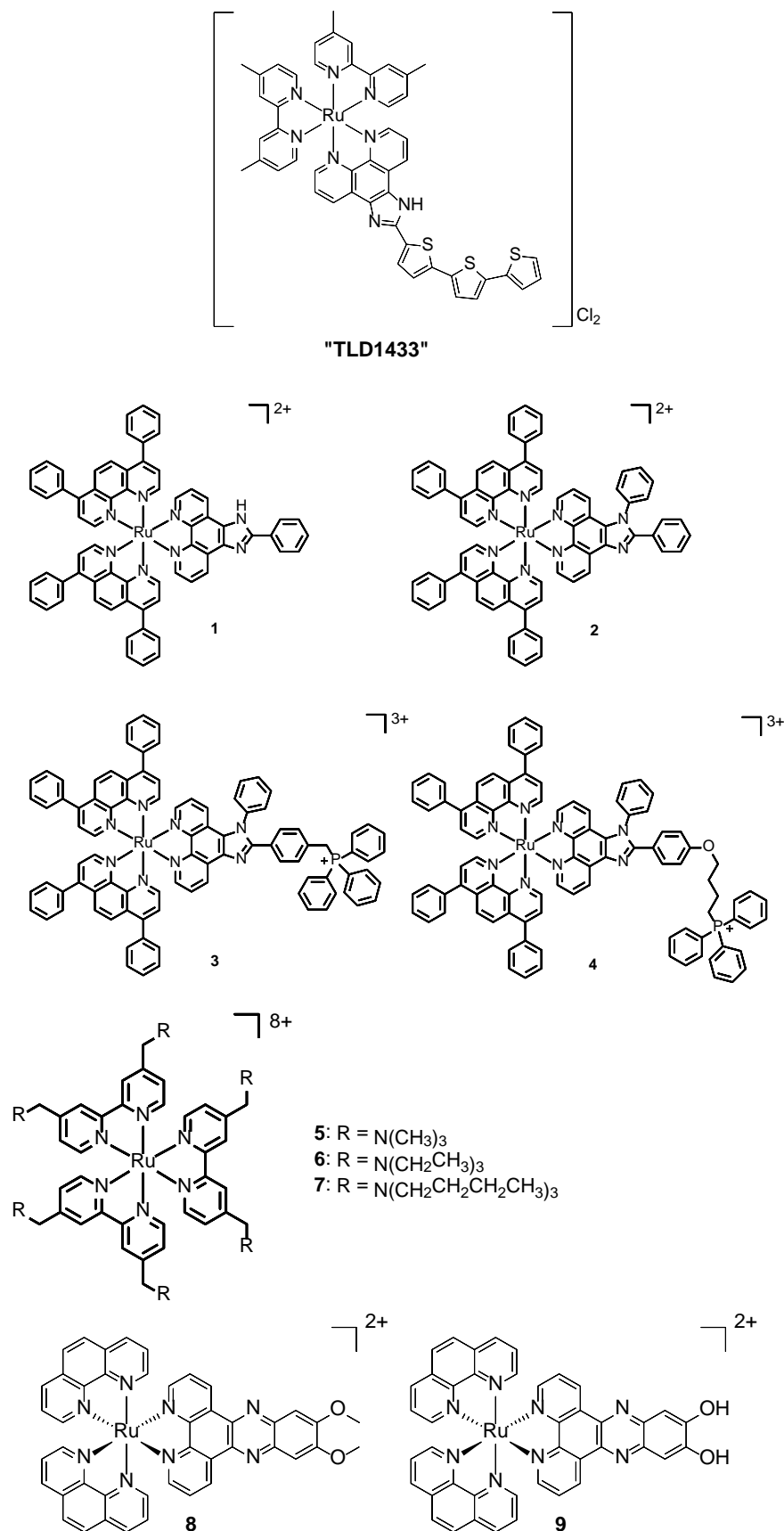


Figure 4. TLD1433 and examples of several other Ru(II) diimine photosensitisers. **1 - 4** are highly lipophilic compounds, numbered RuL1-RuL4 in [39]; compounds **5 - 7** are highly charged (+8) compounds (Ru1 – Ru3 in [40]); compounds **8** and **9** that contain derivatives of a known DNA intercalating ligand dppz are compounds **1** and **2** in [41].

Figure 5

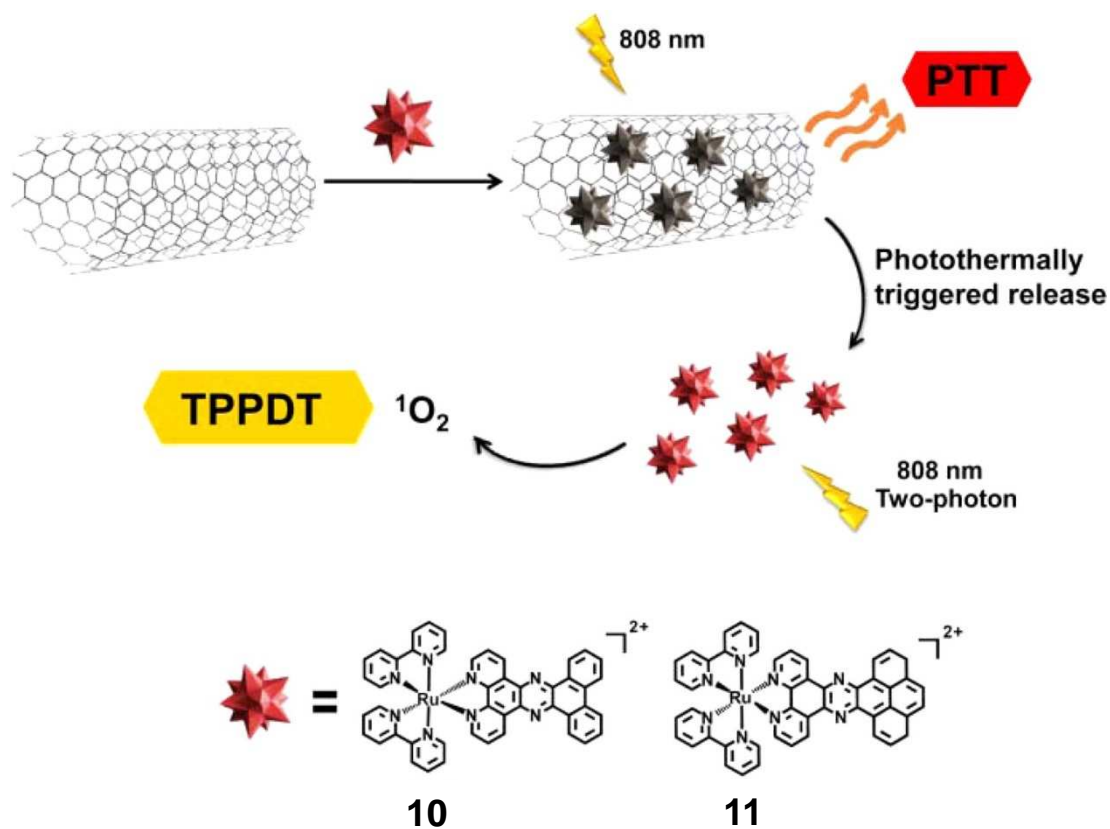


Figure 5. Ru(II) photosensitisers **10** and **11** which in conjunction with single wall carbon nanotubes act as dual photothermal anticancer agents (compounds Ru1 and Ru2 in [42]). Reproduced with permission from the American Chemical Society

Figure 6

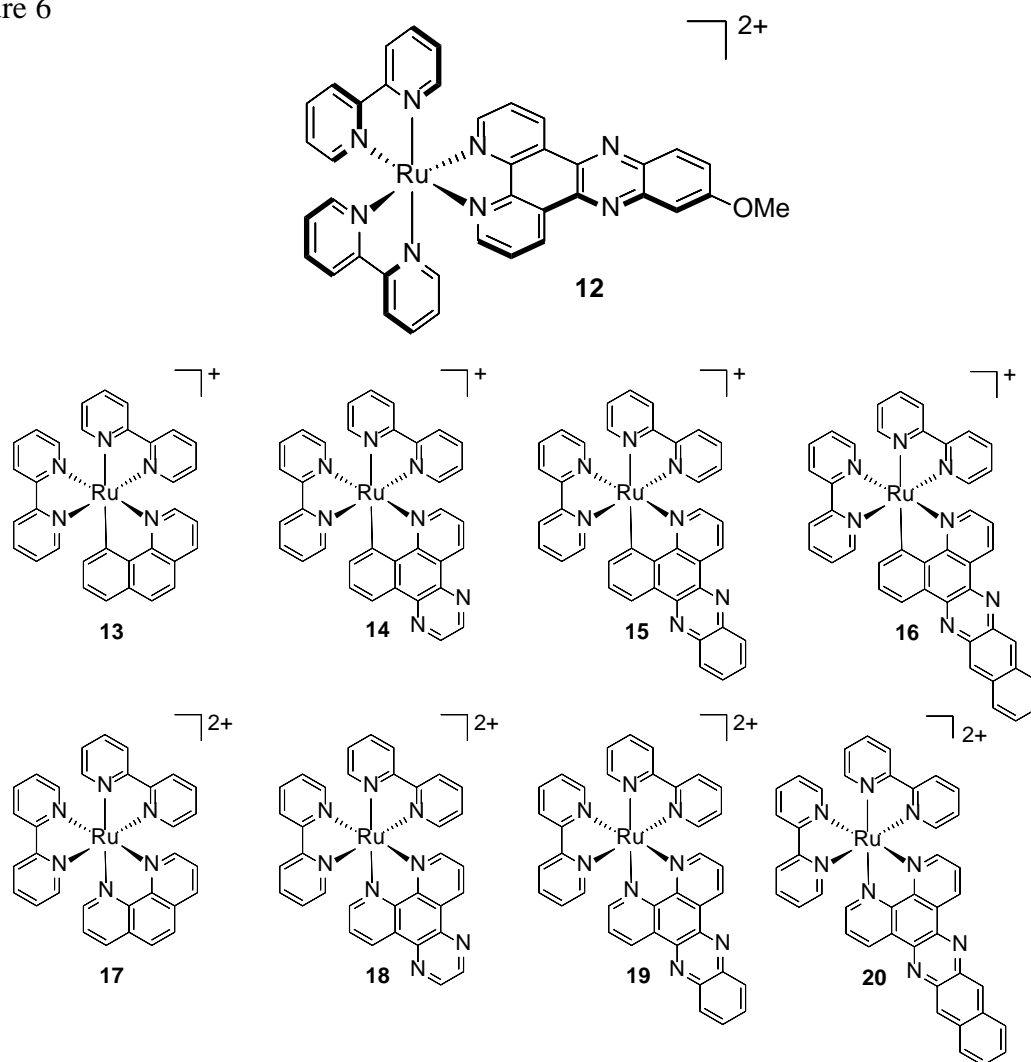


Figure 6. Chemical structures of some Ru(II) photosensitisers. Compound **12** (Ru65 in [43]) is a DNA intercalator. Compounds **13** - **20** (1 - 8 in [45]) contain cyclometallating and diimine ligands. A systematic study of the effect of the extending conjugation in either cyclometalating, or diimine ligands, on photodynamic properties has been performed.

Figure 7

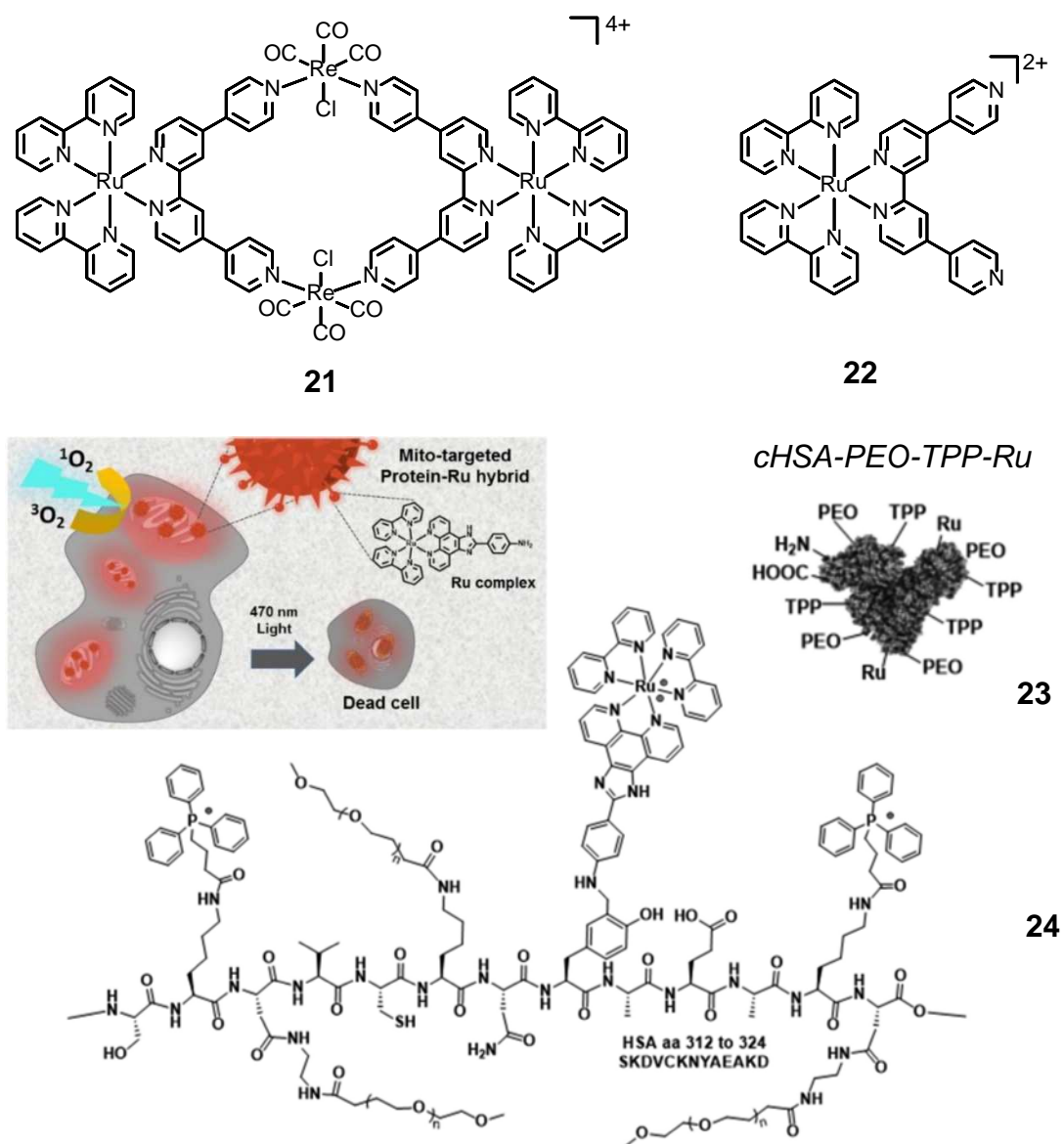


Figure 7. Chemical structures of some Ru(II) based photosensitizers A macrocyclic Ru(II)/Re(I) photosensitizer **21**, and its mononuclear Ru(II) building block **22** [46]. Ru(II) PS conjugated to human serum albumin (**23**) cHSA-PEO-TTP-Ru and to HSA aa 312 to 324 (**24**)[47]. Structures of **23** and **24** and image reproduced from [47] with permission from the American Chemical Society.

Figure 8

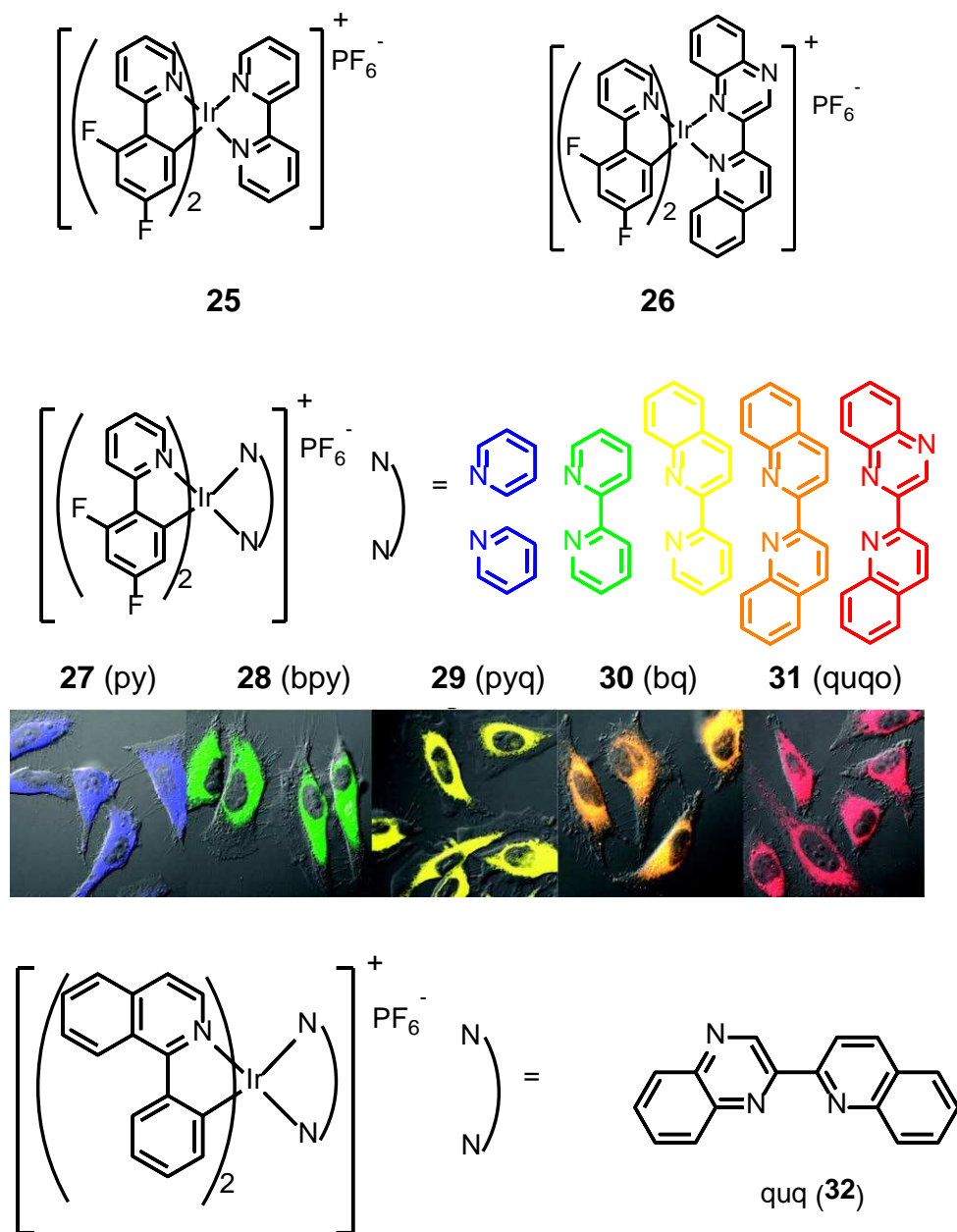


Figure 8. Cyclometallated Ir(III) complexes of general type $[\text{Ir}(\text{C}^{\wedge}\text{N})_2(\text{NN})]^+$. Compounds **25** and **26** are compounds 1 and 2 in [65]; compounds **27** – **32** are compounds 1-6 in [56]. Emission images of HeLa cells incubated with **27-31** (left to right) are also shown. Emission images reproduced from [56] with permission from the American Chemical Society.

Figure 9

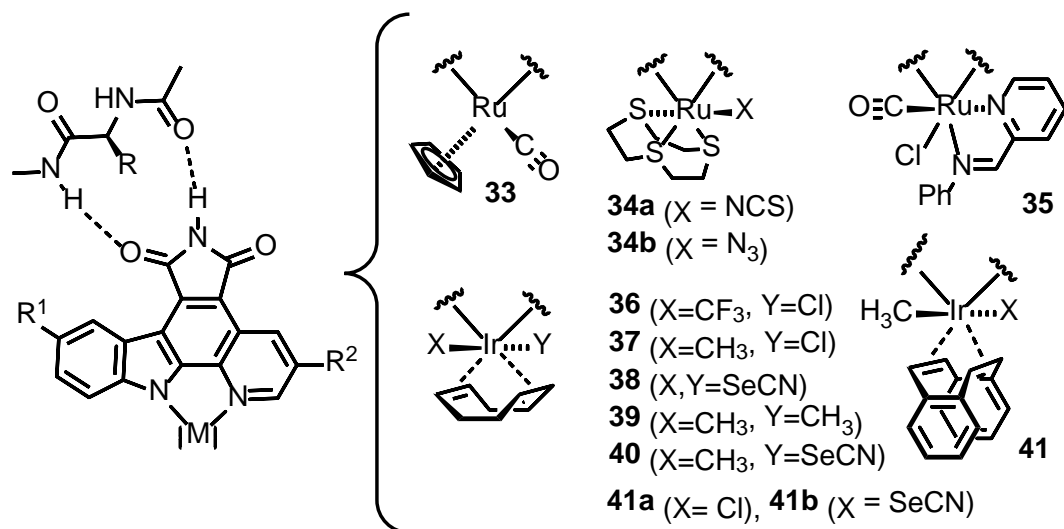


Figure 9. Chemical structures of metallo-pyrido carbazole Ir(III) photosensitisers **33** – **41b** (compounds 1 - 11 in [69]).

Figure 10

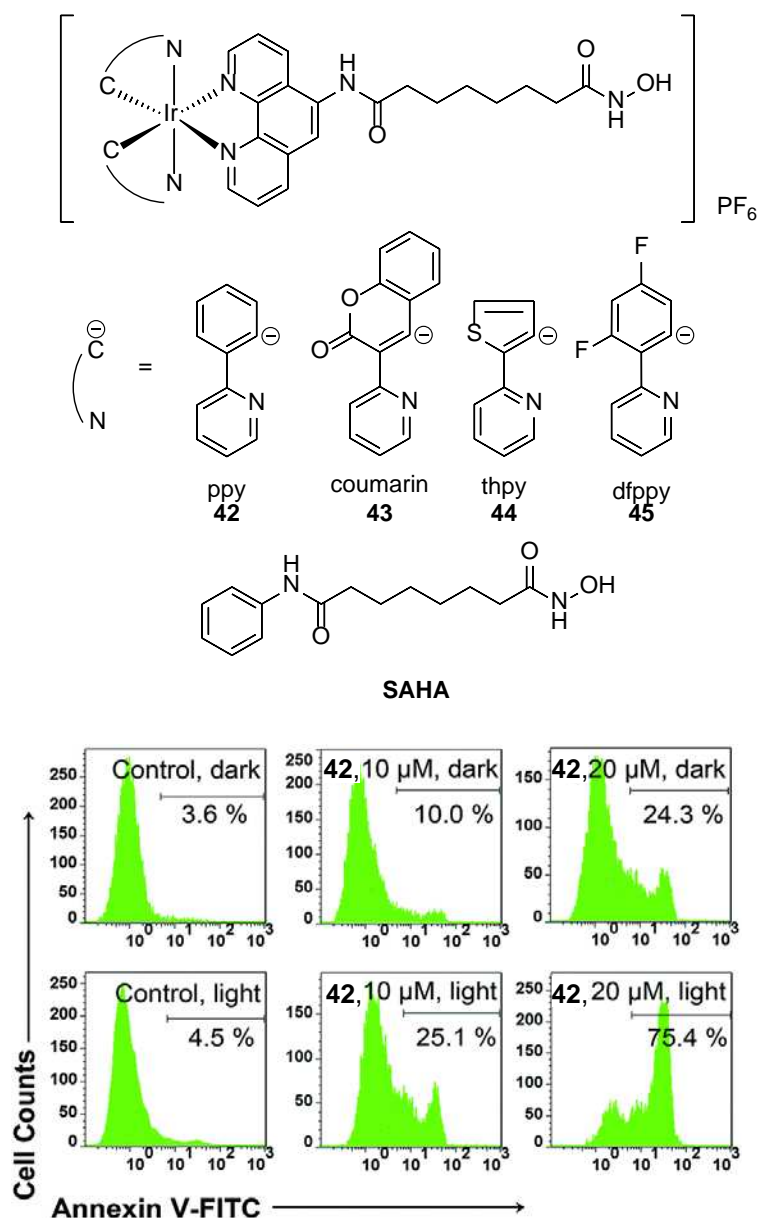


Figure 10. $[\text{Ir}(\text{C}^{\wedge}\text{N})_2(\text{NN})]^+$ photosensitisers designed with the aim of combining photosensitisation with a Histone deacetylases (HDAC) inhibitor, suberanilohydroxamic acid (SAHA). Compounds **42** - **45** are compounds 1 - 4 in [71]. The bottom panel shows characterisation of apoptosis induced in HeLa cells by complex **42** using annexin V-FITC staining, and monitored by flow cytometry, reproduced from [71] with permission from the Royal Society of Chemistry.

Figure 11a

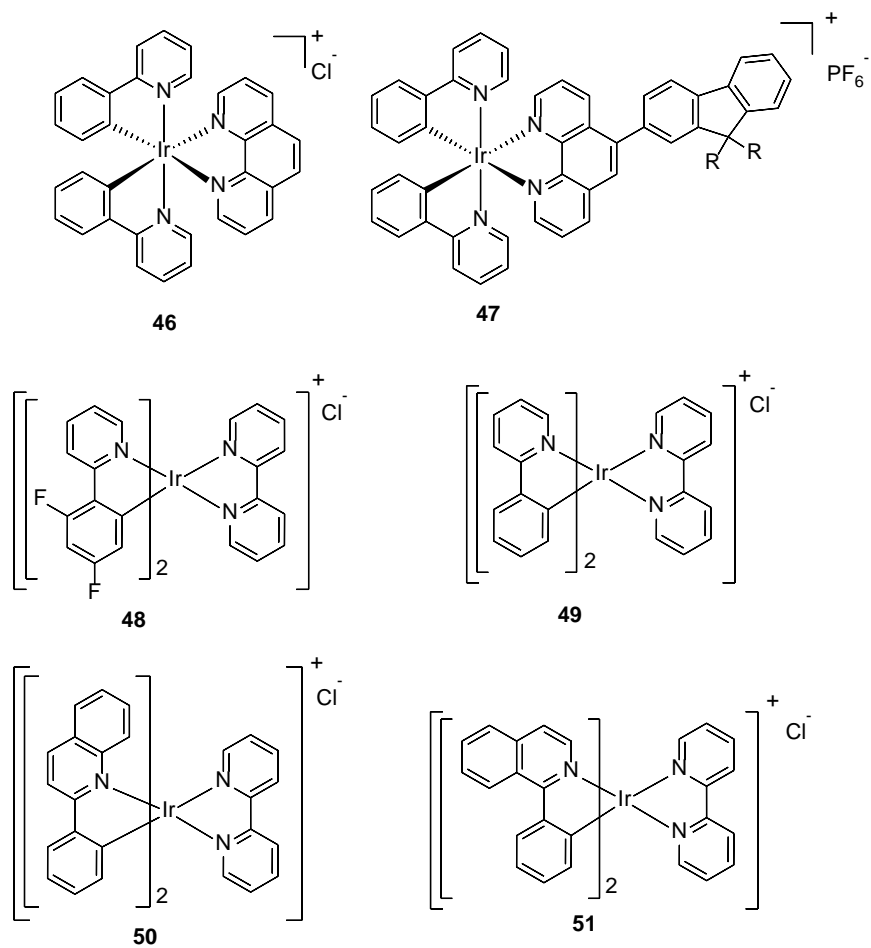


Figure 11a. Chemical structures of some $[\text{Ir}(\text{C}^{\wedge}\text{N})_2(\text{NN})]^+$ photosensitisers: **46**[73]; **47**[74]; **48 - 51** (compounds Tlr1 - Tlr4 in [76]).

Figure 11b

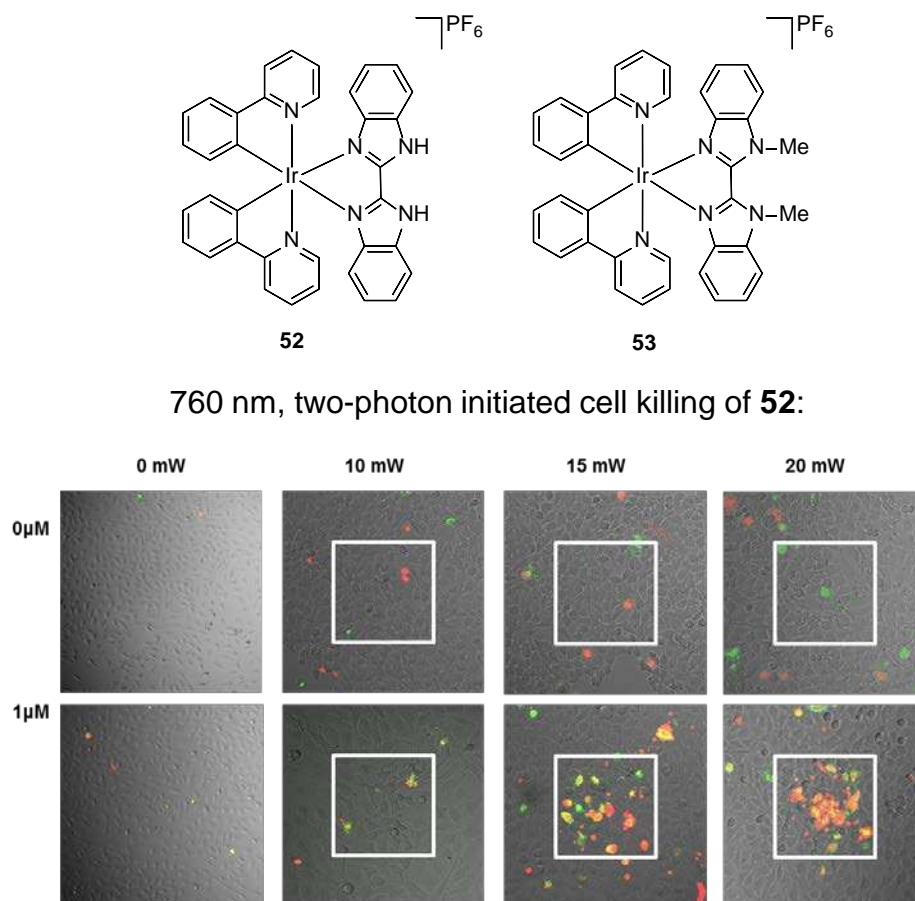


Figure 11b. Chemical structures of Ir(III) compounds **52** and **53**.^[77] **52** and **53** are pH sensitive in the physiological range. **52** has the higher PI index for Ir(III) complexes to date under one-photon excitation, and is also a two-photon PDT agent^[77]. The bottom panel shows two photon absorption activated killing of HeLa cancer cells incubated with **52** ($1 \mu\text{M}$) for two hours, followed by irradiation with 760 nm, ~ 100 fs pulses (irradiated area $225 \times 225 \mu\text{m}$, 1024×1024 pixels, $6.6 \mu\text{s}$ dwell time, 8 scans) with the powers corresponding to 0, 1088, 1632, 2176 J cm^{-2} . Cell apoptosis is indicated in green and necrosis in red. All images are $450 \times 450 \mu\text{m}$ except those in the 0 mW column which are $900 \times 900 \mu\text{m}$. Cell death Images reproduced from [77] with permission from John Wiley & Sons.

Figure 12

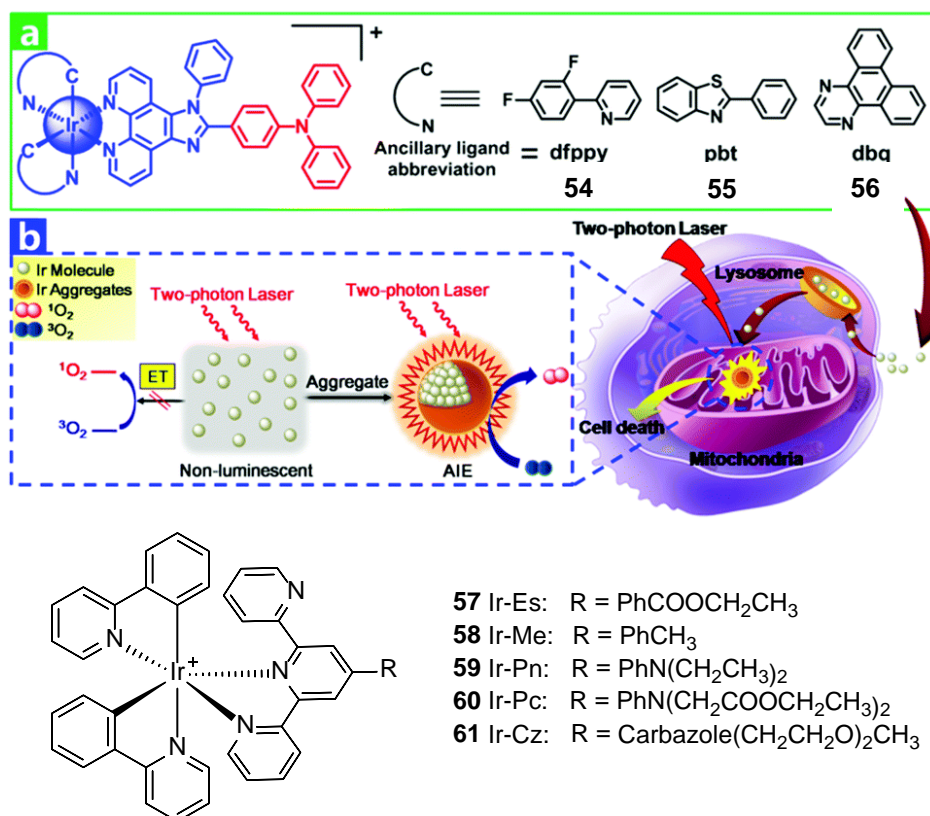


Figure 12. Chemical structures of some of Ir(III) photosensitizers: compounds **54** - **56** are compounds Ir1 – Ir3 in [78]; compounds **57** – **61** are compounds Ir-Es, Ir-Me, Ir-Pn, Ir-Pc and Ir-Cz in [79]. Top panel reproduced from [78] with permission, Copyright The Royal Society of Chemistry.

Figure 13

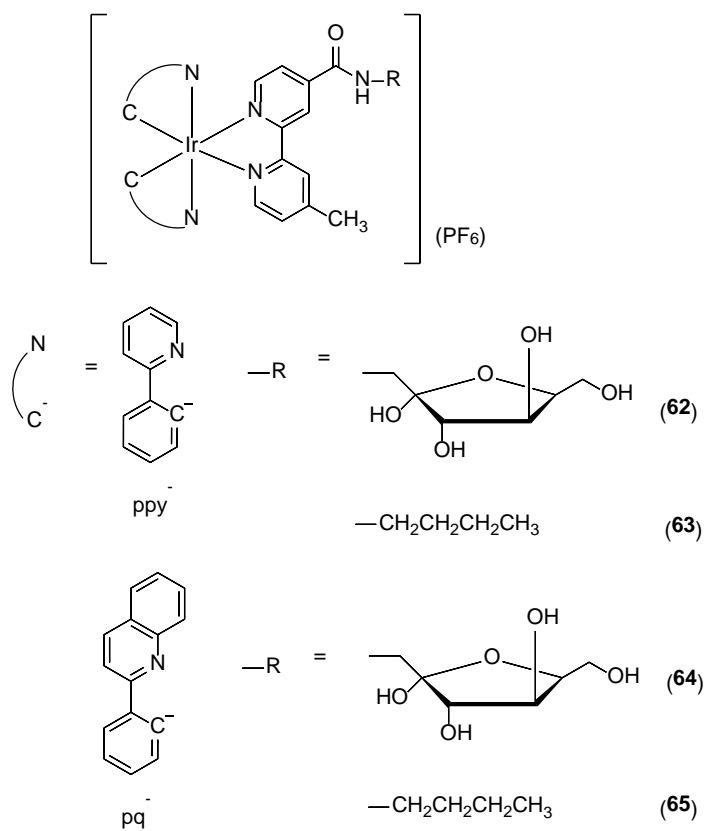


Figure 13. Ir(III) photosensitisers containing fructose, and their fructose-free analogues; compounds **62** – **65** are compounds 1a, 1b, 2a and 2b from [80].

Figure 14

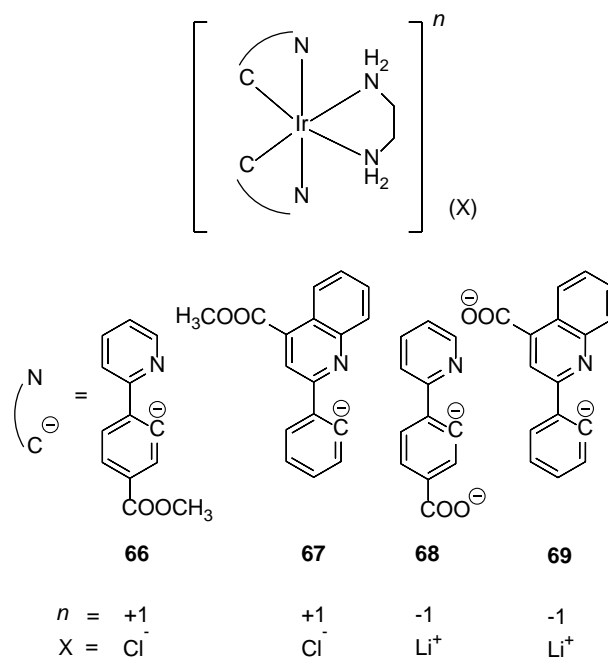


Figure 14. Ir(III) photosensitisers with diverse cyclometallating ligands. Compounds **66** – **69** are compounds 1a, 2a, 1b and 2b from [83].

Figure 15

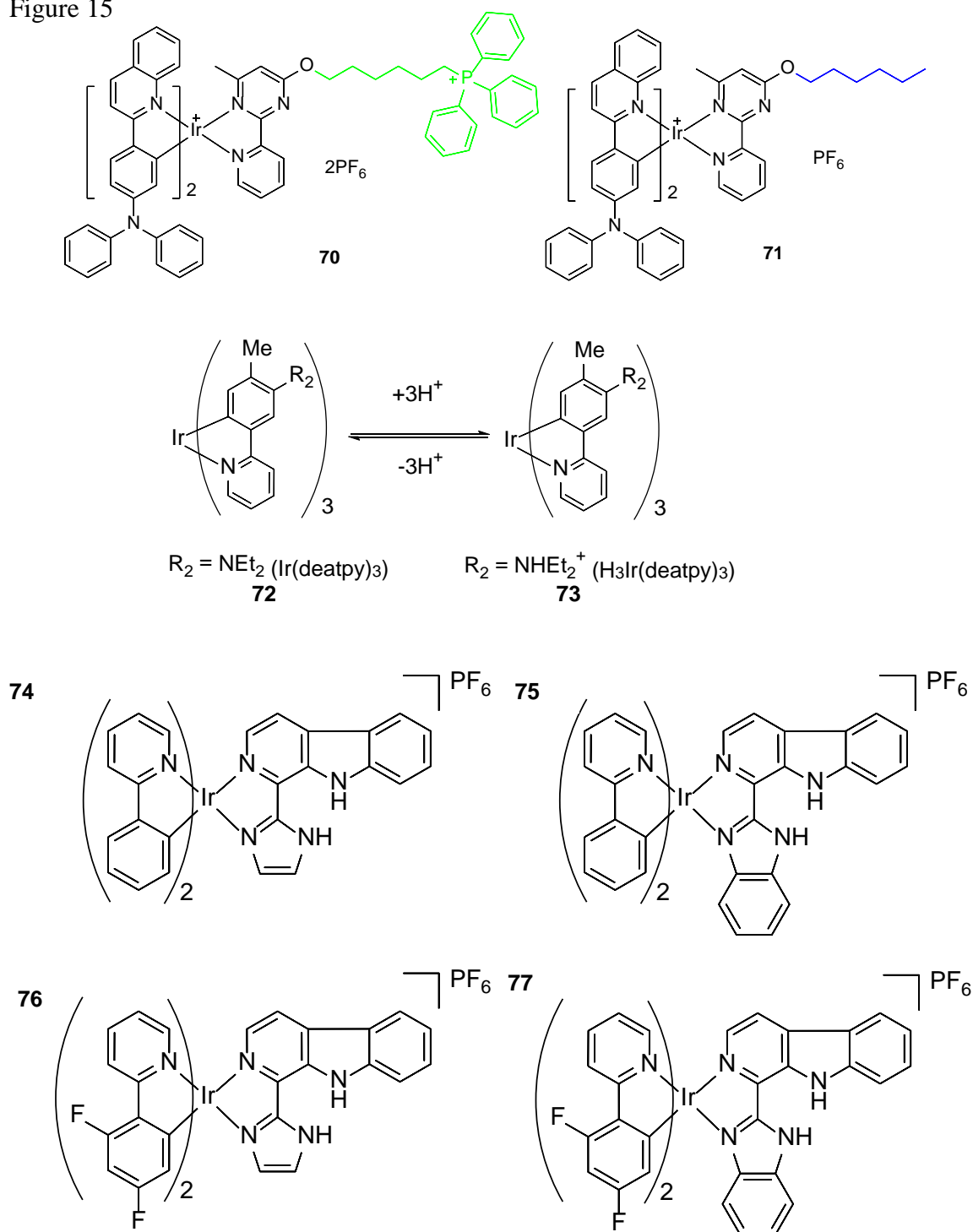


Figure 15. Ir(III) photosensitizers which are lysosome-specific (**70** and **71**, correspond to Ir-P(ph)₃ and Ir-alkyl from [84]); [Ir(N[∧]C)₃]ⁿ pH-responsive photosensitizers **72** and **73** (5 and H3.5 from [85]); and pH-responsive, lysosome-specific [Ir(N[∧]C)₂(NN)]⁺ compounds **74** – **77** (compounds 1 – 4 from [88]).

Figure 16

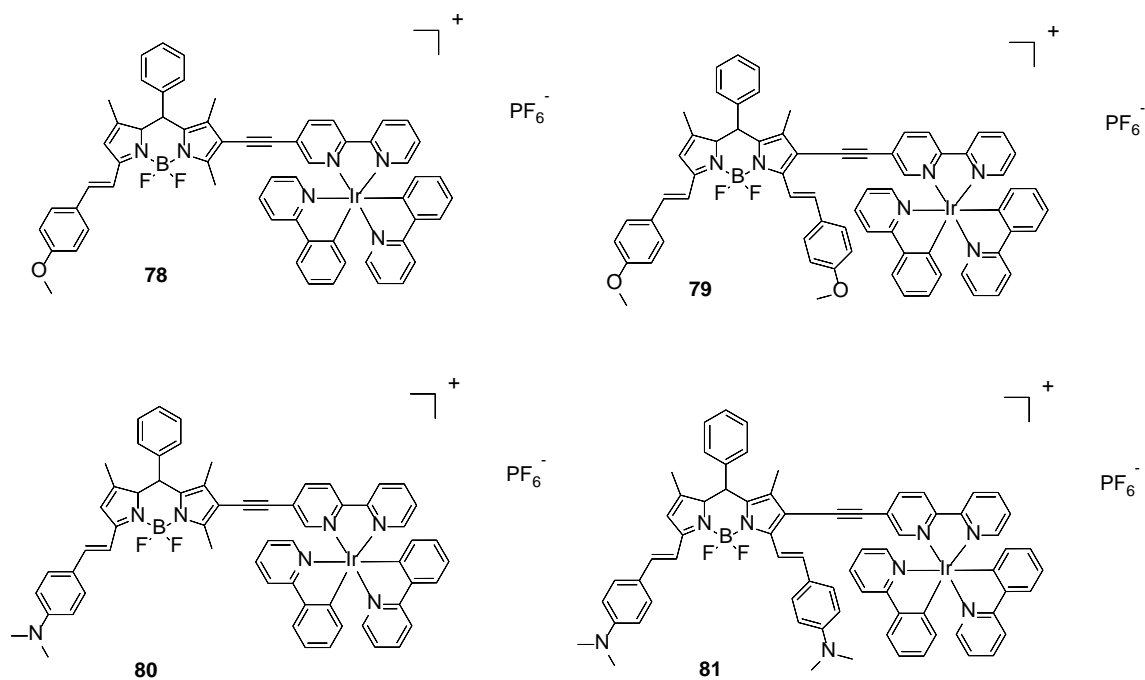


Figure 16. Red-light activated Ir(III) photosensitisers bearing BODIPY groups, **78** – **81** (compounds Ir-1 – Ir-2 from [89]).

Figure 17

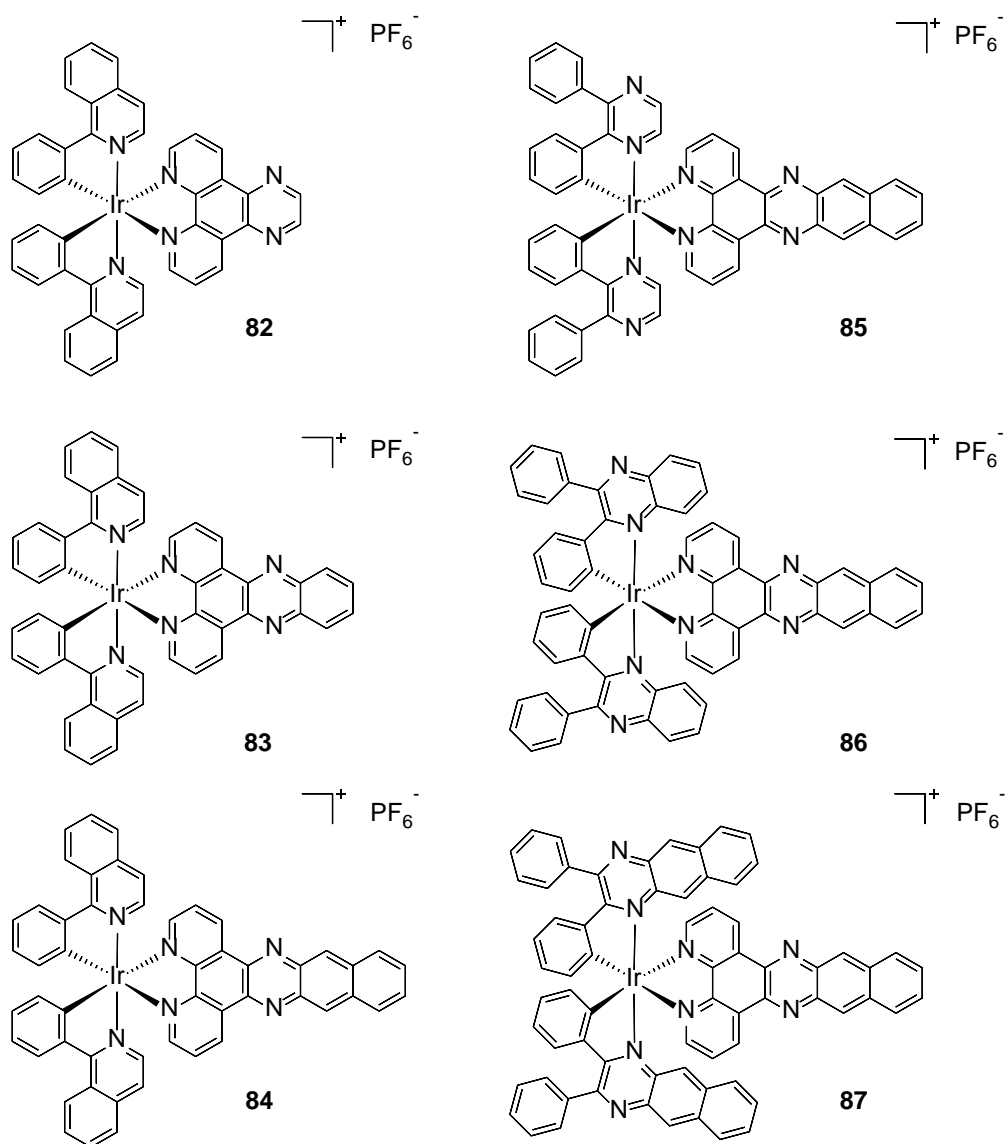


Figure 17. Systematic tuning of light-absorbing properties of Ir(III) complexes through changing conjugation in diimine and cyclometalating ligands, **82** – **87** (compounds 1 – 6 from [90]).

Figure 18

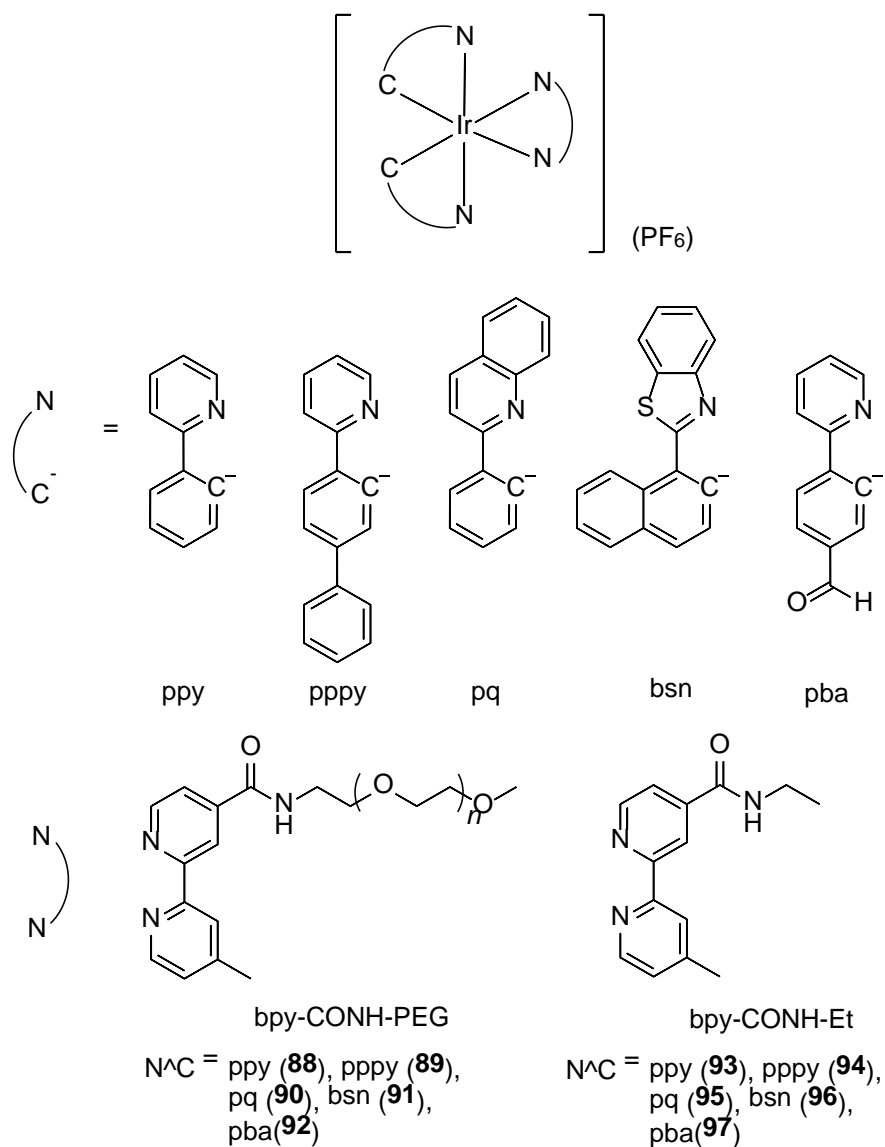


Figure 18. Ir(III) photosensitisers with PEG chains and their analogs. Compounds **88** – **92** are compounds 1a – 5a, compounds 93 – 97 are compounds 1b – 5b from [95].

Figure 19

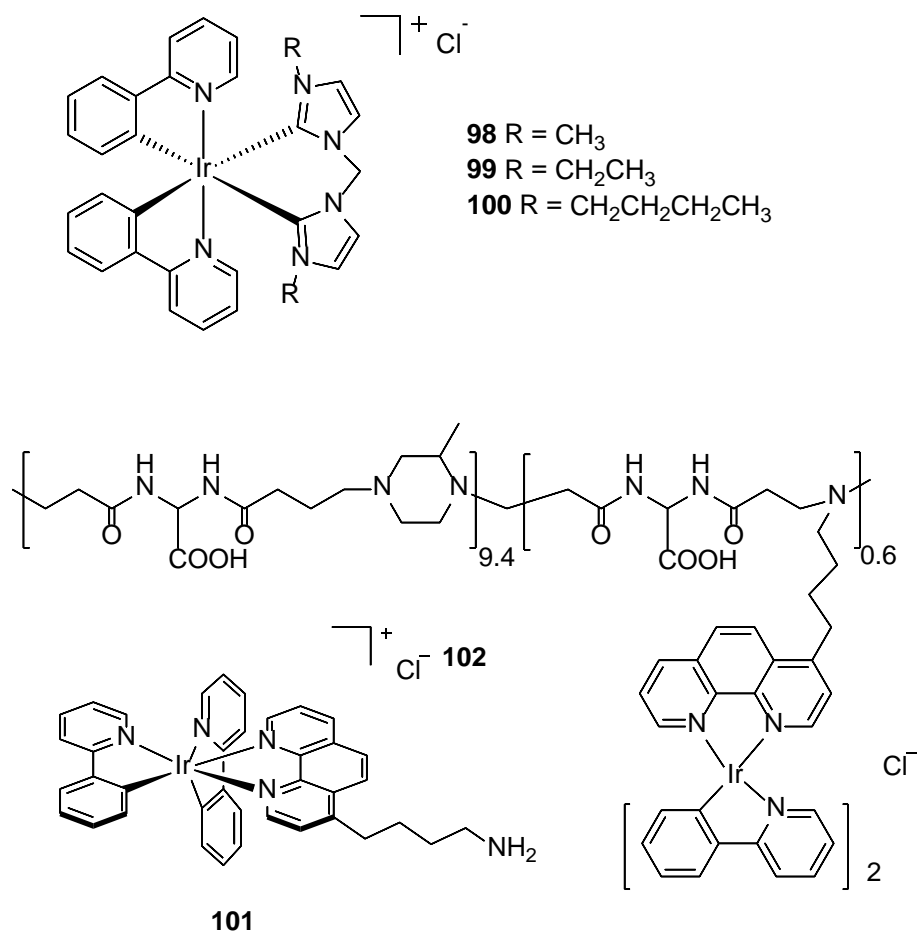


Figure 19. Ir(III) photosensitisers designed for mitochondrial (**98 – 100**, compounds 1 – 3 from [97]) and perinuclear (**101 – 102**, compounds 1M and 1P from [98]) localisation.

Figure 20

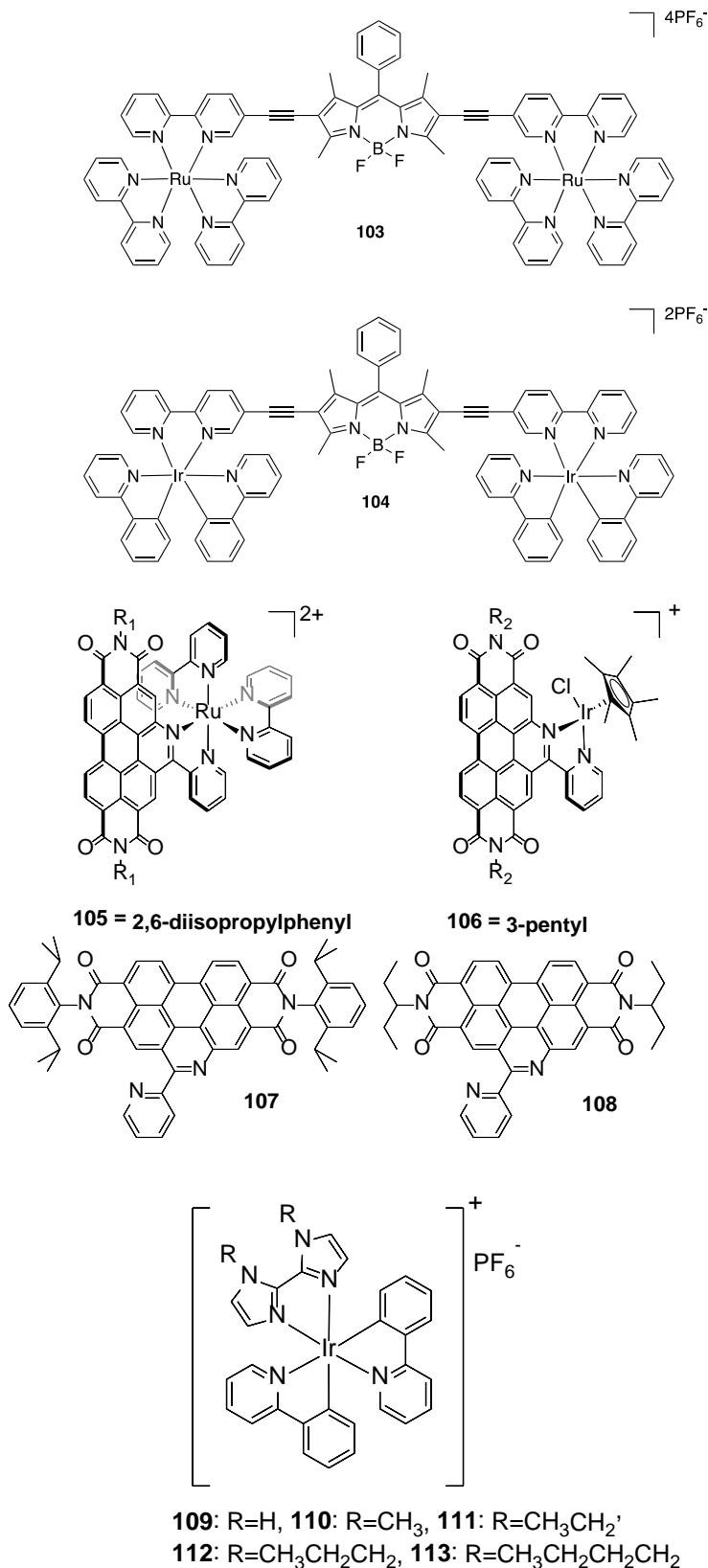


Figure 20. Orange-absorbing photosensitisers **103** and **104** (Ru-2 and Ir-2 from [99]); aromatic acid imide-containing photosensitisers **105** - **108** (R1, R2, L1 and L2 from [100]); mitochondria-targeting photosensitisers **109** - **113** (Ir1 - Ir5 from [101]).

Figure 21

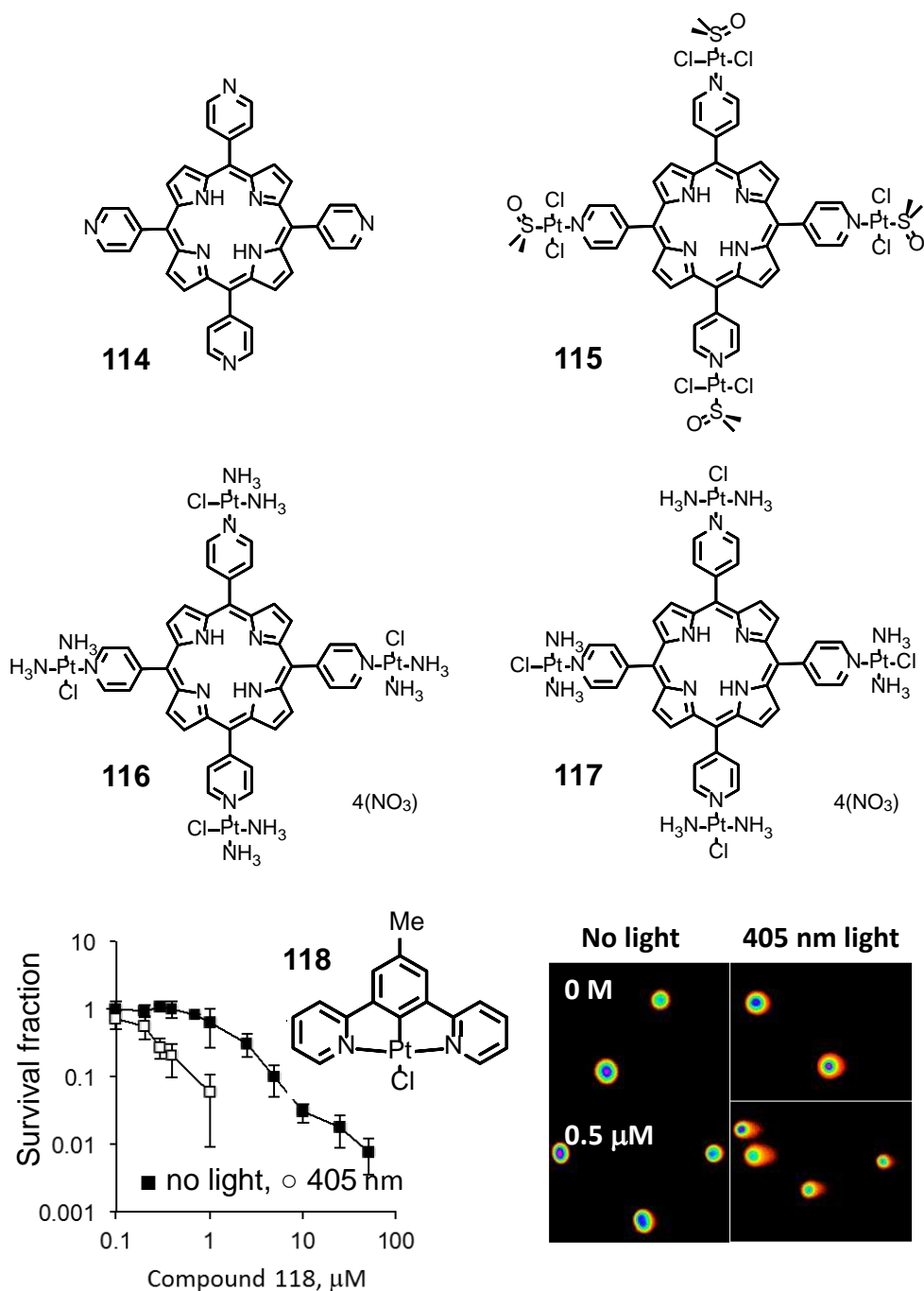
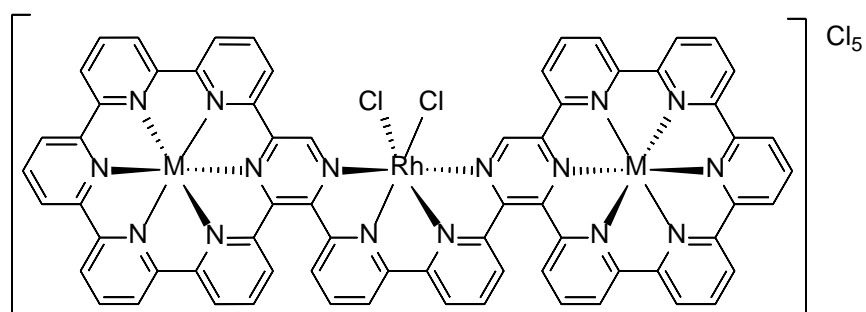
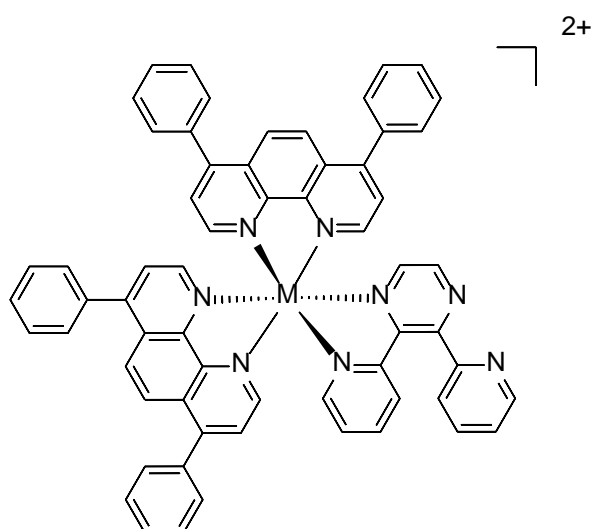


Figure 21. Pt-based photosensitizers. **114** – **117** are compounds 1 – 4 from [108]; compound **118** is compound 1 from [109]. The bottom panel shows a representative COMET assay images for HeLa cells treated with 0.5 μM of **118**, with and without exposure to 405 nm light (3.6 J cm^{-2}) [109].

Figure 22



M = Os(II), 199; M = Ru(II), 120



M = Ru(II), 121; M = Os(II), 122

Figure 22. Multinuclear Os(II) and Ru(II) photosensitisers **119** and **120** [113]; mononuclear Ru(II) and Os(II) photosensitisers **121** and **122** (1 and 2 from [115]).

Figure 23

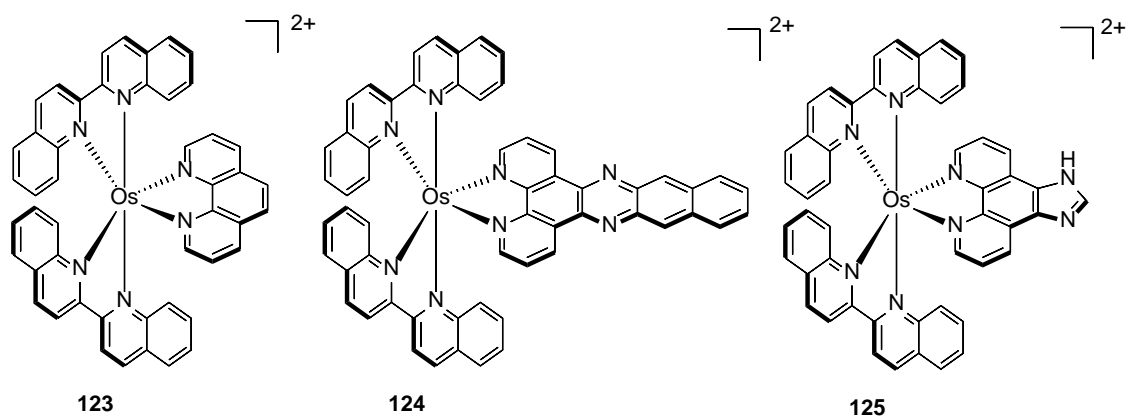


Figure 23. Os(II) photosensitisers **123** – **125** (TLD1822, TLD1824 and TLD1829 from [29]).

Figure 24

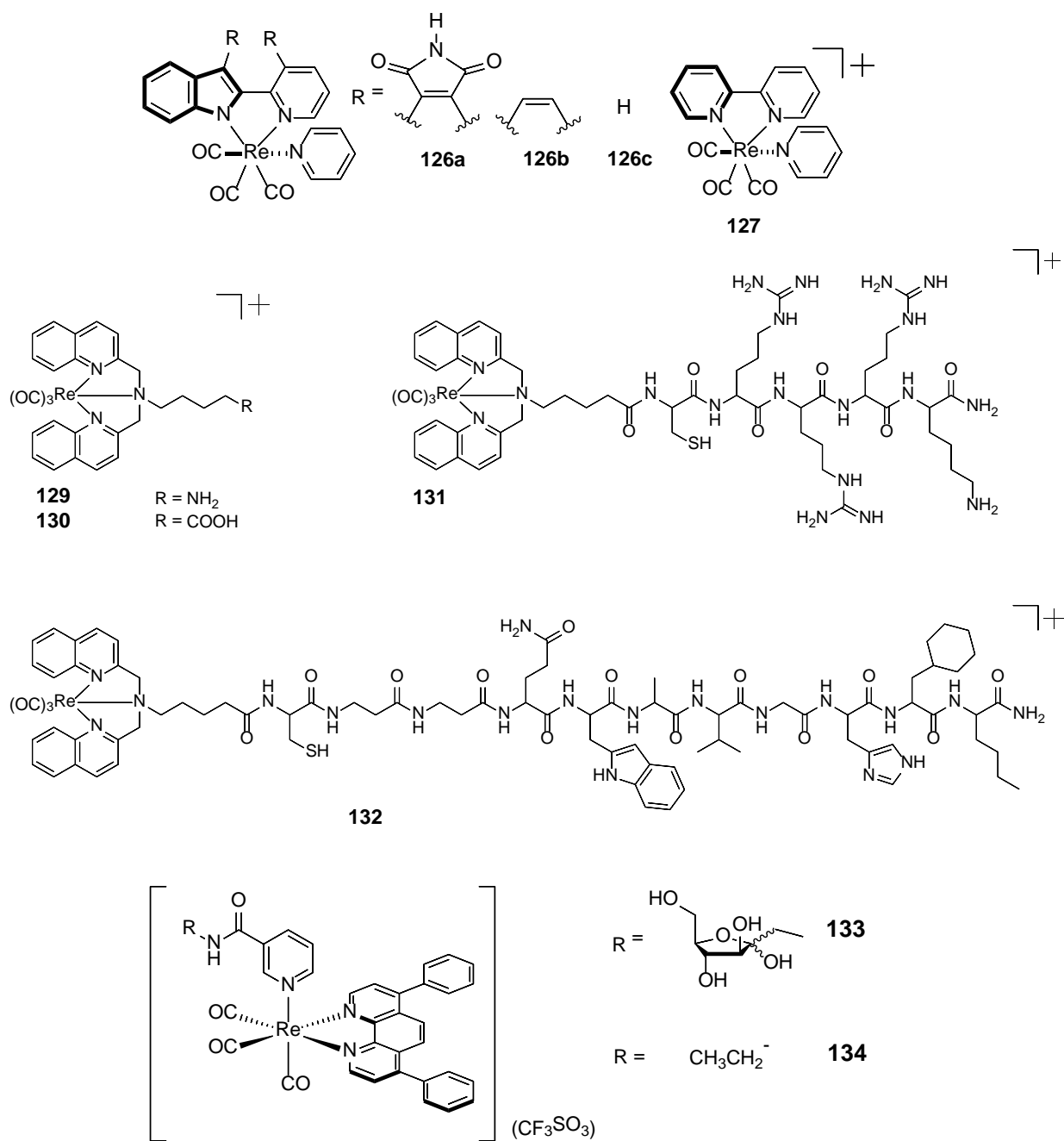
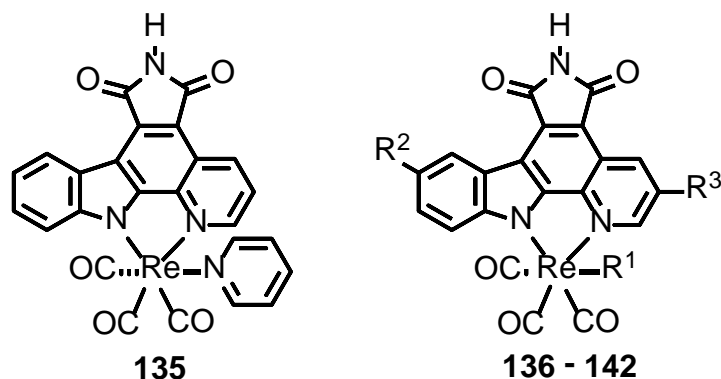


Figure 24. Re(I) photosensitizers **126** – **127** (1-4 from [118]).

Re(I) photosensitizers bearing protein tags, **129** – **132** (Re –NH₂, Re –COOH, Re –NLS and Re –Bombesin from [119]) and fructose unit, **133** - **134** (1 and 2 from [120]), and their tag-free analogues.

Figure 25



	R ¹	R ²	R ³
136	PMe ₃	H	H
137	Imidazole	H	H
138	Imidazole	OH	H
139	Imidazole	NMe ₂	H
140	Imidazole	H	F
141	Imidazole	H	CF ₃
142	imidazole	OMe	F

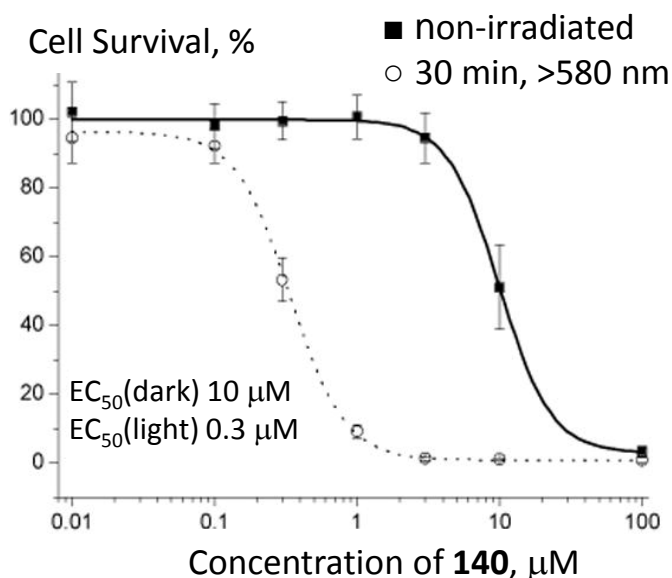


Figure 25. Re(I) pyridocarbazole complexes with tuneable absorption maxima for red-light activated PDT, **135 – 142** (compounds 1 – 8 from [121]); compounds **138-139** are not PDT-active. The bottom panel shows visible-light-induced antiproliferative activity of **140** in HeLa cancer cells which were irradiated for 30 min at $\lambda \geq 580$ nm following 1 h incubation with **140**; cytotoxicity was determined 24 h after addition by MTT assay, reproduced from [121] with permission from John Wiley & Sons.

Figure 26

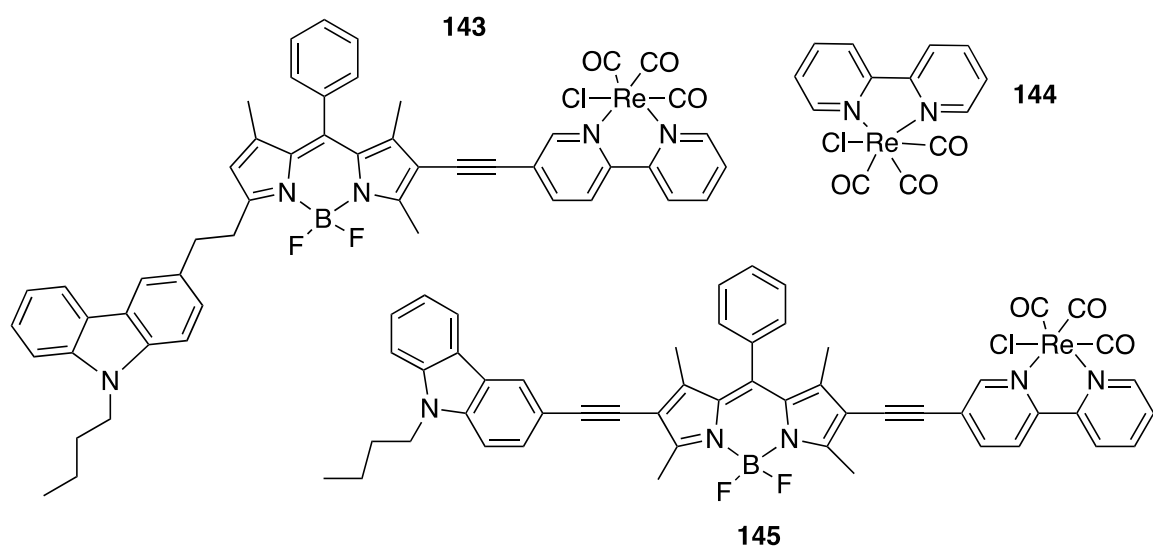


Figure 26. Re(I) photosensitisers **143** and **145** containing BODIPY unit (Re-1 and Re-2 from [122]).

Figure 27

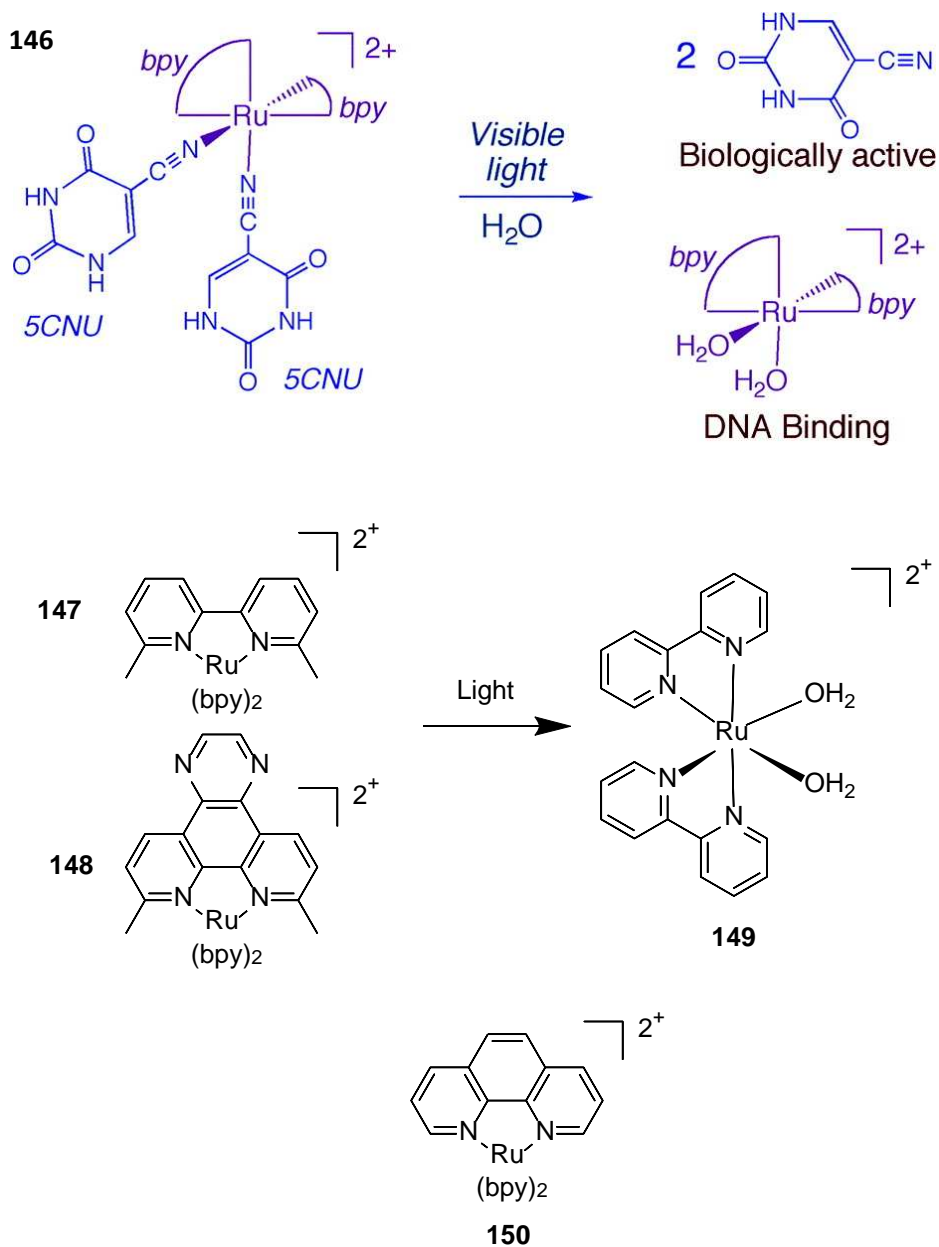


Figure 27. Ru(II) photosensitizers **146** (**1** in [127]) and **147-149** (**2**, **3** and **1** in [132]), and a control compound **150**. Top panel reproduced from [127] with permission from the American Chemical Society.

Figure 28

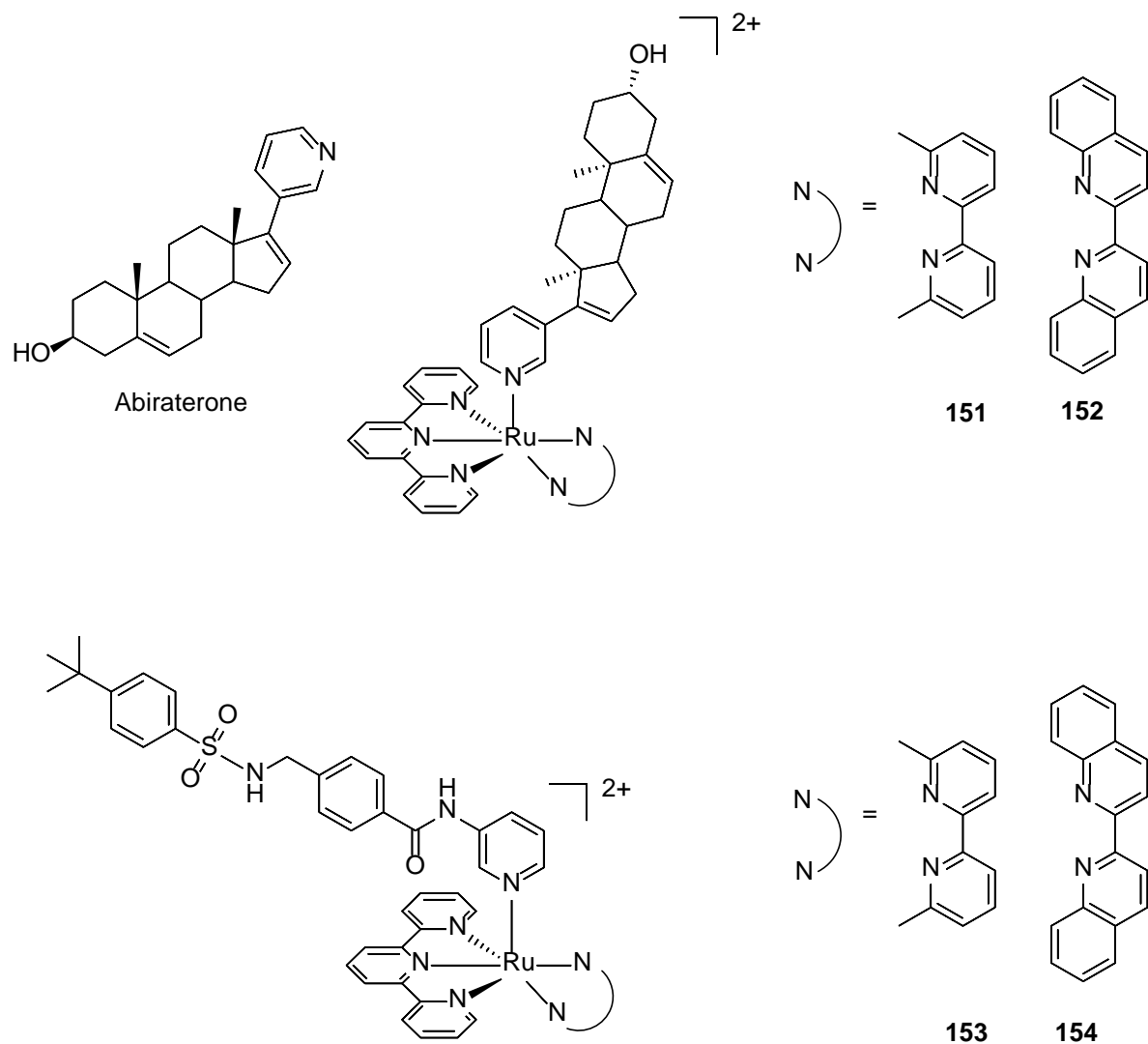


Figure 28. Ru(II) photosensitisers **151** and **152** (1 and 2 in [133]) and **153** and **154** (1 and 2 in [134]).

Transition Metal Complexes as Photosensitisers in one- and two-Photon Photodynamic Therapy

Luke K. McKenzie,^{1,2*} Helen E. Bryant,^{1*} Julia A. Weinstein^{2*}

¹ *Department of Chemistry, The University of Sheffield, Sheffield S3 7HF, U. K.*

² *Department of Oncology, The University of Sheffield, Sheffield S10 2RX, U. K.*

LKMckenzie1@sheffield.ac.uk, H.Bryant@sheffield.ac.uk, Julia.Weinstein@sheffield.ac.uk

Abstract

Photodynamic therapy (PDT) exploits light-activated compounds for therapeutic use. It relies on a photosensitiser (PS) that is inactive in the absence of light. When irradiated, the PS absorbs light and is promoted to a higher energy, “excited” state (PS*), which is either toxic to cells in itself, or triggers formation of other species which are toxic to cells, and hence particular wavelengths of light can be used to induce light-dependent cell killing. In PDT occurring via the so-called type I and type II mechanisms, the PS* engages in energy transfer to dioxygen present in cells and tissues. This process generates highly reactive singlet oxygen (¹O₂) and/or other reactive oxygen species (ROS) which in turn cause damage in the immediate vicinity of irradiation, and ultimately can lead to cell death. Whilst the main focus of research for the last 50 years has been on organic molecules or porphyrins as sensitisers, there is now emerging interest in extending the use of transition metal (TM) complexes can display intense absorption in the visible region, and many also possess high two-photon absorption cross-sections, which enable two-photon excitation with NIR light. As with any other type of photosensitiser, the issues to consider whilst designing a TM complex as a photosensitiser include cell permeability, efficient absorption of NIR light for deeper penetration, preferential affinity to cancer cells over healthy cells, targeted intracellular localisation, and lack of side effects. This review summarises recent developments involving photosensitisers containing, Ru(II), Os(II), Pt, Ir(III), and Re(I), and the approaches used to address the above requirements. Several remarkable recent advances made in this area, including the first clinical trial of a metal complex as a photosensitiser, indicate the bright future of this class of compounds in PDT.

1. Introduction

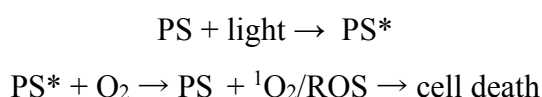
1.1 Photodynamic therapy

The ultimate aim of drug design and discovery is to find a compound that exerts maximal beneficial effects in the target tissue with minimal side effects in other tissues. Yet adverse secondary effects are common for most clinically used drugs, and can in part be attributed to the lack of specificity of their site of action. Photodynamic therapy (PDT) is built on the concept of light-activatable compounds known as photosensitisers (PS) which can be ‘switched on’ at the target site by localised irradiation with light. The PS should be non-toxic in the absence of light, and thus PDT offers the promise of highly targeted therapy with decreased side-effects[1].

In PDT, the patient is treated with the non-active PS either topically, systemically or by other treatment routes such as intravesically, dependent on the condition. The PS is then allowed to accumulate throughout the body in both healthy and non-healthy tissue (Figure 1, top left). Once peak concentration in the unhealthy tissue is reached, the PS is activated by localised irradiation with light of a suitable wavelength, with depth of tissue penetration dependent on wavelength of activating light [2] (Figure 1).

Absorption of light by the PS leads to the population of an electronic excited state, PS*. A currently used classification of the types of PDT is based on the mechanism of action of the PS*. Type I and II mechanisms of PDT operate via an oxygen-dependent pathway and are the focus of this review. In type III mechanism dependent PDT, electron or hydrogen transfer from the PS*, or cytotoxic products from its photodegradation, lead to cell death. These reactions are usually classified as photoactivated chemotherapy (PACT)[3] rather than PDT.

The key step in type I and type II PDT is a reaction of the PS* with molecular oxygen (O₂). This interaction produces singlet oxygen (¹O₂) or reactive oxygen species (ROS) respectively, leading to irreparable cell damage and hence cell death:



Notably, the PS itself is not changed by this process, it merely acts as an “energy relay” to absorb light and transfer energy, therefore the PS can be used in many cycles of light absorption.

PDT is used around the world to treat a range of ailments from acne[4, 5] to age-related macular degeneration[6] as well as in treatment of a subset of cancers[7], often in combination with other types of treatment.

Light therapy is believed to have been employed since ancient times, an example being the treatment of vitiligo using plants containing furocoumarin (psoralen) in India and Egypt[8, 9]. Modern investigations into phototherapy were initiated in the late 19th century by Niels Finsen[10] who used a carbon arc-lamp to treat a condition called *lupus vulgaris*. This revolutionary approach to the treatment of diseases led to Finsen being awarded a Nobel Prize in Physiology and Medicine in 1903[11].

The use of light treatment in combination with photosensitising agents was demonstrated by Raab in 1900[12]: in their studies, dyes were added to single-cell organisms, paramecia, in which, following light treatment, a loss of motion and cell death were observed. Around the same time a physician J. Prime, whilst treating patients for epilepsy with eosin, noticed the side effect of sunlight inducible dermatitis[13, 14]. Inspired by these studies, von Trappeiner started treating skin cancer lesions with eosin and light[11]. The need for oxygen in addition to drug and light was demonstrated by von Trappeiner and Jodlbauer who, in 1907, coined the term ‘photodynamic activation’[14, 15].

In 1913, Meyer-Betz self-administered hematoporphyrin and subsequently experienced a high level of light sensitivity with high levels of swelling in areas exposed to sunlight which lasted for months,[12, 16] adding further evidence to the possibility of photochemical sensitization. In the decades that followed, it was noted that porphyrins show preferential tumour uptake compared to healthy tissue[14, 17], and that the hematoporphyrin derivative, HPD, was particularly tumour specific[9]. This information, coupled with the observations that photosensitization of human tissue occurs with porphyrin type molecules (Figure 2a), led to their investigation for use in light activated therapy and ultimately to the renaissance in photodynamic therapy, which started in the 1970s[16, 18, 19]. The first PS approved for clinical use in the treatment of cancer was Photofrin, for use in bladder cancer in 1993 (Fig. 2b).

1.2 Light delivery to the photosensitiser: one vs. two photons

As mentioned above, light activation is required to populate an excited state of the photosensitiser, PS*, with subsequent interaction of PS* with cellular O₂ leading to the production of ¹O₂ and/or ROS[20]. If one considers a solution model whereby bimolecular

reaction between PS* and O₂ is diffusion-limited, an estimation of the time required for the reaction could be made on the basis of Stern-Volmer equation:

$$\tau_0/\tau = 1+k_{\text{diff}}\tau_0[\text{O}_2],$$

where τ_0 and τ are excited state lifetimes of PS* without and with O₂ respectively; and k_{diff} is the rate constant of a diffusion-limited reaction. Assuming that k_{diff} in water is equal to $2 \times 10^9 \text{ M}^{-1}\text{s}^{-1}$, and that [O₂] in water is 0.2mM; in order for the 50% of PS* to interact with O₂, the τ_0 should be of the order of $1/(k_{\text{diff}}[\text{O}_2])$, $2.5 \times 10^{-6} \text{ s}$. Of course, this estimate does not take into account the presence of O₂ in the first coordination sphere of the PS*, any specific interactions, or any additional mechanisms of energy transport etc., and is given here purely to highlight the order of the timescales involved. Given the above, molecules which readily populate a long lived excited state (ideally, microseconds) are sought after as photosensitisers in PDT[21].

For the majority of molecules, the “ground”, lowest energy electronic state, is a singlet state (S₀). Light absorption leads to initial population of a singlet excited state (S₁) which can deactivate to the ground state in a spin-allowed process that usually occurs on the timescale of nanoseconds. Singlet excited states can also undergo intersystem crossing (ISC), leading to population of a triplet excited state (T₁). The transition T₁ → S₀ is spin-forbidden, hence the lifetime of a triplet excited state is usually microseconds or longer. The long-lived triplet state (T₁, also sometimes noted as ³PS*) can therefore be efficient in interactions with cellular oxygen (Figure 3). However, as S₁ → T₁ transition is also spin-forbidden, it is not competitive with the spin-allowed, fast, deactivation of S₁ to S₀. In order to populate the T₁ state with some meaningful yield, significant spin-orbit coupling (SOC) which promotes interactions of singlet and triplet excited state manifolds is required. Organic molecules usually have weak spin-orbit coupling, and consequently low yields of triplet states. Introduction of a heavy atom, such as a metal centre, dramatically increases spin-orbit coupling, and promotes the population of long-lived triplet excited states – making transition metal complexes potentially efficient PS in PDT.

The wavelength of PS activation is one of the most important considerations in the selection of a PS. Absorption of light between 700 nm and 1100 nm, in the spectral range of relative tissue transparency is important as it allows for more diverse clinical applications, especially when deeper penetration into tissues is required. Traditionally, PS activation has been achieved by one-photon excitation with red/NIR absorbing molecules being especially sought after. Recently, with the advent of multiphoton lasers and light delivery technologies, two-photon activation in PDT is being explored as a possible future treatment modality. In two-photon excitation, absorption of two photons of NIR light leads to the same excited state

as would normally be populated by absorption of one photon of around twice the energy. As such, a PS that absorbs at 350 nm can be activated by 2 x ~700 nm photons. The potential advantages of two-photon excitation (TPE) are that PS which absorb in the UV/Vis region of the spectrum can be used, that intracellular components are not affected by NIR light as they have negligible two-photon absorption (TPA) cross-section in this region, and that the depth of light penetration is much greater[22]. However, TPE imposes further requirements on the photosensitiser – exceptional photostability and high two-photon absorption cross-section.

Current limitations in the development of two-photon PDT include the lack of optical technology for light delivery which would be sufficiently robust for clinical application, and the relatively small excitation volumes currently achievable in the lab. However, recent advances in pulsed fibre-optic lasers, which have been used for light delivery in in-vivo multiphoton microscopy, including that on human volunteers, create exciting possibilities of two-photon PDT developing into a practical approach to treatment[23].

1.3 General requirements of a PS for PDT

While the clinical requirements for a PS can vary dependent on disease type and site, there are some general characteristics usually sought after [24] [21] [16] in type I and II PDT. These include (but are not limited to):

- (i) A long-lived electronic excited state PS* which is capable of energy or electron transfer to O₂, leading to production of ¹O₂ and/or other ROS.
- (ii) Minimal cytotoxicity or biological function of the non-irradiated form of the PS and any products of its metabolic breakdown. This requirement differentiates PDT agents from other chemotherapeutics, and is key to a potentially dramatic reduction in side effects.
- (iii) Accumulation of PS in cells with, ideally, either preferential uptake, and/or higher retention rates in diseased tissue vs. healthy tissue.
- (iv) Targeted subcellular localisation, since reactive oxygen species will cause damage in the immediate vicinity of the PS.[25]
- (v) Absorption of light in the range of relative tissue transparency, 700 – 1100 nm, to increase penetration depth and allow for treatment of a deeper tumours.
- (vi) Chemical and photochemical stability.
- (vii) Prompt PS clearance from the body, most importantly from the cutaneous and ocular tissues, to reduce the risk of long-term photosensitivity.

Whilst presently available clinical PS have proven beneficial in certain types of diseases, a number of current limitations need to be addressed in the design of next generations of PDT agents to widen clinical applications of the method. Absorption in the visible range which limits the depth of tissue penetration, is one of the general limitations of the currently approved PS. Side effects present another problem - for example, the most widely used PS Photofrin, applied with much success in palliative lung and oesophageal cancer among others, causes a side effect of prolonged light sensitivity. From the implementation perspective, the cost of the PS[26] also plays a role.

The need for the therapies with reduced side effects, and for therapies operating under red light, has sparked the design of new generations of PS beyond the originally developed heterocyclic ring structures, and the design of new ways of light delivery to PS, such as two-photon excitation, or the use of upconverting nanoparticles.

1.4 Transition Metal Complexes in Photodynamic Therapy

Following the success of cisplatin in treatments, many other TM complexes started to be explored as anticancer agents[27] in various treatments including PDT. Accordingly, the last decade has seen dramatic expansion in the use of TM complexes as photosensitisers for photodynamic therapy – with the first TM PS, a Ru(II) complex known as “TLD1433” (see below) entering clinical trials in early 2017[28, 29].

The reason for the growing interest in TM complexes is that they meet several essential requirements for a PDT photosensitiser. Such complexes typically absorb light efficiently in the visible region in a one-photon absorption process, whilst often possessing high two-photon absorption cross-section in the NIR region. The presence of a heavy atom promotes spin-orbit coupling leading to ultrafast (usually < 1 ps) and efficient (often close to 100%) population of triplet excited states[30, 31][32][33]. The high yield of triplet excited states leads to generally high yields of singlet oxygen generation. On the other hand, long emission lifetimes make TM complexes sensitive to the intracellular microenvironment – thus potentially offering combined “see and cure” agents. Contrary to the majority of coloured organic compounds, TM complexes are usually photostable (i.e., do not photobleach[33]) under prolonged one- and two-photon illumination, which would allow the prolonged recycling of the PS and hence an overall reduction in the PS dose required. Added to these attractive photo-physical properties is the relative ease with which TM complexes can be synthesised, where several ligands and metal

centres can be combined in an almost combinatorial fashion, offering an opportunity to tune their photophysical properties as required.

The present review does not embark on the impossible task of comprehensive coverage of the field of “transition metal complexes as photosensitisers”, but rather aims to highlight a few of the most recent examples in this area. Common challenges for developing new PS include achieving specific targeting of subcellular structures; high water solubility; intense absorption in visible-NIR regions; possibility of one- and two-photon activation; and understanding of the mechanisms which lead to photoinduced cell death. With these challenges in mind, a number of complexes of Ru(II), Os(II), Ir(III), Pt, and Re(I) proposed as potential PS are discussed. Selected photosensitisers along with their photoactive index (PI, = $LD_{50}(\text{dark})/LD_{50}(\text{light})$), the wavelength of irradiation, the light dose used, and the mechanism of action where known, are summarised in Table 1. The PI normalised by the light dose used, PI/dose, is also discussed.

It is important to emphasize that the data obtained in different laboratories are extremely difficult to compare. This difficulty arises due to a great diversity of the light sources used – continuous wave lasers vs. pulsed lasers, LEDs, broad-band sources, broad-band sources with filters (selecting, e.g., a 10-nm band), broadband sources with cut-off filters, etc.

Consequently, light doses administered are equally hard to compare – it is not possible to estimate the amount of light absorbed by the photosensitiser in live cells, neither is it possible to directly compare power densities applied in different experiments. In an attempt to compare the results from different laboratories, a ratio of photoindex PI to the light dose is given in Table 1. It is interesting to note that whilst high PIs are often reported, the ratio of PI/dose ($J\text{ cm}^{-2}$) is generally low, with only few exceptions noted in Table 1 showing PI/dose > 100. The above applies to one-photon activated photosensitisers. The ways to compare the efficiencies of photosensitisers activated by one-photon vs. two-photon excitation *in vivo* are yet to be fully developed.

The review classifies the photosensitisers by the central metal atom, and where possible, sub-classifies according to the ligands used, the mode of excitation, subcellular targeting strategy, and dual-action agents where photosensitisation is combined with another mode of treatment.

2. Ruthenium (II) complexes in photodynamic therapy

Ru(II) complexes have been the most extensively studied transition metal complexes in relation to PDT. Detailed reviews by Gasser *et al.*[34] and Turro *et al.*[35] describe state of the field up to 2015, with recent progress reviewed in[36, 37]. Notably, the first clinical trials of a TM complex in PDT – a Ru(II)-based agent, **TLD1433**, developed in McFarland's and Lilge's laboratories (Figure 4)[28, 29, 38] for use in non-muscle-invasive bladder cancer with intravesical application, started in early 2017.

2.1. Ru(II) diimine complexes in two-photon activation

Since current clinically approved PS possess low two-photon absorption cross-sections, new PS with high TPA are required to realise what could potentially be a powerful new approach in PDT. The high two-photon absorption cross-section is often associated with the presence of an extended conjugated system. Accordingly, a number of Ru(II) complexes with extended organic ligands have been investigated for use as PS under two-photon excitation (TPE PS). Chao *et al.* reported a series of four mitochondria targeting Ru(II) polypyridyl complexes as potential TPE PS (Figure 4)[39] **1-4** which have strong absorption at around 460 nm due to MLCT transitions, low dark toxicity ($LD_{50} > 100 \mu M$), and high yields of 1O_2 production ($\Phi_{\Delta} = 0.74 - 0.81$). All four compounds partially localise to mitochondria in HeLa cells (64.8% - 70.1 % by ICP MS), with **4** showing a higher affinity of 85.3 % by Pearson's correlation coefficient of $R = 0.88$ against MitoTracker Green. The addition of $-P(Ph)_3$ group increased the TPA cross-section in the region 800 nm – 830 nm, with the values of 124, 155, 170 and 198 GM for **1-4** respectively. Light-induced PS activity in cell monolayers under CW light (450 nm, 20 mW cm^{-2} , 10 min) occurred with a PI of >28 for **4**. Photosensitization in multicellular spheroids was shown under CW activation and under multiphoton activation (Ti:Sapp laser, 800 – 830 nm, 100 mW, 80 MHz, 100 fs, 3 min). A high PI of >52 for **4** was observed under multiphoton activation compared to CW activation, showing the potential of **4** for TPE PDT. Pursuing the aim to reduce dark toxicity, a series of Ru(II) complexes **5 – 7** based on a $[Ru(bpy)_3]^{2+}$ core was designed by Gasser and Chao (Figure 4)[40] to avoid localisation to the nucleus and mitochondria. The compounds carry high positive charge (8+) and tertiary ammonium groups in order to increase binding affinity of the complexes to negatively charged cell membranes and induce cellular internalisation through an engulfing mechanism. This strategy has proved successful: compounds **5-7** localised to the lysosomes in HeLa cells (confirmed by ICP-MS, **5** has a correlation coefficient of 0.85 with LysoTracker Green); the cellular uptake pathway was energy dependent endocytosis. Φ_{Δ} of 0.92 – 0.99 in methanol and

0.49 – 0.67 in D₂O, and a virtual lack of dark toxicity (LD₅₀ > 300 μM) further supported the potential of **5 - 7** for PDT. Continuous irradiation of cells incubated with **5 - 7** with 450 nm (10 J cm⁻²) light led to PS activity with a maximum PI for the series being 313 (for **5**); the mode of cell death was determined to be necrosis with spill of the cytoplasm into the extracellular matrix observed post light treatment. The introduction of pendant ammonium groups increased the TPA cross-sections of **5 - 7** to 185 – 250 GM compared to 66 GM for the [Ru(bpy)₃]²⁺ core, which enabled TPE induced photosensitisation in multicellular spheroids, leading to cell killing at low light doses (800 nm, 10 J cm⁻²). High light-induced activity and exceptionally low dark toxicity make Ru(II) complex **5** a highly promising candidate for two-photon activated photosensitisation of PDT.

Ru(II) complexes of a well-known intercalating ligand dppz, [Ru(phen)₂dppz]²⁺, with various functional groups on the dppz have also been explored for one- and two-photon activated PDT (**8** and **9**, Figure 4).[41] The one-photon absorption spectra of **8** and **9** show MLCT transitions in the range 400-500 nm, typical for Ru(II) complexes; the TPA cross-section values were 145 and 93 GM, and Φ_Δ values of 0.75 and 0.54 for **8** and **9** respectively. Compound **8** had more suitable properties than **9** for photosensitisation: **8** was stable in human plasma whilst only 19% of **9** survived a 48-hour incubation, and **8** accumulated in cytoplasm and nucleus whilst **9** had high affinity to membrane binding. Accordingly, multicellular tumour spheroids were stained throughout with **8**, while **9** was only able to penetrate the outer layer. The increase in cellular uptake of **8** vs. **9** was accompanied by the higher PS effect of **8** resulting in a higher, though still modest, value of the PI of 11.7 for **8** vs. 5.9 for **9**.

2.2 Dual action Ru(II) photosensitisers

One emerging avenue of research is to design photosensitisers which have an additional therapeutic effect, a “dual agent”. In pursuit of such combined therapies, Ru(II) complexes in conjunction with single-walled carbon nanotubes (SWCN) have been explored for photo-thermal therapy (**10** and **11**, Figure 5)[42] as carbon nanotubes are known to convert NIR light (in this case, 808 nm, 0.25 W cm⁻²) to heat. Carbon nanotubes acted both as photo-thermal therapy agents, and as a delivery vehicle of the Ru(II) complexes. Both **10** and **11** possess high two photon absorption cross-sections (494 GM and 428 GM respectively), and considerable yield of ¹O₂ upon excitation with blue light (405 nm, Φ_Δ = 0.30 – 0.35) in D₂O as determined by both a direct and indirect method; a fluorescent ¹O₂ assay (indirect method) showed ¹O₂ production in HeLa cells upon TPE (808 nm, 0.25 W cm⁻²) with **10** and **11**. The photothermal conversion efficiency of the SWCN loaded with ruthenium complexes was found to be 40%,

higher than that of the tubes alone, and led to temperature increases of 36-38 °C said to be sufficient for cancer photo-thermal therapy. Alongside this temperature increase, Ru(II) complexes were released upon excitation (808 nm, 0.25 W cm⁻²), and then acted as TPE PS under 808 nm excitation. The release of **10** and **11** from the nanotubes in cells was shown by multiphoton imaging under conditions when only free **10** and **11** are luminescent. Upon initial imaging of SWCN/Ru(II) incubated cells, no emission is observed; however, following irradiation with 808 nm light, red emission was detected in the lysosomes. The lysosomal localisation (confirmed by co-localisation with LysoTracker green), indicated endocytotic uptake of the **10**- and **11**-loaded carbon nanotubes. The carbon nanotubes alone, Ru(II) complexes alone, and loaded nanotubes showed limited dark toxicity (up to 200 µg/mL). The complexes and carbon nanotube alone caused photo-activated cell death, but the combined treatment led to dramatic reduction in cell viability. The results obtained in cell lines were also confirmed in multicellular spheroids and an *in vivo* mouse model. This study was the first example of combined photo-thermal therapy with transition metal complexes and TPE PDT, the idea that light of the same wavelength, 808 nm, causes both a photo-triggered release of the PS and its two-photon activation is particularly elegant.

Many Ru(II) complexes have been reported to induce DNA damage under irradiation. Gasser, Ferrari *et al.* explored in detail how a nuclear-localised, DNA binding molecule can be used for PDT using an example of a new Ru(II) polypyridyl complex (Figure 6)^[43]. It was shown that **12** generates ¹O₂, causes photoinduced DNA damage with UV-A irradiation (350 nm 2.58 J cm⁻²)^[44] and shows a dose dependant increase in photoinduced nicks in plasmid DNA. Through LC-MS it was shown that guanoside can be photooxidised by **12** indicating a likely source of DNA photodamage. Modest PS activity was observed in all cell lines tested with low light dose (UV-A, 1.29 J cm⁻²). Nuclear localisation of **12** was confirmed in a variety of cell lines (HeLa, U2OS, MCF7 and CAL33 cancer cell lines) with ICP-MS indicating 55% nuclear accumulation in U2OS cells. Both COMET and pulse-field gel electrophoresis indicated intracellular photo-induced DNA double strand breaks with **12** under UV-A irradiation. Importantly, cell cycle arrest studies allowed the authors to confirm guanine oxidation taking place in cells. It was determined that severe DNA damage is the likely trigger of cell death; the 3.6-fold increase in PS activity in mitotic cells compared to non-synchronised cells is ascribed to less efficient photosensitisation in condensed DNA.

2.3. Examples of Ru(II) Photosensitisers other than Ru(II) diimine complexes

Whilst Ru(II) complexes bearing exclusively polypyridyl ligands are most commonly investigated, other Ru(II)-sensitisers have started being explored as well. A few examples of such Ru(II)-based potential PS are given in this section – namely, complexes with cyclometallating ligands, macrocycles, and protein conjugates.

Ru(II) complexes with cyclometallating ligands, $[\text{Ru}(\text{NN})_2(\text{C}^{\wedge}\text{N})]^+$, are an example of such potential photosensitisers. McFarland *et al.* investigated the effect of expansion of the π -system of cyclometallating ligands of Ru(II) complexes (**13** – **20**, Figure 6)[45] on the PS properties of such compounds. The expansion of $\text{C}^{\wedge}\text{N}$ ligands in compounds **13** – **16** was shown to drastically alter the interaction of the compounds with cells. **13** – **15** showed high levels of dark toxicity with limited light activation, whilst **16** can be considered non-toxic in the dark ($\text{LD}_{50} > 300 \mu\text{M}$) whilst exhibiting high levels of PS activity ($\text{PI} > 1400$ in SK-MEL-28 cells) albeit at high light dose (visible light, 100 J cm^{-2}). This high PS activity occurs despite the very low Φ_{Δ} of 0.0056, whilst $\text{O}_2^{\cdot-}$ was suggested to be the ROS formed.

A self-assembled metallomacrocycle (**21**), alongside its mononuclear building block (**22**), was shown to induce photoactivated killing of cancer cells (Figure 7)[46]. Φ_{Δ} values of 0.54 and 0.75 were found for **22** and **21** respectively, and oxygen depended photo-cleavage of DNA was shown with supercoiled plasmid DNA. Both compounds showed photo-induced toxicity with the PI of **22** ($206, 48 \text{ J cm}^{-2}$) being somewhat higher than that of **21**.

A HSA protein-Ru(II) conjugate was designed as a mitochondrial targeting PS (Figure 7)[47], where the blood plasma protein HSA was chosen with the aim of producing a treatment for acute myeloid leukaemia, and triphenylphosphine (TPP) groups were introduced to achieve mitochondrial targeting. Conjugation of the Ru(II) complex to HSA had no effect on its light absorption characteristics, but induced a 8-fold increase in the yield of photo-induced $^1\text{O}_2$ production ($\lambda_{\text{exc}} 470 \text{ nm}$) compared to the unconjugated Ru(II)-complex. Clear localisation to the mitochondria was observed in HeLa cells, with a relatively high PI of 220 ($\lambda_{\text{exc}} 470 \text{ nm}$, $\sim 6 \text{ J cm}^{-2}$) when considering the protein concentration and an estimated 10 Ru(II) complexes per protein. An analogue conjugate without the mitochondria targeting TPP groups was somewhat less photosensitising ($\text{PI} = 75$) indicating the importance of subcellular localisation.

The two-photon absorption cross-section of the conjugate was 5-fold greater than that of the Ru(II) complex alone, making TPE PDT a potential future avenue for protein-PS conjugates.

3. Iridium(III) complexes as photosensitisers

The use of Ir(III) complexes for PDT is in its infancy.[48] Multiple papers have reported cyclometalated Ir(III) complexes as efficient photosensitisers of $^1\text{O}_2$ [48-51] [52] and as cellular imaging agents.[53-61] The emission characteristics of Ir(III) complexes are dependent on the environment, indicating their potential use as pH [62] and hypoxia[63] sensing agents[61] as well as DNA binding agents[64].

The cellular uptake of Ir(III) complexes was demonstrated in 2008 with the example of two cationic complexes, a green emitter $[\text{Ir}(\text{dfpy})_2(\text{bpy})]^+\text{PF}_6^-$ (**25**) and a red emitter $[\text{Ir}(\text{dfpy})_2(\text{quqo})]^+\text{PF}_6^-$ (**26**) [dfpy = 2-(2,4-difluorophenyl)pyridine] (Figure 8)[65] which were seen to accumulate in the cytoplasm of cells. The high photostability of the compounds in the cellular environment in comparison with the ubiquitous nucleic acid stain DAPI make them promising as imaging agents. The compounds caused limited reduction in cell viability at concentrations up to 100 μM , and were therefore deemed non-toxic.

Following this first example, numerous Ir(III) compounds were investigated as imaging agents[33, 54, 57, 66-68]. Of particular note is a paper by Li *et al.* in 2010 demonstrating the ease by which colour tuning from blue to NIR [56] could be achieved in a series of six cationic complexes, $[\text{Ir}(\text{dfpy})_2(\text{N}^{\wedge}\text{N})]^+$ (**27–31**; dfpy = 2-(2,4-difluorophenyl)pyridine, $\text{N}^{\wedge}\text{N}$ = py, bpy, pyp, bq or quqo) and $[\text{Ir}(\text{piq})_2(\text{quq})]^+\text{PF}_6^-$ **32** (piq = 2-phenylisoquinoline), Figure 8. The difference in the emission properties were attributed to different contributions from $^3\text{MLCT}$ and ^3LC to the emissive state. The cellular uptake of the compounds with cytoplasmic localisation was shown by confocal microscopy. Limited dark cytotoxicity up to 100 μM in all compounds was shown following 24 hour incubations of MCF-7 and HCT-8 cells.

3.1. Dual action Ir(III) Photosensitisers

The first example of photosensitized killing of live cells by Ir(III) compounds (**39 – 41**), Figure 9)[69] was reported in 2012. The compounds, Ir(III) metallo-pyridocarbazoles, were designed as protein kinase inhibitors to be used as dual antiangiogenic and photosensitizing agents.

Compounds **39** – **41** were phototoxic at 1 μM under light of $> 450\text{ nm}$, **41b** caused significant apoptosis, and demonstrated a PI of 34.35. The mechanism of action was suggested to be type III with photo-induced ligand substitution by cellular Cl^- leading to photo-induced labilization of the selenocyanate ligand ($^-\text{SeCN}$). However, the separately prepared proposed photo-substitution product, **41a**, showed no dark cytotoxicity, and it therefore remains unclear if the selenocyanate ligand would cause the apoptotic death of the cells. The compound **41b** retains antiangiogenic action, whilst its methylated derivative shows no protein kinase inhibition. In human umbilical vein endothelial cells (HUVEC) which highly express vascular endothelial growth factor receptor kinases (VEGFR), known to be inhibited by **41b**[70] but not the methylated analogue, 24 hour incubation with **41b** (5 μM) caused apoptotic cell death whilst the methylated analogue did not. Photo-induced toxicity to HeLa cells was demonstrated by **41b**, showing its potential as a dual therapeutic agent.

Another example of dual-action agents is a series of Ir(III) complexes $\text{Ir}(\text{C}^{\wedge}\text{N})_2\text{L}](\text{PF}_6)$ ($\text{L} = N^1$ -hydroxy- N^8 -(1,10-phenanthroline-5-yl)octanediamide) **42** - **45**, Figure 10,[71] designed to combine histone deacetylase (HDAC) inhibition with photosensitization. HDACs regulate the histone modification by catalysing the removal of acetyl groups from histones, in this way they can alter gene expression patterns often associated with cancer,[71] thus HDACs are indicated as anticancer drugs with at least two approved by the FDA[72]. One such HDAC is suberanilohydroxamic acid, SAHA. SAHA was incorporated into a phenanthroline ligand for all compounds **42** – **45**. The Φ_{Δ} values for **42** – **45** ($\lambda_{\text{exc}} 425\text{ nm}$) range from 0.21 – 0.75 in ascending order **44**<**43**<**42**<**45**. All compounds localised to the cytoplasm, and showed phototoxicity with UV ($\lambda_{\text{exc}} 365\text{ nm}$, 3.6 J cm^{-2}) and blue excitation ($\lambda_{\text{exc}} 425\text{ nm}$, 7.2 J cm^{-2}) resulting in PIs in the range 2.7 – 18.9. All compounds retained HDAC inhibitory function, with **43** showing a higher inhibitory effect than SAHA. Compound **42** exhibited the strongest photodynamic response in HeLa cells under 365 nm irradiation. Histone H3 acetylation levels, indicative of HDAC inhibition, were higher with **42** and light in comparison with **42** in the dark, indicating that HDAC inhibition was enhanced upon irradiation. Apoptosis levels increased in a dose dependent manner with **42** in the dark whilst light treatment greatly increased the levels as demonstrated by Annexin-V binding and caspase-3/7 activation. Mirroring these results, cellular ROS concentration increased and mitochondrial membrane potential (MMP) decreased in a dose dependent manner in the dark, whilst light treatment

caused a 5-fold increase in ROS levels and a marked drop in MMP. This study demonstrated the promise of HDAC inhibitors incorporated into Ir(III) photosensitizers as dual-action drugs.

3.2. Two-photon activated Ir(III) Photosensitizers

The first example of TPE PS with Ir(III) complexes was demonstrated using a compound $[\text{Ir}(\text{ppy})_2(\text{phen})]\text{Cl}$, **46** (Figure 11, $\Phi_{\Delta} = 0.036$ in H_2O).^[73] 24-hour incubation of live cells with **46** (up to $10 \mu\text{M}$) did not result in visible differences in cell morphology. However, when incubation was followed by irradiation with 800 nm light (30 min, 2.4 mW, 80 MHz), an assessment by eye 150 min later led to the clear, albeit qualitative, conclusion that the compound was phototoxic to cells.

The next report of Ir(III) TPE killing of cells used a cyclometallated fluorenyl Ir(III) complex **47** (Figure 11)^[74], analogous to a Ru(II) compound previously reported by the same group^[75]. The close match of one and two-photon excitation spectra indicated that the same excited states are accessed in both cases, with TPA up to 80 GM in the range 700 – 800 nm. The TPE cell damage effect of the compound was shown in a G6 Glioma cell line, change in morphology of the cells was used to determine cell death. The compound ($1 \mu\text{M}$) and light (740 nm, 220 J cm^{-2}) caused morphological change while light alone did not.

In mid-2016, Lim *et al.* reported a series of Ir(III) compounds as PS (**48** – **51**, Figure 11),^[76] these showed some phototoxicity under one-photon excitation (PI 5.64, albeit with a low light dose - sunlight, estimated as 1 J cm^{-2}). Complex **50** was also phototoxic under two-photon excitation; demonstrated in a single cell at high Ir(III) concentrations ($20 \mu\text{M}$). The cell death mechanism was confirmed to involve the ROS and $^1\text{O}_2$ production in cells under these conditions.

Recently, our groups in collaboration with others, demonstrated that representative of $[\text{Ir}(\text{N}^{\wedge}\text{C})_2(\text{N}^{\wedge}\text{N})]^+$ family of cyclometallated Ir(III) complexes **52** and **53** (Figure 11)^[77] are efficient PS under one photon activation. Furthermore, compound **52** proved to be efficient in two-photon activated cell killing. This study was the first example of TPE PS demonstrated on cell monolayers with an Ir(III) complex. The compounds have appreciable Φ_{Δ} of 0.42 and 0.40 for **52** and **53** respectively. Rapid uptake in HeLa cells was seen for both compounds. Importantly, **52** was virtually non-toxic in the dark up to $100 \mu\text{M}$ concentration (highest concentration tested) while its N-methylated analogue **53** was somewhat more toxic with an LD_{50} of $6.5 \mu\text{M}$. The localisation of **52** changed over time, from mitochondrial (< 4 hrs incubation) to lysosomal at the 24-hr time point, potentially indicating the trafficking of **52** out

of cells. Compound **52** was shown to be an efficient PS under low dose violet light (3.6 J cm^{-2} , 405 nm) in a number of cell lines, with a maximum PI of >555 demonstrated in U2OS cells (osteosarcoma). Apoptosis and ROS production in cells post light treatment were confirmed in HeLa cells. The potential use of the compound in TPE PDT is demonstrated by a relatively high σ_2 of 112 GM at 760 nm and TPE mediated PS of cells was demonstrated on HeLa monolayers by Annexin V and PI staining.

The studies above were concerned with molecular photosensitisers, or their covalent conjugates to specific functional groups. A different approach was reported by Chao *et al.* who designed a series of Ir(III) complexes **54** – **56**, that showed aggregation induced emission (AIE) and associated TPE PS activity (Figure 12)[78]. The hypothesis was that the compounds are non-emissive at low concentrations due to quenching of the excited state by the rotation of the fluorogen group in solution, whilst at increased concentration aggregation prevents the rotation, inhibits this route of excited state quenching, and restores the emission. For **54** – **56** only weak emission was observed (yield 0.001) in DMSO solution, this increased upon addition of water and reached maximum intensity at 90% (v/v) water/DMSO ratio (yield 0.044). Aggregation of the complexes in the 90/10 water/DMSO solution was confirmed by dynamic light scattering, indicating nanoaggregates of 88.99 – 250.09 nm. Φ_{Δ} were also reported to be highest at 90/10 water/DMSO; **54** demonstrated a greater consumption rate of DPBF ($^1\text{O}_2$ scavenger) than the standard used (H_2TPP , $\Phi_{\Delta} = 0.70$ in toluene). **54** was found to have a high TPA of 214 GM at 730 nm. Compound **54** which is more lipophilic than **55** and **56** ($\log P_{o/w} = 1.42$, 1.06 and 0.77 respectively) was shown by ICP-MS to accumulate in the mitochondria ($>80\%$ of accumulated compound) of HeLa and L02 (human hepatic) cells. Lower uptake was observed in the normal cell line and was ascribed to the higher membrane potential of cancer cells. **54** was shown to enter cells via an endocytic pathway. The dark and light (405 nm , 40 mW cm^{-2} , 12 J cm^{-2}) toxicity of the compounds in HeLa and L02 cell lines showed similar dark toxicities (dark- $\text{LD}_{50} = 29.2 - 30.3 \text{ }\mu\text{M}$ and $32.2 - 34.0 \text{ }\mu\text{M}$ for HeLa and L02 respectively) but higher light toxicity in HeLa cells leading to higher PI of **54** in HeLa cells (PI = 75 and 14 for HeLa and L02 cells respectively). A number of measurements indicated that the mitochondrial oxidative phosphorylation pathway is impaired post PS treatment, which, along with the observed activation of caspase-3/7 post light treatment likely indicates apoptotic cell death. The ROS production in cells and PS activity with TPE (730 nm , 0.88 W cm^{-2} , 50 s, 12 J cm^{-2}) shown for

54 indicate the potential use of the compounds for TPE PDT. This was supported by the studies of multicellular spheroids (light-LD₅₀ = 0.35 μM, PI = 100).

In early 2017, a series of organelle specific Ir(III) terpyridine complexes for TPE PDT, (**57-61**, Figure 12)[79] with one-photon absorption in the range 350 nm to 520 nm, and maximum σ_2 values of 60 – 110 GM at around 800 nm were reported. Compound **57** localized to the nucleus, while **58 - 61** localized to the mitochondria in HepG2 (human liver cancer) cells. Inhibition assays showed that **57** entered cells through microtubule-dependent endocytosis, whilst the uptake of **58**, used as a representative of all non-nuclear PS, was partially inhibited by a number of inhibitors, indicating a mixed mode of uptake. By analysis of cell morphology, and annexin V / propidium iodide staining, it was determined that the nuclear localizing **57** caused drastic morphology changes in cells following TPE (800 nm) while, despite their similar ¹O₂ sensitizing capabilities, the mitochondrial targeting **58** did not. TEM imaging of cells treated with **57** and TPE (800 nm, 30 s, 30 min intervals, 2 hrs) showed cells containing multiple vacuoles, indicative of induction of apoptosis. DNA cleavage post light treatment was shown in supercoiled DNA incubated with **57**.

3.3. Subcellular targeting with Ir(III) photosensitisers

As with all PS, disease-specific uptake and intracellular targeting are aims of molecular design of Ir(III) PS.

Zhang *et al.* reported two fructose containing Ir(III) polypyridine complexes alongside their fructose free analogues in 2013 (Figure 13)[80]. This work exploits the fact that highly prolific cells require more energy and hence overexpress glucose transporters (GLUTs). Therefore, incorporation of sugar molecules may allow for increased uptake in neoplastic cells. Whilst an exciting prospect, the results with these particular complexes indicated that the fructose containing compounds showed lower cellular uptake than their fructose-free counterparts – the result was ascribed to the increased hydrophilicity imparted by the sugar molecule, as cellular uptake of TM complexes is often dependent on the level of lipophilicity of the complex[61, 81, 82]. Addition of unmodified fructose reduced the uptake of the fructose containing **64**, whilst **65** uptake was unaffected, indicating regulation of uptake of **65** by membrane bound fructose transporters. The compounds showed mitochondrial localisation, but displayed high dark toxicities and therefore light toxicities were not explored further.

Lo *et al.* developed this approach of targeted accumulation further. In one example, a series of compounds in which ligands were equipped with either ester groups, **66** and **67**, or carboxylate groups, **68** and **69**, displayed significant differences in cellular internalization (Figure 14)[83]. The complexes with ester groups were taken up by the cells readily via an energy dependent pathway and localised in mitochondria and endosomes, whilst the carboxylate compounds were not easily taken up by cells – the effect was ascribed to limited membrane permeability as confirmed by emission imaging which detected the compounds at the cell membrane. Compounds **66**, **68** and **69** showed low levels of dark toxicity ($LD_{50} > 200 \mu M$) whilst **67** was somewhat more toxic ($LD_{50} = 8.6 \pm 0.1 \mu M$). The carboxylate compounds showed no increase in toxicity upon light treatment, whilst both ester compounds demonstrated increased light toxicity with PI values of 11.56 and 17.2 for **66** and **67** respectively. The light dose is quoted as ‘irradiated at 365 nm with a 6 W UV-A lamp (Spectroline, USA) for 1 h’.

Two related Ir(III) complexes, **70** and **71** (Figure 15), which share the same central cyclometallated Ir(III) resulting in similar photophysical properties (Φ_{Δ} 0.17 and 0.21 for **70** and **71** respectively), showed different organelle specific subcellular localisation, mitochondrial and lysosomal one, resp. [84]. The intracellular localisation was confirmed by co-localisation with mitotracker green and LysoGreen for **70** and **71** respectively (Pearson’s correlation coefficients 0.85 and 0.91, respectively). Cellular uptake studies indicated an energy-dependent endocytosis pathway for the uptake. Hypoxic incubation with **70** and **71** altered the decrease in O_2 levels in the culture media compared to untreated cells. In complex treated cells an 18 % and 29% decrease in oxygen was observed after 15 min in the hypoxic environment in comparison a 44 % decrease was observed in untreated cells. This indicated that cellular respiration was decreased when cells were treated with either **70** or **71** with a less marked decrease in O_2 for the mitochondrial targeting **70** (18 % vs 29 %). Both compounds had low dark cytotoxicity in HeLa cells, however, under hypoxic conditions the mitochondrial localized PS had somewhat higher phototoxic activity than the lysosomal PS. The authors attributed this difference to the advantages of mitochondrial localisation in hypoxic conditions, although it could also be due to a higher effect of the mitochondria-localised PS.

3.4. pH sensitive Ir(III) photosensitisers

A number of pH sensitive Ir(III) complexes have been proposed as PS due to the potential of preferential localisation. A representative example, a pH-sensitive Ir(III) complex *fac*-

$\text{Ir}(\text{deatpy})_3$ (**73**, $\text{deatpy} = 2\text{-}(5'\text{-}N,N\text{-diethylamino-4'}\text{-tolyl})$ pyridine, Figure 15),[85] with a pK_a of 7, shows negligible emission at pH 7.4 but strong emission ($\lambda_{\text{em}} 497 \text{ nm}$) at $\text{pH} < 7$ attributed to a reversible formation of its protonated form, **72**. In HeLa-S3 cells **72** co-localised with LysoTracker indicating lysosomal localization, with passive uptake mechanism confirmed by uptake studies at 4°C . **72** was shown to result in production of $^1\text{O}_2$ upon excitation with 366 nm. Following prolonged excitation (30 min) at both 366 nm and 470 nm, cells incubated with $10 \mu\text{M}$ solution of **72** were shown to exhibit cell membrane swelling indicating cell death. Cell death at 366 nm was confirmed, and determined to be mainly necrotic, by Annexin and Propidium Iodide staining. Several related pH-responsive compounds were reported in 2013,[86] and later expanded to a series of pH-sensitive Ir(III) complexes which showed photoinduced toxicity[87].

A series of pH-responsive Ir(III) complexes showing clear lysosomal staining and a high PI of >833 (although at the high light dose of 36 J cm^{-2}) have been reported (**64 – 77**, Figure 15)[88]. One of the compounds was shown to have selectivity for cancer cells although, the authors state that the need to excite at 425 nm would limit its clinical application.

3.5.Red/NIR activated Ir(III) photosensitisers

A possible approach to efficient PDT under red/NIR light is to create a hybrid organic-inorganic agent, which would allow one to utilise the broad visible/NIR absorption of the organic fluorophore whilst retaining the ISC offered by the TM centre.

In realisation of this idea, four Ir(III) complexes were investigated, here bulky organic fluorophore mono/di-styryl BODIPY derivatives were attached to the coordination centre via an acetylide linker (**78 – 81**, Figure 16)[89]. This design allows π -conjugation across the molecule, so that following absorption of red light by the fluorophore, the resulting singlet excited state undergoes efficient ISC to the desired triplet excited states. Whilst the complex without BODIPY is characterised by relatively weak visible light absorption ($\epsilon 1.51 \times 10^4 \text{ M}^{-1} \text{ cm}^{-1}$ at 385 nm) and no NIR absorption, the BODIPY-Ir conjugates had strong absorption in the red region: **78** ($\epsilon 1.14 \times 10^5 \text{ M}^{-1} \text{ cm}^{-1}$ at 606 nm), **79** ($\epsilon 8.96 \times 10^4 \text{ M}^{-1} \text{ cm}^{-1}$ at 644 nm), **80** ($\epsilon 9.89 \times 10^4 \text{ M}^{-1} \text{ cm}^{-1}$ at 644 nm) and **81** ($\epsilon 7.98 \times 10^4 \text{ M}^{-1} \text{ cm}^{-1}$ at 729 nm). Fluorescence of **78 – 81** was weaker than in their non-coordinated BODIPY ligand counterparts indicating some interaction with the metal centre. Transient absorption studies established that the long-lived triplet excited states were localized on the styryl-BODIPY ligand rather than the coordination

centre; the lifetimes of the triplet excited states were determined to be in the range $\sim 156 \mu\text{s}$ to $31.4 \mu\text{s}$, where the decrease in the lifetime correlates with the decrease in the excited state energy. Φ_{Δ} varied dramatically between the compounds, from 0.53, 0.83 to 0.06 and 0.02 for **78** - **81**, respectively. **78** – **80** were shown by emission microscopy to accumulate in lung cancer cells, whilst **81** - the compound with the lowest yield of $^1\text{O}_2$ production, the shortest emission lifetime, but the longest absorption wavelength of $>700 \text{ nm}$ - did not permeate into cells. In the cell lines 1121 and LLC **78** was shown to have PIs of 3.8 and 1.32 and **79** PIs of 2.17 and 1.59 respectively. Whilst modest, and difficult to compare with other studies as the light doses were not specified, these PI values are rather remarkable for TM complexes with excitation at 635 nm.

Late 2016 saw the publication by McFarland, Sun *et al.* of a series of six Ir(III) complexes (**82** – **87**, Figure 17)[90]. The compounds were designed using the idea that extended diimine π -conjugation can increase the triplet state lifetimes in complexes containing diimine ligands with the ^3IL state slightly lower in energy than the $^3\text{MLCT}$ state for the complex [91]. This idea was previously shown to increase photosensitising activity of Ru(II) complexes,[92] as well as increasing the lifetime of charge-transfer triplet excited states in some cases [93, 94].

Accordingly, a series of complexes with extended π -conjugation of the diimine ligand (**82** – **84**) and the cyclometallating ligand (**85** – **87**) were designed. Complexes **85** – **87** had absorption band red shifted relative to **82** – **84**. The extension of the diimine π -conjugated system shown to affect the ground state absorption but not the triplet state emission energy, while extension of the π -conjugated system in the cyclometallating ligand was shown to affect both the ground state and the emitting triplet state. The extension of the cyclometallating π -conjugation visible absorption into the red/NIR was ascribed to a direct $\text{S}_0 - \text{T}_n$ transition via a $^3\pi, \pi^*/^3\text{CT}$ transition. The PS effects of **82** – **83** were tested in SK-MEL-28 (melanoma) and HL60 (leukaemia) cell lines under irradiation with broadband visible light (400-700 nm, 34.2 mW cm^{-2}) or red light (625 nm, 29.1 mW cm^{-2}) at a rather high light dose for both (100 J cm^{-2}). Compounds **82** – **86** were somewhat toxic in the dark to both cell lines ($\text{LD}_{50} \leq 2.11 \mu\text{M}$ and $\leq 4.51 \mu\text{M}$ for SK-MEL-28 and HL60 respectively) whilst **87** was significantly less toxic ($\text{LD}_{50} = 144 \mu\text{M}$ and $83.8 \mu\text{M}$). All compounds had PS activity in both cell lines with greater effect under visible light (PI = 22 – 407 and 12 – 143 for SK-MEL-28 and HL60 respectively) compared to red light (PI = 1.2 – 32 and 1.5 – 16 for SK-MEL-28 and HL60 respectively). A mixture of subcellular localisations was observed for the compounds, with **87** showing nuclear

staining in adherent cells and cytosolic staining in suspension. Irradiation of light to plasmid DNA in the presence of **87** was not found to induce strand breaks but to aggregate or condense the DNA. **87** showed the greatest promise in both cell lines at each wavelength with the greatest PI of 407 with visible light activation in SK-MEL-28; however, the light dose administered was high, 100 J cm⁻².

3.6. Other examples of Ir(III) photosensitisers

A series of cyclometalated Ir(III) polypyridine compounds incorporating polyethylene glycol (PEG) chains and their PEG free counterparts were investigated by Lo *et al.* (**88** – **97**, Figure 18)[95]. The PEG chains were added with the aim of increasing the water solubility of the Ir(III) complexes and reducing the dark cytotoxicity as the addition of PEG chains is often linked to reduced interaction of the complexes with biological entities such as DNA and proteins[66, 96]. The Φ_{Δ} for the compounds were in the range 0.24 - 0.79 (in aerated DMSO against the standard methylene blue) and generally increased across the series **88** < **92** and **93** < **97**. The PEG variants were found to be less lipophilic than their PEG-free counterparts, with ICP-MS indicating higher cellular uptake of the PEG free complexes. This is an interesting finding as it may indicate that PEG addition is not the best route for PS design. **90** localised to mitochondria (Pearson's correlation coefficient 0.909), as expected given the cationic and lipophilic nature of the compound. The low dark cytotoxicity of the PEG compounds (LD₅₀ > 300 μ M in all cases) is considerably lower than that of the PEG free compounds although this cumulative effect was, perhaps, to be expected due to lower cellular uptake imparted by incorporation of the PEG chains. The PEG containing compounds, except **92**, were phototoxic in HeLa cells with appreciable PI values in the range of >12.9 to >88.2, although the light dose appears likely to be large (365 nm, 30 min with a 6 W UV-A lamp) and may need to be optimised to become relevant to the clinic.

Incredibly high light toxicities (as low as LD₅₀ 0.00086 μ M, PI 3488 in A549R cells) have been demonstrated by mitochondria targeting complexes **98** – **100** (Figure 19),[97] whilst dark toxicity against a number of cell lines was remarkably low, in the range LD₅₀ 1.0 μ M - 17.3 μ M. This value is the highest PI of an Ir(III) compound reported. Interestingly, the PIs in HeLa cells were much lower (up to 49) and the light dose used was reasonably high (20 J cm⁻²) in the UV region (365 nm) which would severely limit the clinical application of the compounds. The lipophilicity of the compounds was found to correlate with both their uptake and photosensitizing efficiency of the compounds, a finding further supporting the link between

lipophilicity and intracellular uptake of small molecules. The compounds were shown to induce apoptosis by mitochondrial damage but cell cycle analysis indicated that the compounds were not genotoxic.

Maggioni *et al.* reported water soluble compounds **101** and its conjugate to a poly-(amidoamide) copolymer **102**, which localised in the perinuclear region, and induced apoptosis under Xe lamp illumination (Figure 19)[98]. The molecules of **102** self-assembled in water into spherical nano-aggregates of roughly ~30 nm diameter. Compared to the polymer conjugate **102**, compound **101** had twice as high Φ_{Δ} , and required much shorter incubation times to accumulate in cells (2 hr vs. 12 hr). It was also significantly more toxic in the dark, but showed higher photosensitizing activity with lower levels of necrosis.

A dinuclear Ir(III) complex containing a bridging boron-dipyrromethene (BODIPY) chromophore and its Ru(II) analogue were reported by Draper *et al.* (**103** and **104**, Figure 20)[99]. Both compounds absorbed strongly in the visible range (567 nm, ϵ 105713 dm³ mol⁻¹ cm⁻¹ and 570 nm, ϵ 113317 dm³ mol⁻¹ cm⁻¹) for the Ir(III) and Ru(II) complexes respectively, showed low dark toxicity (LD₅₀ = 300 μ M), considerable light toxicity (although their light toxicities were not determined quantitatively), and are therefore promising PDT agents.

Gasser, Chao, *et al.* reported Ir(III) and Ru(II) complexes bearing aromatic acid diimides as additional light absorbers (**105** and **106**, Figure 20)[100]. Both compounds were shown to sensitise production of ¹O₂ under at 420 nm irradiation through an indirect and direct detection method, although no signal could be measured for **105** by the direct method, perhaps due to the limits of the detection (detection limit Φ_{Δ} = 0.24) with Φ_{Δ} = 0.29 in CH₃CN by the indirect method. No Φ_{Δ} was observed for either compound under excitation at 575 nm. The PS effect of **105** and **106**, and associated ligands **107** and **108**, was tested in three cancer cell lines: A2780 and A2780R, cisplatin-sensitive and cisplatin-resistant ovarian epithelial cancer cell lines and HeLa. The two ligands showed no PS effect whilst both **105** and **106** showed photosensitization in all cell lines (λ_{exc} 420 nm, 9.27 J cm⁻²) with **106** showing higher PI in all cells (PI up to >23 in A2780 cells). The subcellular localisation of **105** and **106** was determined, by ICP-MS, to be nuclear for **105** and mainly mitochondrial for **106**; it was suggested that the higher dark toxicity of **105** may be imparted by the nuclear localisation with DNA interaction a possible source of the toxicity.

A series of 5 mitochondrial targeting PS for PDT of the general formula $[\text{Ir}(\text{ppy})_2(\text{L})]^+$ where L is a 2,2'-bisimidazole ligand equipped with varying length alkyl chains to alter the lipophilicity of the compounds, have been investigated (**109** – **113**, Figure 20)[101]. The Φ_{Δ} of the compounds were 0.17, 0.21, 0.28, 0.51 and 0.59 for **109** - **113** respectively. The octanol/water partition coefficients ($\text{Log } P_{o/w}$) indicated increasing lipophilicity with increasing chain length; **110** < **111** < **112** < **109** < **113** with the exception of the non-alkylated **109**. All complexes were readily taken up by HeLa cells and localised to the mitochondria as shown by colocalisation with MitoTracker Red (Pearson's correlation coefficients in the range 0.8 – 0.87) and confirmed by ICP-MS. Their PS activity in HeLa cells is characterised by PI, as follows: **113** (150) > **112** (64.6) > **109** (49.7) > **111** (42.2) under irradiation at 405 nm (20 mW cm⁻², 5 min, 6 J cm⁻²). Importantly, the authors reported lower PI in the non-cancerous cell line LO2 indicating a potential preferential killing of cancer cells. **113** was shown to kill cells via apoptosis with ROS shown to increase in HeLa cells post light treatment with loss of mitochondrial membrane potential indicated.

4. Platinum complexes as photosensitisers

A large number of octahedral Pt(IV) compounds have been explored as photoactivatable drugs, which could be photo-converted into Pt(II). These Pt(IV) complexes induce cell death via the non-oxygen dependent 'Type III' pathway and as such are deemed to work as photoactivated chemotherapeutics (PACT) rather than as PDT agents. A large body of work has been published harnessing the relative ease of interconversion between the oxidation states of platinum, where non-cytotoxic octahedral Pt(IV) compounds could be photochemically converted to cytotoxic square planar Pt(II) complexes exhibiting cisplatin-like activity. These compounds would circumvent the issues associated with hypoxia and PDT but may fall foul of cisplatin resistance. This exciting work is summarised in detail in many recent reviews, for example [102][103][104][105].

Despite numerous studies indicating Pt(II) complexes as efficient singlet oxygen sensitizers,[48] very few platinum compounds have been shown to exhibit photosensitizing effects via a type I or II mechanism.

Having noted that previous papers had shown photosensitizing properties of porphyrin complexes with peripherally conjugated ruthenium complexes[106, 107], Spingler et al designed three tetra-platinated porphyrins (**115** – **117**, Figure 21) based on the naked porphyrin **114**[108]. The Φ_{Δ} were in the range 0.54 - 0.41 for **114** - **117**, respectively. Photo-induced action of **114** – **117** was tested in MCF-7, HeLa, A2780 and CP70, a cisplatin resistant cell line with low dose violet light (420 nm, 6.95 J cm⁻²). Incorporation of the peripheral platinum groups drastically increased the photosensitisation effect in HeLa cells, increasing from PI =17.3 for **114** to an incredibly high PI of 1210 for **117**, with light induced LD₅₀ for **115** – **117** in the nanomolar range. Photosensitisation was also shown at a higher wavelength (575 nm, 6.95 J cm⁻²) albeit to a lesser degree. Following these outstanding results **115** – **117** were tested in a cisplatin resistant ovarian cancer cell line, A2780, again with violet light (420 nm, 6.95 J cm⁻²) leading to remarkable PIs of 1110, 1930 and >5260 for **115**, **116** and **117** respectively. The compounds were shown to enter the nucleus by confocal microscopy with the nuclear uptake of **117** confirmed by ICP-MS confirmed to be at 99.5 % (0.5 % cytoplasmic). Having demonstrated nuclear localization, **117** was shown to exhibit strong binding with calf thymus DNA (ctDNA) with an apparent binding constant calculated by competitive binding experiments with ethidium bromide (EB) to be $K_{app} = 7.5 \times 10^6 \text{ M}^{-1}$. The intercalative nature of the binding was confirmed by circular dichroism studies. No DNA cleavage was observed with **117** in the dark but light treatment caused an increase in DNA damage indicating DNA as the likely target of the compound.

In 2016, in collaboration with other groups, we reported the first example of oxygen mediated photosensitization of cell death by a small cyclometallated Pt(II) complex, Pt(II) 2,6-dipyrido-4-methyl-benzenechloride (**118**, Figure 21)[109]. The molecule demonstrated an appreciable Φ_{Δ} of 0.7 and was capable of inducing photosensitization of a number of cancer cell lines with low dose violet light (405 nm, 3.6 J cm⁻²). The compound, previously shown to accumulate predominantly in the nucleus with some cytoplasmic staining[110], was shown here to bind to DNA by metaphase spread indicating chromosomal staining. Bimodal DNA binding was deemed likely due to the biexponential emission decay of the DNA-bound compound ascribed to a mixture of intercalation and groove binding. Competitive binding with EB confirmed at least partial intercalation with a binding constant calculated to be $1.19 (\pm 0.08) 10^5 \text{ M}^{-1}$. The light induced DNA damage of the compound was investigated by agarose gel electrophoresis, induction of single strand breaks (SSB) in plasmid DNA was found with the combination of

compound and light but not compound or light alone. Oxygen was also implicated as hypoxic conditions reduced the formation of SSB, competitive EB binding also reduced SSB formation indicating that the intercalated binding mode was responsible for the damage. Induction of SSBs in cells was confirmed by COMET assay with significantly more damage observed when cells were treated with compound and light versus light or compound alone. The compound had a PI of 8.

Whilst the tetraplatinated porphyrin molecule showed high PS activity in a number of cell lines, the small cyclometallated Pt(II) molecule had relatively high levels of toxicity in the dark. This feature might have hindered exploration of Pt(II) complexes as photosensitisers of cell death in the past, as there are such limited reports of Pt(II) mediated PS of cells via a type I or II mechanism.

5. Osmium (II) complexes as photosensitisers

While there are reports of DNA photocleavage by Os(II) compounds[111, 112] there are very few reports of their PS activity in cells. The first such report, published in 2007 by Brewer et al, discussed two trinuclear metal complexes consisting of a central co-ordinating Rhodium between two metal centres, either Ru(II) or Os(II) (**119** and **120**, Figure 22)[113]. The design rationale was built on the reports of rhodium and mixed metal complexes having induced photo-cleavage of DNA[114], in which metal-to-metal charge-transfer (³MMCT) from the Os(II) or Ru(II) to the rhodium centre was considered to be responsible for the DNA cleavage. The irradiation of Vero cells incubated with **119** and **120** ($\lambda_{exc} > 460$ nm, 4 min) led to higher levels of cell death relative to non-irradiated cells.

In 2016, two polyazine complexes, of Os(II) and Ru(II), were reported (**121** and **122**, Figure 22)[115]. The absorption spectrum of the Os(II) complex, **122**, is slightly red shifted compared to the Ru(II) complex ($\Delta \lambda = 20$ nm) and shows greater absorption (24x higher) in the red (λ 650 nm, ³MLCT absorbance) attributed to the higher spin-orbit coupling from the heavier metal. The Os complexes demonstrated modest PIs of 9.86 and 5.8 under 470 nm and 625 nm excitation, respectively, in F98 (rat malignant glioma cells) – this is the first example of transition metal PS in glioma cells.

In April 2017 McFarland, Lilge, Mandel, *et al.* reported three Os(II) complexes as PS, these were tested in diverse cell lines and in mice (**123** – **125**, Figure 23)[29]. In order to have several charge-transfer transitions involving different ligands and achieve pan-chromatic absorption to harness as much light as possible, the Os(II) complexes bore two different diimine ligands, bipyridine and 2,2'-biquinoline (biq). All three compounds **123**, **124**, and **125** showed some absorption across the region 200 nm – 1000 nm with ligand centred transitions in the UV, a transition around 550 nm associated with MLCT from the Os(II) to the non-biq ligand and the broad absorption into the NIR associated with the MLCT to the biq ligand, with additional contributions from the spin –forbidden singlet-triplet transitions induced by high SOC of the Os center. Important in the context of antitumor treatments is the low Φ_{Δ} of 0.04 for **123** and **124** with no $^1\text{O}_2$ detected for **125**, the finding is consistent with the lack of O_2 quenching of photoluminescence of the compounds and indicates an O_2 independent pathway for the PS cell killing. The three compounds showed low dark toxicities in both U87 (human glioblastoma) and HT1276 (human bladder cancer) cell lines ($\text{LD}_{50} = 416 \mu\text{M} - 744 \mu\text{M}$) with modest PIs with red light excitation ($\text{PI} = 3.3 - 9.6$) at relatively high dose (625 nm, 90 J cm^{-2}) and with one-photon NIR light ($\text{PI} = 2.6 - 12$) at another high light dose (808 nm, 600 J cm^{-2}). Whilst these light doses are extremely high it is worth noting that this excitation is in the NIR using non-multiphoton lasers. The compounds were tested in mice and showed variability in their maximum tolerated doses (MTD) ('defined as the highest dose (mg kg^{-1}) that does not cause an animal distress'). The MTD for **123** was 1.25 mg kg^{-1} (below the acceptably limit for *in vivo* studies). For **125** the MTD was 6.25 mg kg^{-1} , and for **124** the MTD was high with tolerability at 47.0 mg kg^{-1} . **125** was therefore tested in mice with a subcutaneous colon tumour model. PS alone (at half the MTD) and light alone showed no significant increase in survival whilst PS and 192 J cm^{-2} red light slowed tumour growth and increased survival significantly ($P < 0.01$) compared to light only but not compared to PS only controls. A higher light dose (266 J cm^{-2}) combined with **125** led to complete tumour regression in most animals. The PDT effect was also tested in the NIR (808 nm, 600 J cm^{-2}) and caused significant survival gains compared to PS and light alone.

The lack of Os(II) complexes reported for PDT is somewhat surprising considering the relative wealth of Ru(II) complexes presented in the literature. One possible explanation is the usually shorter excited state lifetime of Os(II) complexes[116, 117] due to energy gap law – however,

recent results clearly show the potential of Os(II) complexes and assemblies thereof to act as photosensitisers for photoinduced cell death.

6. Rhenium(I) complexes as photosensitisers

The first report of photosensitizing activity of a Re(I) compound in 2013 described a series of three photosensitizing compounds **126a** – **126c** alongside a nontoxic luminescent probe **127** (**126** – **127**, Figure 24)[118]. The authors observed a surprising result that replacing the 2,2'-bipyridine ligand of the Re(I) complex **127** with 2-(2'-pyridyl)indolato ligand (and its derivatives) led to the loss of luminescence of the complex whilst leading to light-induced anticancer activity. Complex **126a** had a PI of 1000 in HeLa cells, although the light dose was incredibly high (>505 nm, 60 min, 29.2 mW cm⁻² (giving 105.12 J cm⁻²)) with cell death determined to be via apoptosis. Whilst **126a** showed light induced toxicity at longer wavelengths (≥ 505 nm) both **126b** and **126c** required shorter wavelengths for activation (≥ 415 nm) and **127** showed no phototoxicity even under UV irradiation (≥ 330 nm). Cell blebbing consistent with cell killing was observed by emission microscopy in cells incubated with **1** (1 μM) and a dose of light (LED light source) as high as 7 W, for 15 min. The efficiency of light-induced cell death mirrored the efficiency of singlet oxygen sensitisation by **126a** – **126c** at various wavelengths (≥ 505 nm, ≥ 415 nm and ≥ 330 nm), implicating ¹O₂ as the toxic agent produced. This hypothesis was further supported by the reduction in the efficiency of light-induced cell killing in cells co-incubated with **126a** and the anti-oxidant α-tocopherol (vitamin E). The PS ability of **126a** was also confirmed in melanoma spheroids. Although the extremely high light doses required would make developments of these specific compounds impractical, the work has clearly demonstrated the potential of the Re(I) complexes as photosensitisers for light-induced cell killing.

Specific intracellular targeting with Re(I) complexes was achieved by, for example, Gasser *et al.* by conjugating Re(I) diimine cores to known receptor-targeting peptide conjugates - a short nuclear localization signal (NLS), **131**, and a derivative of the neuropeptide bombesin, **132** (Figure 24) [119]. The NLS was conjugated with the aim of localising the PS in the nucleus in order to cause DNA damage upon activation, while **132** was designed to target receptors overexpressed in certain cancers. The Φ_Δ of the two control complexes, which did not contain targeting conjugates, **129** and **130**, assessed by indirect (RNO/Histidine assay) and direct (NIR emission of ¹O₂) methods were found to be in the range 0.2-0.26 and 0.72-0.79 in water and

acetonitrile, respectively. The subcellular localisation of the compounds assessed by emission microscopy indicated that **129** localises to the cytoplasm, **130** displays homogeneous distribution throughout the cell and **131** specifically locates to the nucleoli. The intracellular luminescence from **132** was too weak to evaluate its subcellular localisation. The toxicity of compounds **129** – **132** was assessed in HeLa and MCR-5 (human fibroblast) cell lines. **129** and **130** showed low levels of dark toxicity in both cell lines ($LD_{50} > 100 \mu\text{M}$). Both **131** and **132** were relatively toxic to MCR-5 cells ($LD_{50} = 17.8$ and 44.1 respectively), while in HeLa cells **131** was toxic ($LD_{50} = 35.1 \mu\text{M}$) yet **132** was not ($LD_{50} > 100 \mu\text{M}$). All compounds show light induced toxicity with UV excitation (350 nm , 2.58 J cm^{-2}), with an important result that conjugation to Bombesin led to ~ 20 fold increase in phototoxicity.

Specific targeting of Re(I) complexes was tackled by Lo *et al.* by conjugating a Re(I) core to a fructose group (**133** – **134**, Figure 24) [120]; the approach used by the same group to target-delivery of Ir(III) bipyridine D-fructose compounds[80]. Glucose transporters (GLUTs) are transmembrane proteins overexpressed in a number of cancers, hence conjugation of metal complexes to the fructose moiety might allow one to specifically target these overexpressing cells. Photoexcitation of **133** led to long-lived $^3\text{MLCT}$ emission ($505 - 553 \text{ nm}$) which was not affected by addition of the fructose. As with the Ir(III) complexes addition of the sugar led to a decrease in lipophilicity and a drop in cellular uptake compared to the sugar-free analogue (0.42 mM vs 1.83 mM for **133** and **134** respectively as determined by ICP-MS). A reduction in uptake at $4 \text{ }^\circ\text{C}$ indicated an energy dependent uptake pathway and both compounds were shown to localise to the mitochondria by colocalisation with MitoTracker deep red (Pearson's colocalisation coefficients of 87% and 80%). Both complexes were shown to be somewhat toxic in the dark in MCF7 cells ($LD_{50} = 9.6 \mu\text{M}$ and $3.9 \mu\text{M}$ for **133** and **134** respectively) and demonstrated PS activity following longwave UV radiation ($\lambda_{\text{exc}} > 365 \text{ nm}$, 30 min) with PIs of 4.8 and 13 for **133** and **134** respectively. The yield of singlet oxygen sensitisation was determined indirectly, by photo-oxidation of 1,5-dihydroxynaphthalene, and found to be 67.7 % and 67.1 % for **133** and **134** respectively. To assess relative uptake of the two complexes, a number of cell lines were tested, including two breast cancer lines overexpressing fructose transporters (MCF-7 and MDA-MB-231), two non-breast cancer cell lines which do not overexpress the fructose transporter (A549 and HepG2) alongside two non-cancer cell lines (NIH/3T3 and HEK293T). In all cell lines the uptake of the non-fructose containing complex **134** was higher as expected due to the higher lipophilicity but whilst **134** showed no major

difference in uptake between cell lines, the fructose containing **133** showed significantly higher uptake in the two breast cancer cell lines. To show that uptake was dependent on the fructose the cell lines were incubated with **133**, with and without exogenous fructose. It was found that exogenous fructose decreased the uptake of **133** only in the cell lines overexpressing the fructose transporter. This finding further indicates the potential for incorporation of fructose as a targeting moiety despite the drawbacks in terms of lipophilicity.

The work towards developing PSs which absorb more of the red part of the spectrum than traditional Re(I) diimines has been described in a paper from Meggers *et al.* in 2014 who designed derivatives, **136** – **142**, of their original compound **135** for this purpose (Figure 25) [121]. The substitution of monodentate π -acceptor pyridine ligand in **135** by σ -donor PMe_3 in **136**, or an imidazole in **137** did not lead to significant change in the absorption maxima. However, modifications of the cyclometallating ligand with accepting and donating moieties, **138** – **142**, led to significant changes in the energy of the lowest absorption band, with the largest red shift of 49 nm in complex **5** which bears a π -donating $-\text{NMe}_2$ -group in position 5 of the indole moiety. Interestingly, introducing a π -donating substituent in position 5 on the indole led to complete suppression of Φ_Δ (compounds **138** and **139**) and to a substantial reduction in Φ_Δ when $-\text{MeO}$ substituent was used (complex **142**). Compounds **140** and **141**, on the other hand, were shown to efficiently produce $^1\text{O}_2$ even under excitation in the red region of the spectrum (≥ 620 nm). Compounds **140** – **142** had PS effect in HeLa cells under red light excitation (1 hour, ≥ 620 nm, 7W LED). The PI of compound **140** was determined as 33.3 (30 min, ≥ 580 nm, 7W LED).

In another approach to developing broadly absorbing Re(I) photosensitisers, Zhao *et al.* employed the same strategy as discussed above for Ir(III) photosensitisers, namely, conjugation to a light-absorbing fluorophore, BODIPY (Figure 26)[122]. The Φ_Δ of **143** and **145** in DCM were 0.16 and 0.06 respectively which is surprisingly low, and was attributed to the increased bulk from the Bodipy chromophore. **144** and **143** were found to be somewhat toxic in the dark ($\text{LD}_{50} = 18.72 \mu\text{M}$ and $20.63 \mu\text{M}$ respectively) to the LLC cells used; PI **143** was determined as 1.59 (625 nm, unknown dose). The number of Re(I) photosensitisers studied to date is relatively small, perhaps due to potential toxicity of the standard tricarbonyl moiety, lack of strong absorbance in visible/NIR region unless coupled to an additional photosensitiser, and a modest, capacity to modulate and enhance two-photon absorption propensity as only one

diimine ligand is present in [Re(diimine)(CO)₃Cl] vs. polypyridyl Ru(II), Os(II), or Pt(II) complexes with multiple diimine ligands. Nonetheless, given the success of Re(I) compounds in emission imaging in life sciences, there is a clear potential, especially through selective targeting of subcellular structures, for the development of this group of PS in the future.

7. Ruthenium (II) complexes for photoactivated chemotherapy

The primary concerns regarding practical development of type I and II PDT is that of light delivery, and the requirement for cellular oxygen. The tumour microenvironment in solid tumours can be substantially different to that of healthy tissues. Significant differences in the vasculature of the tumour, arising due to the growth of neoplastic cells outpacing the process of angiogenesis, can result in a restriction in fresh nutrients and oxygen reaching areas of the tumour [123, 124]. A natural result of restriction in oxygen coupled with fast paced growth of cells is hypoxia. This lack of oxygen renders PDT ineffective in these areas and a breakdown of vasculature during PDT treatment combined with the depletion of cellular oxygen by the treatment itself can exacerbate the situation [125].

Photoactivated chemotherapy (PACT) in which photosensitisation of cells takes place by the oxygen independent type III pathway is an exciting alternative to PDT. As mentioned before the early work with TM complexes for PACT focussed on Pt(IV) complexes and has been extensively reviewed elsewhere [102-105]. More recently Ru(II) complexes have been explored for use as PACT PS [34, 35, 126]. This review does not attempt to cover Ru(II) PACT in any great detail however a few select examples are given to summarise the types of approaches groups have taken in designing Ru(II) PSs for PACT.

A common design strategy for PACT PS is to design complexes with photolabile, cytotoxic, ligands. In 2011, C. Turro *et al.* proposed a cationic complex, *cis*-[Ru(bpy)₂(5CNU)₂]²⁺ (bpy = 2,2'-bipyridine; 5CNU = 5-cyanouracil), for use in PACT (**146**, Figure 27) [127]. Upon irradiation, solvent-ligand exchange efficiently releases the biologically active compound 5CNU. 5CNU is a derivative of the chemotherapeutic agent 5-fluorouracil. Coordination to the Ru(II) complex renders 5CNU inactive and would allow for photo-release at the target site. While not reported in cells, the complex was effectively shown to release the chemotherapeutic upon visible excitation ($\lambda_{irr} \geq 395$ nm) demonstrating its potential. Following this work, C.

Turro's group, in collaboration with others, have explored Ru(II) complexes exhibiting photo-induced ligand release[128-131].

In 2012 Glazer *et al.* reported Ru(II) complexes **147** and **148** which have low toxicity in the dark, but photo-release a bidentate ligand under visible light ($\lambda_{\text{exc}} > 450$ nm) forming a highly toxic, DNA-binding Ru(II) complex **149** (Figure 27)[132]. Chemical analysis confirmed rapid dissociation of the sterically strained ligand upon irradiation in **147** and **148** while a non-sterically strained control compound, **150**, was found to be photo-stable. **147** photobinds to DNA (visible light, 200 W, 1 hour) while **150** photocleaves DNA and **148** both photobinds to, and photocleaves DNA. The PS activity of the compounds was tested in HL60 leukaemia and A549 lung cancer cell lines with visible light excitation ($\lambda_{\text{exc}} > 450$ nm, 410 W, 3 min) leading to a PI of 208 for **148** in A549 cells.

More recently Kodanko, *et al.* explored the Ru(II)-caged abiraterone complexes, **151** and **152**, for photorelease of the potent Cytochrome P450 enzyme (CYP) inhibitor abiraterone (AB) (Figure 28)[133]. Abiraterone acetate is an FDA approved therapeutic for metastatic prostate cancer however the anti-androgenic action of the drug is not limited to the tumour leading to negative effects in healthy tissue. In both **151** and **152** AB is photo-released through ligand exchange with the solvent (CH_3CN or H_2O) with visible light irradiation (λ_{exc} 500 nm). The bulkier N^N ligand in **151** led to faster photo-release of AB compared to the less sterically strained complex **152**[35]. Both **151** and **152** were tested in a AB sensitive cell line DU145. **151** and light ($\lambda_{\text{exc}} \geq 395$ nm, 250 W, 10 min) was deemed as toxic as AB while **151** administered in the dark showed limited toxicity up to 100 μM .

A similar strategy was subsequently used by Bonnet *et al.* who demonstrated photo-release of a cytotoxic nicotinamide phosphoribosyltransferase (NAMPT) inhibitor from Ru(II) complexes, **153** and **154** (Figure 28)[134]. NAMPT can be upregulated in cancer cells, with NAMPT inhibition able to induce apoptosis in cancer cells. However, the side-effects of NAMPT can include blindness making NAMPT inhibitors a good target for photo-release. A known inhibitor of NAMPT, STF-31, was coordinated to the same photo-caging scaffold as in [133]. Photo-release of STF-31 was demonstrated with both compounds (λ_{exc} 625 nm) with **153** more efficiently releasing STF-31 as predicted due to the bulkiness of the associated ligand. Both **153** and **154** were tested in three cancer cell lines (A549, MCF-7, and A431) and a normal cell line (MRC-5) in normoxic (21% O_2) and hypoxic (1% O_2) conditions in the dark and with red

light treatment (628 nm, 20.6 J cm⁻²). **153** proved unsuitable for use due to the lability of STF-31 in the dark. However, **154** proved promising as a PACT PS with similar PI values in normoxic and hypoxic conditions with low dose red light (628 nm, 20.6 J cm⁻²). These findings clearly demonstrate the potential offered by Ru(II) complexes in PACT.

8. Summary

The exploration of transition metal complexes as photosensitisers for PDT has seen rapid development in the past decade. The diversity of approaches used is immense, clearly demonstrating the adaptability of design of TM complexes as PS. Whilst Ru(II) is considered the leader in this field, Ir(III) is proving a worthy contestant, with some Os(II), Pt, and Re(I) PS emerging as important players as well. Many TM photosensitisers have demonstrated high photoindices, $PI = LD_{50}(\text{light})/LD_{50}(\text{dark})$. It is important to note the practical difficulties of comparing efficiency of photosensitisers reported by different laboratories. This difficulty is intrinsic to the diversity of light sources used – from pulsed lasers to broad-band arch lamps with vastly different spectral characteristics and power densities. Normalising of the PI reported for the light dose used may be the first step to more realistic comparisons between different photosensitisers activated by one-photon excitation. Three compounds (Table 1) stand out as the most promising ones, demonstrating the best PI/dose parameter of >100: Ir(III) complex **52** [77] which is also active under 2-photon excitation, Ir(III) complex **100** [97], and Pt(II) compound **117** [108]. Several other PS show PI/dose values between 40 and 10, whilst the majority of the photosensitisers have PI/dose values <10. The relatively high two-photon absorption cross-sections exhibited by some of metal complexes aids in the development of two-photon excitation in PDT. Increased targeting is badly needed to achieve disease specificity in patient care. Use of 2-photon PDT, development of complexes which absorb more in the red spectral region and/or the addition of targeting moieties to TM complexes offers hope for a revolution in the age old use of light for therapy; the first proof of which is offered with the advent of the first TM complex in a PDT clinical trial.

9. Acknowledgements

We thank the University of Sheffield, CRUK, YCR, and the EPSRC for financial support, and Dr Elizabeth Edwards (*nee* Baggaley), and Professor J. A. Gareth Williams (University of Durham, UK) for fruitful collaborations.

10. References

- [1] D. Phillips, *Pure and applied chemistry*, 67 (1995) 117-126.
- [2] E. Ruggiero, S. Alonso-de Castro, A. Habtemariam, L. Salassa, *Dalton Trans*, 45 (2016) 13012-13020.
- [3] N.J. Farrer, L. Salassa, P.J. Sadler, *Dalton Trans*, (2009) 10690-10701.
- [4] Y. Itoh, Y. Ninomiya, S. Tajima, A. Ishibashi, *Arch Dermatol*, 136 (2000) 1093-1095.
- [5] C. Sandberg, A.-M. Wennberg, O. Larkö, *Photodynamic Therapy of Acne*, in: *Photodynamic Therapy in Dermatology*, Springer, 2011, pp. 91-96.
- [6] J.S. Heier, D.S. Boyer, T.A. Ciulla, P.J. Ferrone, J.M. Jumper, R.C. Gentile, D. Kotlovker, C.Y. Chung, R.Y. Kim, *JAMA Ophthalmol*, 124 (2006) 1532-1542.
- [7] D.E. Dolmans, D. Fukumura, R.K. Jain, *Nat. Rev. Cancer*, 3 (2003) 380-387.
- [8] T.B. Fitzpatrick, M. Pathak, *J. Investig. Dermatol.*, 32 (1959) 229-231.
- [9] K. Kalka, H. Merk, H. Mukhtar, *J Am Acad Dermatol*, 42 (2000) 389-413.
- [10] N. Finsen, *Phototherapy*, Edward Arnold, 1901.
- [11] R. Bonnett, *Chem. Soc. Rev.*, 24 (1995) 19-33.
- [12] E.D. Sternberg, D. Dolphin, C. Brückner, *Tetrahedron*, 54 (1998) 4151-4202.
- [13] J. Prime, *Jouve and Boyer*, Paris, (1900).
- [14] R. Ackroyd, C. Kelty, N. Brown, M. Reed, *J. Photochem. Photobiol.*, 74 (2001) 656-669.
- [15] H. von Trappeiner, A. Jodebauer, *Gesammte Untersuchungen über die photodynamische erscheinung*, (1907).
- [16] L.B. Josefsen, R.W. Boyle, *Met Based Drugs*, 2008 (2008) 276109.
- [17] A. Policard, *CR Soc Biol*, 91 (1924) 1423-1424.
- [18] J.A. Parrish, T.B. Fitzpatrick, L. Tanenbaum, M.A. Pathak, *N. Engl. J. Med.*, 291 (1974) 1207-1211.
- [19] A. Siddiqui, R. Cormane, *Br. J. Dermatol.*, 100 (1979) 247-250.
- [20] D. Phillips, in: *Proc. R. Soc. A, The Royal Society*, 2016, pp. 20160102.
- [21] R. Bonnett, *Chemical Aspects of Photodynamic Therapy*, GORDONBREACH, Amsterdam, 2000.
- [22] E. Baggaley, J.A. Weinstein, J. A. G. Williams, *Coord. Chem. Rev.*, 256 (2012) 1762-1785.
- [23] B. Sherlock, S.C. Warren, Y. Alexandrov, F. Yu, J. Stone, J. Knight, M.A. Neil, C. Paterson, P.M. French, C. Dunsby, *J. Biophotonics*, (2017), doi: 10.1002/jbio.201700131.
- [24] B.C. Wilson, M.S. Patterson, *Phys. Med. Biol.*, 53 (2008) R61.
- [25] D. Kessel, Y. Luo, Y. Deng, C. Chang, *J. Photochem. Photobiol.*, 65 (1997) 422-426.
- [26] T.U. Shah, S. Keilin, *Gastrointestinal Malignancies: New Innovative Diagnostics and Treatment*, 22 (2015) 141.
- [27] P. Zhang, P.J. Sadler, *J. Organomet. Chem.*, 839 (2017) 5 - 14.
- [28] J. Fong, K. Kasimova, Y. Arenas, P. Kaspler, S. Lazic, A. Mandel, L. Lilge, *Photochem. Photobiol. Sci.*, 14 (2015) 2014-2023.
- [29] S. Lazic, P. Kaspler, G. Shi, S. Monroe, T. Sainuddin, S. Forward, K. Kasimova, R. Hennigar, A. Mandel, S. McFarland, *J. Photochem. Photobiol.*, 93 (2017) 1248-1258.
- [30] J.W. Tucker, C.R. Stephenson, *J. Org. Chem.*, 77 (2012) 1617-1622.

- [31] C.K. Prier, D.A. Rankic, D.W. MacMillan, *Chem. Rev.*, 113 (2013) 5322-5363.
- [32] H. Wang, Q. Liao, H. Fu, Y. Zeng, Z. Jiang, J. Ma, J. Yao, *J. Mater. Chem.*, 19 (2009) 89-96.
- [33] Q. Zhao, C. Huang, F. Li, *Chem. Soc. Rev.*, 40 (2011) 2508-2524.
- [34] C. Mari, V. Pierroz, S. Ferrari, G. Gasser, *Chem. Sci.*, 6 (2015) 2660-2686.
- [35] J.D. Knoll, C. Turro, *Coord. Chem. Rev.*, 282 (2015) 110-126.
- [36] F. Bolze, S. Jenni, A. Sour, V. Heitz, *ChemComm*, 53 (2017) 12857-12877.
- [37] F. Heinemann, J. Karges, G. Gasser, *Acc. Chem. Res.*, 50 (2017) 2727-2736.
- [38] Y. Arenas, S. Monro, G. Shi, A. Mandel, S. McFarland, L. Lilge, *Photodiagnosis Photodyn Ther*, 10 (2013) 615-625.
- [39] J. Liu, Y. Chen, G. Li, P. Zhang, C. Jin, L. Zeng, L. Ji, H. Chao, *Biomaterials*, 56 (2015) 140-153.
- [40] H. Huang, B. Yu, P. Zhang, J. Huang, Y. Chen, G. Gasser, L. Ji, H. Chao, *Angew. Chem. Int. Ed.*, 127 (2015) 14255-14258.
- [41] J. Hess, H. Huang, A. Kaiser, V. Pierroz, O. Blacque, H. Chao, G. Gasser, *Chem. Eur. J.*, 23 (2017) 9888-9896.
- [42] P. Zhang, H. Huang, J. Huang, H. Chen, J. Wang, K. Qiu, D. Zhao, L. Ji, H. Chao, *ACS Appl. Mater. Interfaces*, 7 (2015) 23278-23290.
- [43] V. Pierroz, R. Rubbiani, C. Gentili, M. Patra, C. Mari, G. Gasser, S. Ferrari, *Chem. Sci.*, 7 (2016) 6115-6124.
- [44] C. Mari, V. Pierroz, R. Rubbiani, M. Patra, J. Hess, B. Spingler, L. Oehninger, J. Schur, I. Ott, L. Salassa, *Chem. Eur. J.*, 20 (2014) 14421-14436.
- [45] T. Sainuddin, J. McCain, M. Pinto, H. Yin, J. Gibson, M. Hetu, S.A. McFarland, *Inorg. Chem*, 55 (2016) 83-95.
- [46] M.G. Walker, P.J. Jarman, M.R. Gill, X. Tian, H. Ahmad, P.A. Reddy, L. McKenzie, J.A. Weinstein, A.J. Meijer, G. Battaglia, *Chem. Eur. J.*, 22 (2016) 5996-6000.
- [47] S. Chakraborty, B.K. Agrawalla, A. Stumper, N.M. Vegi, S. Fischer, C. Reichardt, M. Kögler, B. Dietzek, M. Feuring-Buske, C. Buske, *J. Am. Chem. Soc.*, 139 (2017) 2512-2519.
- [48] X. Jiang, N. Zhu, D. Zhao, Y. Ma, *Sci China Chem*, 59 (2016) 40-52.
- [49] R. Gao, D.G. Ho, B. Hernandez, M. Selke, D. Murphy, P.I. Djurovich, M.E. Thompson, *J. Am. Chem. Soc.*, 124 (2002) 14828-14829.
- [50] P.I. Djurovich, D. Murphy, M.E. Thompson, B. Hernandez, R. Gao, P.L. Hunt, M. Selke, *Dalton Trans*, (2007) 3763-3770.
- [51] V.L. Whittle, J. A. G. Williams, *Inorg. Chem.*, 47 (2008) 6596-6607.
- [52] Z. Liu, P.J. Sadler, *Acc. Chem. Res.*, 47 (2014) 1174-1185.
- [53] C. Li, M. Yu, Y. Sun, Y. Wu, C. Huang, F. Li, *J. Am. Chem. Soc.*, 133 (2011) 11231-11239.
- [54] K.Y. Zhang, H.-W. Liu, T.T.-H. Fong, X.-G. Chen, K.K.-W. Lo, *Inorg. Chem.*, 49 (2010) 5432-5443.
- [55] K.K.-W. Lo, P.-K. Lee, J.S.-Y. Lau, *Organometallics*, 27 (2008) 2998-3006.
- [56] Q. Zhao, M. Yu, L. Shi, S. Liu, C. Li, M. Shi, Z. Zhou, C. Huang, F. Li, *Organometallics*, 29 (2010) 1085-1091.
- [57] H. Wu, T. Yang, Q. Zhao, J. Zhou, C. Li, F. Li, *Dalton Trans*, 40 (2011) 1969-1976.
- [58] P.-K. Lee, H.-W. Liu, S.-M. Yiu, M.-W. Louie, K.K.-W. Lo, *Dalton Trans*, 40 (2011) 2180-2189.
- [59] L. Murphy, A. Congreve, L.-O. Pålsson, J.G. Williams, *ChemComm*, 46 (2010) 8743-8745.
- [60] P. Steunenberg, A. Ruggi, N.S. van den Berg, T. Buckle, J. Kuil, F.W. van Leeuwen, A.H. Velders, *Inorg. Chem.*, 51 (2012) 2105-2114.
- [61] K.K.-W. Lo, S.P.-Y. Li, K.Y. Zhang, *New J. Chem.*, 35 (2011) 265-287.

- [62] T. Myochin, K. Kiyose, K. Hanaoka, H. Kojima, T. Terai, T. Nagano, *J. Am. Chem. Soc.*, 133 (2011) 3401-3409.
- [63] S. Zhang, M. Hosaka, T. Yoshihara, K. Negishi, Y. Iida, S. Tobita, T. Takeuchi, *Cancer Res.*, 70 (2010) 4490-4498.
- [64] S. Stimpson, D.R. Jenkinson, A. Sadler, M. Latham, D.A. Wragg, A.J. Meijer, J.A. Thomas, *Angew. Chem. Int. Ed.*, 54 (2015) 3000-3003.
- [65] M. Yu, Q. Zhao, L. Shi, F. Li, Z. Zhou, H. Yang, T. Yi, C. Huang, *ChemComm*, (2008) 2115-2117.
- [66] S.P.Y. Li, H.W. Liu, K.Y. Zhang, K.K.W. Lo, *Chem. Eur. J.*, 16 (2010) 8329-8339.
- [67] W. Jiang, Y. Gao, Y. Sun, F. Ding, Y. Xu, Z. Bian, F. Li, J. Bian, C. Huang, *Inorg. Chem.*, 49 (2010) 3252-3260.
- [68] H.-W. Liu, K.Y. Zhang, W.H.-T. Law, K.K.-W. Lo, *Organometallics*, 29 (2010) 3474-3476.
- [69] A. Kastl, A. Wilbuer, A.L. Merkel, L. Feng, P. Di Fazio, M. Ocker, E. Meggers, *ChemComm*, 48 (2012) 1863-1865.
- [70] L. Feng, Y. Geisselbrecht, S. Blanck, A. Wilbuer, G.E. Atilla-Gokcumen, P. Filippakopoulos, K. Kräling, M.A. Celik, K. Harms, J. Maksimoska, *J. Am. Chem. Soc.*, 133 (2011) 5976 - 5986.
- [71] R.-R. Ye, C.-P. Tan, L. He, M.-H. Chen, L.-N. Ji, Z.-W. Mao, *ChemComm*, 50 (2014) 10945-10948.
- [72] A.C. West, R.W. Johnstone, *J. Clin. Invest*, 124 (2014) 30-39.
- [73] S.-y. Takizawa, T. Breitenbach, M. Westberg, L. Holmegaard, A. Gollmer, R.L. Jensen, S. Murata, P.R. Ogilby, *Photochem. Photobiol. Sci.*, 14 (2015) 1831-1843.
- [74] E.M. Boreham, L. Jones, A.N. Swinburne, M. Blanchard-Desce, V. Hugues, C. Terryn, F. Miomandre, G. Lemerrier, L.S. Natrajan, *Dalton Trans*, 44 (2015) 16127-16135.
- [75] G. Bœuf, G.V. Roullin, J. Moreau, L. Van Gulick, C. Terryn, D. Ploton, M.C. Andry, F. Chuburu, S. Dukic, M. Molinari, *ChemPlusChem*, 79 (2014) 171-180.
- [76] J.S. Nam, M.-G. Kang, J. Kang, S.-Y. Park, S.J.C. Lee, H.-T. Kim, J.K. Seo, O.-H. Kwon, M.H. Lim, H.-W. Rhee, *J. Am. Chem. Soc.*, 138 (2016) 10968-10977.
- [77] L.K. McKenzie, I.V. Sazanovich, E. Baggaley, M. Bonneau, V. Guerchais, J. A. G. Williams, J.A. Weinstein, H.E. Bryant, *Chem. Eur. J.*, 23 (2017) 234-238.
- [78] J. Liu, C. Jin, B. Yuan, X. Liu, Y. Chen, L. Ji, H. Chao, *ChemComm*, 53 (2017) 2052-2055.
- [79] X. Tian, Y. Zhu, M. Zhang, L. Luo, J. Wu, H. Zhou, L. Guan, G. Battaglia, Y. Tian, *ChemComm*, 53 (2017) 3303-3306.
- [80] K.K.-W. Lo, W.H.-T. Law, J.C.-Y. Chan, H.-W. Liu, K.Y. Zhang, *Metallomics*, 5 (2013) 808-812.
- [81] K.K.-W. Lo, A.W.-T. Choi, W.H.-T. Law, *Dalton Trans*, 41 (2012) 6021-6047.
- [82] K.K.-W. Lo, K.Y. Zhang, *RSC Adv.*, 2 (2012) 12069-12083.
- [83] T.S.-M. Tang, K.-K. Leung, M.-W. Louie, H.-W. Liu, S.H. Cheng, K.K.-W. Lo, *Dalton Trans*, 44 (2015) 4945-4956.
- [84] W. Lv, Z. Zhang, K.Y. Zhang, H. Yang, S. Liu, A. Xu, S. Guo, Q. Zhao, W. Huang, *Angew. Chem. Int. Ed.*, 128 (2016) 10101-10105.
- [85] S. Moromizato, Y. Hisamatsu, T. Suzuki, Y. Matsuo, R. Abe, S. Aoki, *Inorg. Chem.*, 51 (2012) 12697-12706.
- [86] A. Nakagawa, Y. Hisamatsu, S. Moromizato, M. Kohno, S. Aoki, *Inorg. Chem.*, 53 (2013) 409-422.
- [87] A. Kando, Y. Hisamatsu, H. Ohwada, T. Itoh, S. Moromizato, M. Kohno, S. Aoki, *Inorg. Chem.*, 54 (2015) 5342-5357.

- [88] L. He, Y. Li, C.-P. Tan, R.-R. Ye, M.-H. Chen, J.-J. Cao, L.-N. Ji, Z.-W. Mao, *Chem. Sci.*, 6 (2015) 5409-5418.
- [89] P. Majumdar, X. Yuan, S. Li, B. Le Guennic, J. Ma, C. Zhang, D. Jacquemin, J. Zhao, *J. Mater. Chem. B*, 2 (2014) 2838-2854.
- [90] C. Wang, L. Lystrom, H. Yin, M. Hetu, S. Kilina, S.A. McFarland, W. Sun, *Dalton Trans*, 45 (2016) 16366-16378.
- [91] Y. Sun, L.E. Joyce, N.M. Dickson, C. Turro, *ChemComm*, 46 (2010) 2426-2428.
- [92] R. Lincoln, L. Kohler, S. Monro, H. Yin, M. Stephenson, R. Zong, A. Chouai, C. Dorsey, R. Hennigar, R.P. Thummel, *J. Am. Chem. Soc.*, 135 (2013) 17161-17175.
- [93] Y. Li, N. Dandu, R. Liu, Z. Li, S. Kilina, W. Sun, *J. Phys. Chem. C*, 118 (2014) 6372-6384.
- [94] H. Yin, M. Stephenson, J. Gibson, E. Sampson, G. Shi, T. Sainuddin, S. Monro, S.A. McFarland, *Inorg. Chem.*, 53 (2014) 4548-4559.
- [95] S.P.-Y. Li, C.T.-S. Lau, M.-W. Louie, Y.-W. Lam, S.H. Cheng, K.K.-W. Lo, *Biomaterials*, 34 (2013) 7519-7532.
- [96] J.M. Harris, R.B. Chess, *Nat. Rev. Drug Discov.*, 2 (2003) 214-221.
- [97] Y. Li, C.-P. Tan, W. Zhang, L. He, L.-N. Ji, Z.-W. Mao, *Biomaterials*, 39 (2015) 95-104.
- [98] D. Maggioni, M. Galli, L. D'Alfonso, D. Inverso, M.V. Dozzi, L. Sironi, M. Iannaccone, M. Collini, P. Ferruti, E. Ranucci, *Inorg. Chem.*, 54 (2015) 544-553.
- [99] J. Wang, Y. Lu, N. McGoldrick, C. Zhang, W. Yang, J. Zhao, S.M. Draper, *J. Mater. Chem. C*, 4 (2016) 6131-6139.
- [100] C. Mari, H. Huang, R. Rubbiani, M. Schulze, F. Würthner, H. Chao, G. Gasser, *Eur. J. Inorg. Chem.*, (2017) 1745-1752.
- [101] M. Ouyang, L. Zeng, K. Qiu, Y. Chen, L. Ji, H. Chao, *Eur. J. Inorg. Chem.*, (2017) 1764-1771.
- [102] M. Fanelli, M. Formica, V. Fusi, L. Giorgi, M. Micheloni, P. Paoli, *Coord. Chem. Rev.*, 310 (2016) 41-79.
- [103] K. Mitra, *Dalton Trans*, 45 (2016) 19157-19171.
- [104] J.S. Butler, P.J. Sadler, *Curr. Opin. Chem. Biol*, 17 (2013) 175-188.
- [105] U. Schatzschneider, *Eur. J. Inorg. Chem.*, 2010 (2010) 1451-1467.
- [106] T. Gianferrara, I. Bratsos, E. Iengo, B. Milani, A. Oštrić, C. Spagnol, E. Zangrando, E. Alessio, *Dalton Trans*, (2009) 10742-10756.
- [107] F. Schmitt, P. Govindaswamy, O. Zava, G. Süss-Fink, L. Juillerat-Jeanneret, B. Therrien, *J. Biol. Inorg. Chem.*, 14 (2009) 101-109.
- [108] A. Naik, R. Rubbiani, G. Gasser, B. Spingler, *Angew. Chem. Int. Ed.*, 126 (2014) 7058-7061.
- [109] R.E. Doherty, I.V. Sazanovich, L.K. McKenzie, A.S. Stasheuski, R. Coyle, E. Baggaley, S. Bottomley, J.A. Weinstein, H.E. Bryant, *Sci. Rep.*, 6 (2016) 22668.
- [110] S.W. Botchway, M. Charnley, J.W. Haycock, A.W. Parker, D.L. Rochester, J.A. Weinstein, J.A.G. Williams, *Proc. Natl. Acad. Sci. U.S.A.*, 105 (2008) 16071-16076.
- [111] Y. Sun, L.E. Joyce, N.M. Dickson, C. Turro, *ChemComm*, 46 (2010) 6759-6761.
- [112] S. Swavey, K. Li, *Eur. J. Inorg. Chem.*, 2015 (2015) 5551-5555.
- [113] A.A. Holder, D.F. Zigler, M.T. Tarrago-Trani, B. Storrie, K.J. Brewer, *Inorg. Chem.*, 46 (2007) 4760-4762.
- [114] J. Wang, J. Newman, S.L. Higgins, K.M. Brewer, B.S. Winkel, K.J. Brewer, *Angew. Chem. Int. Ed.*, 52 (2013) 1262-1265.
- [115] J. Zhu, A. Dominijanni, J.Á. Rodríguez-Corrales, R. Prussin, Z. Zhao, T. Li, J.L. Robertson, K.J. Brewer, *Inorganica Chim. Acta*, 454 (2017) 155-161.
- [116] N. Sutin, C. Creutz, Properties and reactivities of the luminescent excited states of polypyridine complexes of ruthenium (II) and osmium (II), in *Inorganic and*

- Organometallic Photochemistry; Wrighton, M. S., Ed.; Advances in Chemistry 168; American Chemical Society: Washington, DC, 1978; pp. 1–27.
- [117] R.H. Fabian, D.M. Klassen, R.W. Sonntag, *Inorg. Chem.*, 19 (1980) 1977-1982.
- [118] A. Kastl, S. Dieckmann, K. Wähler, T. Völker, L. Kastl, A.L. Merkel, A. Vultur, B. Shannan, K. Harms, M. Ocker, *ChemMedChem*, 8 (2013) 924-927.
- [119] A. Leonidova, V. Pierroz, R. Rubbiani, J. Heier, S. Ferrari, G. Gasser, *Dalton Trans*, 43 (2014) 4287-4294.
- [120] K. Yin Zhang, K. Ka-Shun Tso, M.-W. Louie, H.-W. Liu, K. K.-W. Lo, *Organometallics*, 32 (2013) 5098-5102.
- [121] K. Wähler, A. Ludewig, P. Szabo, K. Harms, E. Meggers, *Eur. J. Inorg. Chem.* 2014 (2014) 807-811.
- [122] F. Zhong, X. Yuan, J. Zhao, Q. Wang, *Sci China Chem*, 59 (2016) 70-77.
- [123] R.A. Medina, G.I. Owen, *Biol Res*, 35 (2002) 9-26.
- [124] D.W. Siemann, *Cancer treatment reviews*, 37 (2011) 63-74.
- [125] Z. Huang, H. Xu, A.D. Meyers, A.I. Musani, L. Wang, R. Tagg, A.B. Barqawi, Y.K. Chen, *Technology in Cancer Res. & treatment*, 7 (2008) 309-320.
- [126] C. Mari, G. Gasser, *CHIMIA International Journal for Chemistry*, 69 (2015) 176-181.
- [127] R.N. Garner, J.C. Gallucci, K.R. Dunbar, C. Turro, *Inorg. Chem.*, 50 (2011) 9213-9215.
- [128] R.N. Akhimie, J.K. White, C. Turro, *Inorganica Chim. Acta*, 454 (2017) 149-154.
- [129] L.M. Loftus, J.K. White, B.A. Albani, L. Kohler, J.J. Kodanko, R.P. Thummel, K.R. Dunbar, C. Turro, *Chem. Eur. J.*, 22 (2016) 3704-3708.
- [130] A. Li, J.K. White, K. Arora, M.K. Herroon, P.D. Martin, H.B. Schlegel, I. Podgorski, C. Turro, J.J. Kodanko, *Inorg. Chem.*, 55 (2015) 10-12.
- [131] M. Huisman, J.K. White, V.G. Lewalski, I. Podgorski, C. Turro, J.J. Kodanko, *ChemComm*, 52 (2016) 12590-12593.
- [132] B.S. Howerton, D.K. Heidary, E.C. Glazer, *J. Am. Chem. Soc.*, 134 (2012) 8324-8327.
- [133] A. Li, R. Yadav, J.K. White, M.K. Herroon, B.P. Callahan, I. Podgorski, C. Turro, E.E. Scott, J.J. Kodanko, *ChemComm*, 53 (2017) 3673-3676.
- [134] L.N. Lameijer, D. Ernst, S.L. Hopkins, M.S. Meijer, S.H. Askes, S.E. Le Dévédec, S. Bonnet, *Angew. Chem. Int. Ed.*, 56 (2017) 11549-11553.
- [135] A.B. Ormond, H.S. Freeman, *Materials*, 6 (2013) 817-840.

Table 1. A summary of photophysical data for compounds with highest PI in reviewed literature. NR = not reported. ^a Subcellular localisation: mito = mitochondrial; lyso = lysosomal; PN = perinuclear; Nuc = nuclear; cyto = cytoplasmic; ER = endoplasmic reticulum. ^b Mode of cell death: A = apoptosis; N = necrosis.

Compound	Metal center	LD50 light (μM)	LD50 dark (μM)	PI	λ _{exc} (nm)	Dose (J cm ⁻²)	PI/dose	Localisation ^a	ROS/ ¹ O ₂ (Φ _Δ)	Cell death ^b	One-/two-photon	ref
4	Ru(II)	3.5	>100	>28	450	12	2.33	Mito	¹ O ₂ , 0.81	-	both	[39]
5	Ru(II)	1.5	470	313	450	10	31.3	Lyso	¹ O ₂ , 0.99	N	both	[40]
8	Ru(II)	3.1	36.5	11.7	420	9.27	1.26	NR	¹ O ₂ , 0.75	-	both	[41]
16	Ru(II)	0.206	>300	>1,400	Vis light	100	>14	NR	¹ O ₂ , 0.0056	-	One	[45]
21	Ru(II)/Re(I)	61.7	0.3	206		48	4.29	NM / ER	¹ O ₂ , 0.54	N	One	[46]
12	Ru(II)	20	>100	>5	UV-A	1.29	>3.87	nuclear	¹ O ₂	A	One	[43]
23	Ru(II)	0.0349	7.7	220	470	6	36.7	Mito	¹ O ₂	-	One	[47]
41b	Ir(III)	0.23	7.9	34.35	≥450	NR	-	NR	-	A	One	[69]
45	Ir(III)	1.6	30.2	18.9	425	7.2	2.625	Cyto	¹ O ₂ , 0.75	A	One	[71]
46	Ir(III)	NR	NR	NR	TPE 800	-	-	Mito	¹ O ₂ , 0.54	-	TPE	[73]
47	Ir(III)	NR	NR	NR	TPE 740	-	-	NR	¹ O ₂	-	Both	[74]
51	Ir(III)	0.65	3.67	5.64	sunlight (+ TPE 860)	<1	>5.64	ER	¹ O ₂ , 0.78	A	Both	[76]
52	Ir(III)	0.18	>100	>555	760 TPE 405	3.6	>154.1	Mito + lyso	¹ O ₂ , 0.42	A	Both	[77]
54	Ir(III)	0.4	30.3	75	405	12	6.25	mito	¹ O ₂	-	Both	[78]
57	Ir(III)	NR	NR	NR	808	-	-	nuclear	¹ O ₂	A	TPE	[79]
62	Ir(III)	5	>498.4	99.68	> 365 nm	NR	-	mito	¹ O ₂ , 0.409	-	one	[80]
67	Ir(III)	0.5	8.6	17.2	UV-A	6 W 1h	-	mito	¹ O ₂ , 0.082	-	one	[83]
70	Ir(III)	NR	NR	NR	475	39.6		Mito + lyso	ROS + ¹ O ₂	A+N	one	[84]
72	Ir(III)	NR	NR	NR	377	NR		lyso	¹ O ₂	N	one	[85]

Compound	Metal center	LD50 light (μM)	LD50 dark (μM)	PI	λ_{exc} (nm)	Dose (J cm^{-2})	PI/dose	Localisation ^a	ROS/ ¹ O ₂ (Φ_{Δ})	Cell death ^b	One-/two-photon	ref
75	Ir(III)	0.12	>100	>833	425 nm	36	23.14	lyso	¹ O ₂ 0.05 (pH 7.4) 0.51 (pH 3)	A	one	[88]
78	Ir(III)	2.58	9.81	3.80	635	NR	-	NR	¹ O ₂ , 0.53	-	one	[89]
87	Ir(III)	0.354	144	407	broad vis light	100	4.07	Nuc + cyto	-	-	one	[90]
91	Ir(III)	3.4	>300	>88.2	365	NR	-	mito	¹ O ₂ , 0.69	N	one	[95]
100	Ir(III)	0.00086	3.1	3488	365	20	174.4	mito	¹ O ₂ , 0.62	A	one	[97]
101	Ir(III)	NR	NR	NR	Xe lamp	NR	-	PN	-	A	one	[98]
104	Ir(III)	NR	>300	NR	600 nm	NR	-	cyto	¹ O ₂ , 0.748	-	one	[99]
106	Ir(III)	0.17	>4	>23	420	9.27	>2.48	mito	¹ O ₂ , 0.87	-	one	[100]
113	Ir(III)	0.15	22.5	150	405	6	25	mito	¹ O ₂ , 0.59	A	one	[101]
117	Pt(II)	0.019	>100	>5260	420	6.95	>756	nuclear	¹ O ₂ , 0.54	-	one	[108]
118	Pt(II)	0.2	1.6	8	405	3.6	2.22	nuclear	¹ O ₂ , 0.7	-	one	[109]
119	(Os(II)) ₂ -Rh	NR	NR	NR	>460	NR	NR	NR	NR	-	one	[113]
122	Os(II)	86.1	>500	>5.8	625	13.5	0.43	NR	NR	-	one	[115]
		50.7	>500	>9.86	470	13.5	0.73	NR	NR	-	one	
125	Os(II)	57	550	9.6	625	90	0.0154	NR	¹ O ₂ , 0.04	-	both	[29]
		45	550	12.0	808	600	0.02					
126	Re(I)	0.1	100	1000	>505	105.12	9.512	membrane	¹ O ₂	A	one	[118]
132	Re(I)	5.3	>100	18.87	350	2.58	7.313	NR	¹ O ₂	-	one	[119]
134	Re(I)	0.3	3.9	13	>365	NR	-	mito	¹ O ₂	-	one	[120]
140	Re(I)	0.3	10	33	>580	NR	-	NR	¹ O ₂	-	one	[121]
143	Re(I)	12.94	20.63	1.59	625	NR	-	NR	¹ O ₂ , 0.16	-	one	[122]

Figure captions.

Figure 1. A schematic of PDT treatment of cancer: a) non-active form of drug is administered; b) drug is left to accumulate in tumour and healthy tissue; c) specific radiation of tumour tissue leads to production of singlet oxygen/ reactive oxygen species leading to targeted cell death. Top left: Depth of tissue penetration by varying wavelengths of light [2].

Figure 2. a) Structure of Psoralen and related molecules, adapted from [135]; b) Structure of Photofrin.

Figure 3. A simplified Jablonski diagram showing typical energy levels and transitions relevant to the formation of the triplet state of photosensitiser, and photosensitization of molecular oxygen. IC = internal conversion, VR = vibrational relaxation, ISC = intersystem crossing.

Figure 4. TLD1433 and examples of several other Ru(II) diimine photosensitisers. **1 - 4** are highly lipophilic compounds, numbered RuL1-RuL4 in [39]; compounds **5 - 7** are highly charged (+8) compounds (Ru1 – Ru3 in [40]); compounds **8** and **9** that contain derivatives of a known DNA intercalating ligand dppz are compounds **1** and **2** in [41].

Figure 5. Ru(II) photosensitisers **10** and **11** which in conjunction with single wall carbon nanotubes act as dual photothermal anticancer agents (compounds Ru1 and Ru2 in [42]).

Figure 6. Chemical structures of some Ru(II) photosensitisers. Compound **12** (Ru65 in [43]) is a DNA intercalator. Compounds **13 - 20** (1 - 8 in [45]) contain cyclometalating and diimine ligands. A systematic study of the effect of the extending conjugation in either cyclometalating, or diimine ligands, on photodynamic properties has been performed.

Figure 7. Chemical structures of a macrocyclic Ru(II)/Re(I) photosensitiser **21**, and its mononuclear Ru(II) building block **22** [46]; Ru(II) PS conjugated to human serum albumin (**23**) cHSA-PEO-TTP-Ru and to HSA aa 312 to 324 (**24**).[47]

Figure 8. Cyclometallated Ir(III) complexes of general type $[\text{Ir}(\text{C}^{\wedge}\text{N})_2(\text{NN})]^+$.

Compounds **25** and **26** are compounds 1 and 2 in [65]; compounds **27 – 32** are compounds 1-6 in [56]. Emission images of HeLa cells incubated with **27-31** (left to right) are also shown.

Figure 9. Chemical structures of metallo-pyrido carbazole Ir(III) photosensitisers **33 – 41b** (compounds 1 - 11 in [69]).

Figure 10. $[\text{Ir}(\text{C}^{\wedge}\text{N})_2(\text{NN})]^+$ photosensitisers designed with the aim of combining photosensitisation with a Histone deacetylases (HDAC) inhibitor, suberanilohydroxamic acid (SAHA). Compounds **42 - 45** are compounds 1 - 4 in [71]. The bottom panel shows characterisation of apoptosis induced in HeLa by complex **42** using annexin V-FITC staining, and monitored by flow cytometry.

Figure 11a. Chemical structures of some $[\text{Ir}(\text{C}^{\wedge}\text{N})_2(\text{NN})]^+$ photosensitisers: **46**[73]; **47**[74]; **48 - 51** (compounds T1r1 - T1r4 in [76]).

Figure 11b. Chemical structures of Ir(III) complexes **52** and **53**; emission properties of **52** are pH sensitive in the physiological range. **52** has the higher PI index for Ir(III) complexes to date under one-photon excitation, and is also a two-photon PDT agent[77]. The bottom panel shows two photon absorption activated killing of HeLa cancer cells incubated with **52** (1 μM) for two hours, followed by irradiation with 760 nm, ~ 100 fs pulses (irradiated area 225 x 225 μm , 1024 x 1024 pixels, 6.6 μs dwell time, 8 scans) with the powers corresponding to 0, 1088, 1632, 2176 J cm^{-2} . Cell apoptosis is indicated in green, necrosis in red. Images are 450 x 450 μm except those in the 0 mW column which are 900 x 900 μm .

Figure 12. Chemical structures of some of Ir(III) photosensitisers: compounds **54 - 56** are compounds Ir1 – Ir3 in [78]; compounds **57 – 61** are compounds Ir-Es, Ir-Me, Ir-Pn, Ir-Pc and Ir-Cz in [79].

Figure 13. Ir(III) photosensitisers containing fructose, and their fructose-free analogues; compounds **62 – 65** are compounds 1a, 1b, 2a and 2b from [80].

Figure 14. Ir(III) photosensitisers with diverse cyclometallating ligands. Compounds **66** – **69** are compounds 1a, 2a, 1b and 2b from [83].

Figure 15. Ir(III) photosensitisers which are lysosome-specific (**70** and **71**, correspond to Ir-P(ph)₃ and Ir-alkyl from [84]); [Ir(N[^]C)₃]ⁿ pH-responsive photosensitisers **72** and **73** (5 and H3.5 from [85]); and pH-responsive, lysosome-specific [Ir(N[^]C)₂(NN)]⁺ compounds **74** – **77** (compounds 1 – 4 from [88]).

Figure 16. Red-light activated Ir(III) photosensitisers bearing BODIPY groups, **78** – **81** (compounds Ir-1 – Ir-2 from [89]).

Figure 17. Systematic tuning of light-absorbing properties of Ir(III) complexes through changing conjugation in diimine and cyclometallating ligands, **82** – **87** (compounds 1 – 6 from [90]).

Figure 18. Ir(III) photosensitisers with PEG chains and their analogs. Compounds **88** – **92** are compounds 1a – 5a, compounds **93** – **97** are compounds 1b – 5b from [95].

Figure 19. Ir(III) photosensitisers designed for mitochondrial (**98** – **100**, compounds 1 – 3 from [97]) and perinuclear (**101** – **102**, compounds 1M and 1P from [98]) localisation.

Figure 20. Orange-absorbing photosensitisers **103** and **104** (Ru-2 and Ir-2 from [99]); aromatic acid imide-containing photosensitisers **105** - **108** (R1, R2, L1 and L2 from [100]); mitochondria-targeting photosensitisers **109** – **113** (Ir1 – Ir5 from [101]).

Figure 21. Pt-based photosensitisers. **114** – **117** are compounds 1 – 4 from [108]; compound **118** is compound 1 from [109]. The bottom panel shows a representative COMET assay images for HeLa cells treated with 0.5 μM of **118**, with and without exposure to 405 nm light (3.6 J cm⁻²).

Figure 22. Multinuclear Os and Ru photosensitisers **119** and **120** [113]; mononuclear Ru(II) and Os(II) photosensitisers **121** and **122** (1 and 2 from [115]).

Figure 23. Os(II) photosensitisers **123 – 125** (TLD1822, TLD1824 and TLD1829 from [29]). Re(I) photosensitisers **126 – 127** (1 -4 from [118]).

Figure 24. Re(I) photosensitisers bearing protein tags, **129 – 132** (Re –NH₂, Re-COOH, Re-NLS and Re-Bombesin from [119]) and fructose unit, **133 - 134** (1 and 2 from [120]), and their tag-free analogs.

Figure 25. Re(I) pyridocarbazole complexes with tuneable absorption maxima for red-light activated PDT, **135 – 142** (compounds 1 – 8 from[121]); compounds **138-139** are not PDT-active. The bottom panel shows visible-light-induced antiproliferative activity of **140** in HeLa cancer cells which were irradiated for 30 min at $\lambda \geq 580$ nm following 1 h incubation with **140**; cytotoxicity was determined 24 h after addition by MTT assay.

Figure 26. Re(I) photosensitisers **143** and **145** containing BODIPY unit (Re-1 and Re-2 from [122]).

Figure 27. Ru(II) photosensitisers **146** (1 in [127]) and **147-149** (2, 3 and 1 in [132]), and a control compound **150**.

Figure 28. Ru(II) photosensitisers **151** and **152** (1 and 2 in [133]) and **153** and **154** (1 and 2 in [134]).